EXPERIMENTAL INVESTIGATION OF COLLAPSE IN EOLIAN SOIL: A CASE STUDY IN MAYAPO, COLOMBIA.

INVESTIGACIÓN EXPERIMENTAL DEL COLAPSO EN SUELOS EÓLICOS: UN CASO DE ESTUDIO EN MAYAPO COLOMBIA

Kandy Manuela Teheran Ochoa

Universidad Nacional de Colombia
Facultad de Minas, Departamento de Ingeniería Civil
Medellín, Colombia
2021

EXPERIMENTAL INVESTIGATION OF COLLAPSE IN EOLIAN SOIL: A CASE STUDY IN MAYAPO, COLOMBIA.

INVESTIGACIÓN EXPERIMENTAL DEL COLAPSO EN SUELOS EÓLICOS: UN CASO DE ESTUDIO EN MAYAPO COLOMBIA

Kandy Manuela Teheran Ochoa

Research thesis presented as partial requirement to obtain the title:

Master in Geotechnical Engineering

Director:
Manuel Roberto Villarraga Herrera
Codirector:
Oscar Echeverri Ramirez

Research line:
Unsaturated soils Mechanic

Universidad Nacional de Colombia
Facultad de Minas, Departamento de Ingeniería Civil
Medellín, Colombia
2021

To my dear Mother: Olga Lucia Ochoa

To my brother: Juan Diego Teheran

For their love and support throughout this travel

ACKNOWLEDGMENTS

Es un placer para mí expresar mi más sincero agradecimiento a DIOS, y a todas las personas que con su soporte científico y humano han contribuido al desarrollo y finalización de esta tesis de maestría.

Quisiera expresar mi más profundo agradecimiento a mi director de tesis, al profesor Manuel Villarraga Herrera por su apoyo incondicional y acertada orientación desde el día en que se inició esta investigación hasta la última discusión del contenido, por creer en mí desde el principio y por ser una gran fuente de inspiración.

Mi más sincero agradecimiento a mi codirector de tesis, el profesor Oscar Echeverri Ramírez, quien fue un apoyo incondicional durante el desarrollo del proyecto de tesis y en mi estancia en Francia, su orientación y soporte fue fundamental para la finalización de este proyecto.

Un agradecimiento muy especial al Dr. Daniel Ruiz Restrepo por su apoyo incondicional durante la tesis de maestría, por su orientación y aliento a lo largo de este esfuerzo. Trabajar con Daniel ha sido una experiencia de aprendizaje memorable, y los resultados que aquí se presentan son posibles gracias a su apoyo y su experiencia.

Pour le soutien durant mon stage, je tiens à remercier mes collègues du groupe REEG au CEREMA Toulouse, France. Mon cher chief Didier Virely pour son soutien dans le travail expérimental et sa compréhension dans les moments difficiles. Je tenais aussi à remercier, pour le soutien et l'aide durant le stage, Stéphane MOULIGNE, Florence, Philippe, Jean Claude, les directeurs Pascal SAUVAGNAC et Quentin GAUTIER, et le groupe REGG pour avoir toujours voulu m’aider dans le dans le travail expérimental et de m’avoir fait me sentir comme chez moi dans un pays qui m’était inconnu.

Agradezco también a las instituciones que han hecho posible la realización del trabajo presentado por la ayuda económica brindada por la Universidad Nacional de Colombia, por el Centre d'études et d'expertise sur les risques, l'environnement, la mobilité et l'aménagement CEREMA y por Colciencias. Gracias por la ayuda y confianza en mi depositada.

Finalmente, agradezco a mi familia por su apoyo, compresión, comunicación constante y sacrificio en circunstancias muy difíciles. Especialmente, a mí madre Olga Lucia, quien ha compartido mis alegrías y angustias, por su aliento a superarme cada día. Esta tesis va dedicada a ella.

A todas aquellas personas que colaboraron en la realización de este trabajo, Gracias.

Content

List of Figures

List of Tables

ABSTRACT

The principal target of this research is to focus on the study of the volumetric behavior of the eolian soil and the influence of the geology, the soil structure, and suction on possible collapse behaviour of the eolian soils. An experimental program of laboratory tests was designed including geotechnical classification tests, Micro-structure tests, suction measurement, and oedometer tests included classical and unsaturated in order to know the characteristics and properties of the eolian soils.

The experimental investigation was realized on undisturbed samples of the eolian soil from Mayapo, Colombia. The geology was studied by thin sections and DRX, and the soil structure of the eolian soils was characterized by a scanning electronic microscope. The distribution of the elements is analyzed by energy dispersive diffraction EDS. The suction and total suction is measured by the paper filter method and the osmotic suction by the electrical conductivity of the pore water of the soil. The volumetric behaviour is studied by double oedometer and oedometer at different vertical effective stress to know the collapse potential and the load where the soil suffers the most collapse.

Suction-controlled oedometer tests were developed. The experimental tests included an increase in the vertical net stress at constant suction levels and variations in stress and suction paths. The principal aspect analyzed was the volumetric behaviour at suction levels, the yield stress generated by increased in the vertical net stress or increased in suction levels.

The eolian soil was classified as silty sand (SM) poorly graded, with very low fines percentage. The main minerals of the eolian soil of Mayapo are quartz, plagioclases, and feldspars. Also, there are salt particles in the soil and bonding materials of aluminum and iron oxides bordering the grains.

There are large and continuous macropores between grains and a low amount of micropores. The macropores could control the volumetric behaviour of the eolian soils. the presence of macropores is also demonstrated in the double water retention curve (WRC), where it is demonstrated that the soil present low suction levels and it behaviour is controlled by macropores of the soil.

The salt concentration influences the osmotic suction and the total suction of the eolian soil, affecting its hydraulic condition. It can govern the water flow and attract more water to the soil, increasing the saturation degree, causing a decrease in total suction in the soil. This change in suction component influence the collapse behaviour, increasing the strain with the decrease in suction.

The collapse potential of the eolian soils was classified as a moderated problem. The collapse potential increase with the increment of the initial void ratio. The suction also plays an important role in the collapse potential. As suction decreases and soil wets, water menisci between liquid and vapour phase disappears, and the empty pores are flooded, and it causes a loss in the soil stiffness.

The unsaturated oedometer tests allowed to understand the influence of suction on the volumetric behaviour of the eolian soils. The suction allows the soil to sustain higher applied stress: The higher the suction, the higher is the stress that can be sustained before yield. The suction increases the stiffness of the eolian soils. A constitutive model was proposed to describe the volumetric behaviour of the eolian soil. The model is represented by a Loading Collapse (LC) curve, and to allow knowing the reversible compressive volumetric strains for any stress path of loading (L), collapse (C), or both in the elastic domain and to predict irreversible compressive volumetric strain for any stress loading or collapse paths. There is an important dependence of collapse and loading paths in the volumetric behaviour of the eolian soils. The deformations are very small at suction changes. The soils will suffer higher deformations in loading paths at low suction levels due to the soil stiffness is less.

At last, an experimental procedure was proposed for sampling and characterization of the volumetric behaviour of undisturbed eolian soils.

Key words: Collapse, Eolian soils, Strain

RESUMEN

El objetivo principal de esta investigación es centrarse en el estudio del comportamiento volumétrico del suelo eólico y la influencia de la geología, la estructura del suelo y la succión en el posible colapso de los suelos eólicos. Se diseñó un programa experimental de ensayos de laboratorio que incluye ensayos de clasificación geotécnica, ensayos de visualización de la microestructura, medición de succión y ensayos edométricos convencionales realizados con el procedimiento clásico de la norma y ensayos edométricos no saturados, para conocer las características y propiedades de los suelos eólicos.

La investigación experimental se realizó sobre muestras inalteradas del suelo eólico de Mayapo, Colombia. La geología se estudió mediante secciones delgadas y DRX, y la estructura del suelo de los suelos eólicos se caracterizó mediante un microscopio electrónico de barrido. La distribución de los elementos se analiza mediante EDS por difracción de energía dispersiva. La succión y succión total se mide por el método de filtro de papel y la succión osmótica por la conductividad eléctrica del agua de los poros del suelo. El comportamiento volumétrico se estudia mediante edómetro doble y edómetro a diferentes esfuerzos verticales efectivos para conocer el potencial de colapso y la carga donde el suelo sufre más colapso.

Se desarrollaron pruebas de edómetro controladas por succión. Las pruebas experimentales incluyeron un aumento en la tensión neta vertical a niveles de succión constantes y variaciones en las trayectorias de tensión y succión. El principal aspecto analizado fue el comportamiento volumétrico a los niveles de succión, el límite elástico generado por el aumento de la tensión neta vertical o el aumento de los niveles de succión.

El suelo eólico fue clasificado como arena limosa (SM) pobremente graduada, con muy bajo porcentaje de finos. Los principales minerales del suelo eólico de Mayapo son el cuarzo, las plagioclasas y los feldespatos. Además, hay partículas de sal en el suelo y materiales de unión de óxido de hierro y aluminio que bordean los granos.

El suelo presenta gran cantidad de macroporos entre los granos y una pequeña cantidad de microporos. Los macroporos podrían controlar el comportamiento volumétrico de los suelos

eólicos. la presencia de estos se demuestra en la doble curva de retención de agua (WRC), donde se demuestra que el suelo presenta bajos niveles de succión y su comportamiento está controlado por macroporos del suelo.

La concentración de sal influye en la succión osmótica y la succión total del suelo eólico, afectando su condición hidráulica. Puede gobernar el flujo de agua y atraer más agua al suelo, aumentando el grado de saturación, provocando una disminución de la succión total en el suelo. Este cambio en el componente de succión influye en el comportamiento de colapso de los suelos eólicos estudiados, aumentando la deformación al disminuir la succión.

El potencial de colapso de los suelos eólicos se clasificó como un problema moderado. El potencial de colapso aumenta con el incremento de la proporción de vacíos inicial. La succión también juega un papel importante en el potencial de colapso. A medida que la succión disminuye y el suelo se humedece, los meniscos de agua desaparecen y los poros vacíos se inundan, lo que provoca una pérdida de rigidez del suelo.

Las pruebas en el edómetro no saturado permitieron comprender la influencia de la succión en el comportamiento volumétrico de los suelos eólicos. El componente de succión en el suelo hace que este soporte una mayor tensión aplicada: cuanto mayor es la succión, mayor es la tensión que se puede sostener antes del rendimiento. La succión aumenta la rigidez de los suelos eólicos. Se utilizó el Modelo Básico de Barcelona, propuesto por Alonso et al, 1999, para describir el comportamiento volumétrico de los suelos eólicos de Mayapo, Colombia. El modelo está representado por una curva de colapso de carga (LC) y permite conocer las deformaciones volumétricas compresivas reversibles para cualquier trayectoria de carga (L), colapso (C) o ambos en el dominio elástico y para predecir deformaciones volumétricas compresivas irreversibles. para cualquier carga de tensión o rutas de colapso. Existe una dependencia importante de las rutas de colapso y carga en el comportamiento volumétrico de los suelos eólicos. Las deformaciones son muy pequeñas en los cambios de succión. Los suelos sufrirán mayores deformaciones en los caminos de carga a bajos niveles de succión debido a que la rigidez del suelo es menor.

Finalmente, se propuso un procedimiento experimental para el muestreo y caracterización del comportamiento volumétrico de suelos eólicos no perturbados.

Palabras claves: Colapso, Suelos eólicos, Deformación.

CHAPTER 1 – INTRODUCTION

1.1. General aspects

The collapse phenomenon is defined as a significant volume reduction caused by water content changes in an unsaturated soil under load (Delage et al., 2005). The collapse phenomenon is well understood as a sudden and significant volume change due to wetting, the additional presence of loading, or a combination of both (Jennings & Knight, 1957). It is fundamental to consider this behaviour when investigating the mechanical response of the soil.

The eolian deposits are known for their high potential of collapse behaviour. Many researchers have studied these soils because of problems related to stability in trains lines (Delage et al., 2005), landslide induced by irrigation (Leng et al., 2018), slope failures related to internal erosion, tunnel gullying (Yates et al., 2018). These problems are the result of a strong volume reduction of soil caused by water content changes.

In the north of Colombia, near to Riohacha, capital of the department of La Guajira, there is a town called Mayapo. This town present extensive areas covered by sand deposits attributed to eolian processes. Although the precipitation is rare in these regions, heavy rain episodes may occur generated by storms from the Caribbean sea (Arango et al., 2014). The soil features, along with the climate, can trigger the soil collapse.

The area studied has been enhancing tourism (Mejia and Bolaño, 2014), which has a remarkable effect on urban development, value the landscape, and generate infrastructure demands. However, indiscriminate use of soil is present without widespread attention of the deformation behaviour of eolian soils, aggravated by a lack of urban and tourism planning (CCG, 2017). Major projects could face increasing problems related to unsaturated eolian deposits, which result in pathological affectations as structural failures associated with differential settlements, cause major economic losses (Gaaver, 2012). From this point of view, it is important to identify and analyze problems related to the soil collapse in this area.

1.2. Aims of the research

This research intends to determinate influencing factors in the possible collapse of the eolian deposits in Mayapo, Colombia.

The specific objectives of this work included:

- To realize the geological characterization of eolian soil from the Eolic Deposit Formation (Qe), correlating the current properties with the geological history of this area, including types of soils, mineralogy, cementation, chemical composition.
- Determinate the collapse potential of sand eolian soils from Eolic Deposit Formation (Qe) in Mayapo, Colombia.
- To correlate the structure, the physical, chemical, and mineralogical properties, and the suction in the possible collapse of the eolian soils.
- To propose a sampling and characterization protocol to evaluate the collapse behaviour in eolian soils.

1.3. Relevance of the research

This research is a first approach to knowledge in the eolian soils in the country. It is due to no serious study tackling a comprehensive investigation of the collapse in eolian soils in Colombia. The neglect in studying these soils is understandable because they are usually present in predominantly regions where economic development is limited. Thus, it will make a valuable contribution to the research communities at regional and national levels.

On the other hand, this research will impulse to more scientific investigations will be carried out in other parts of the country where the eolian soils are present, to establish whether the collapse phenomenon and geotechnical problems related to this are presented.

Besides, it is convenient for the local authorities to consider the results obtained in this research within the territorial arrangement planning. Thus, the soil will be distributed effectively in engineering projects. And include the collapse phenomenon of this soils in the potential risk for the area.

It is also significant the process carried out of the installation and assembly from scratch of a controlled suction oedometer for unsaturated soils in the CEREMA geotechnical laboratory in Toulouse, France, and the creation of a manual of the equipment for future research. Also, this stage allowed knowing the deformational behaviour of the eolian soil and obtaining parameters to model the soil, which has extended the scope initially proposed in this research.

1.4. Hypothesis

The eolian soils of Mayapo exhibit characteristic and properties of collapsible soils.

1.5. Thesis layout

To fulfil the objectives mentioned above, the thesis is organized in six chapters, as follows:

Chapter 2 reviews the state of the art of unsaturated soils and suction, a summary of collapsible soils, collapse mechanism, properties, and the analysis and criteria for estimating the collapse. Also, the theory of stress-strain behaviour of unsaturated soils, the axis translation technique used in the unsaturated test, and a brief description of the Barcelona Basic Model (BBM) used to model the soil.

Chapter 3 gives brief information about the site. It presents the site localization and describes the climate, geology, geomorphology of the region, and the area studied.

Chapter 4 refers to the methodology and experimental techniques, where the procedures attached to the preparation of tests and the laboratory are described.

Chapter 5 presents the results and analysis of experimental tests. The micro-visualization analysis (X-ray diffractogram, microscopic analysis, and Scanning Electronic Microscope SEM) and their influence on volumetric behaviour are presented. The water retention curves of the total and matric suction and the results of osmotic suction are also detailed. The volumetric behaviour analysis of the eolian soils of Mayapo is presented by the classic and unsaturated oedometer test results. By last, it presents the parameters obtained from the experimental tests in the oedometer with controlled suction. The parameters are used to model the eolian soils using the constitutive model Barcelona Basic Model (BBM).

Finally, Chapter 6 summarizes this work and presents general conclusions and future work.

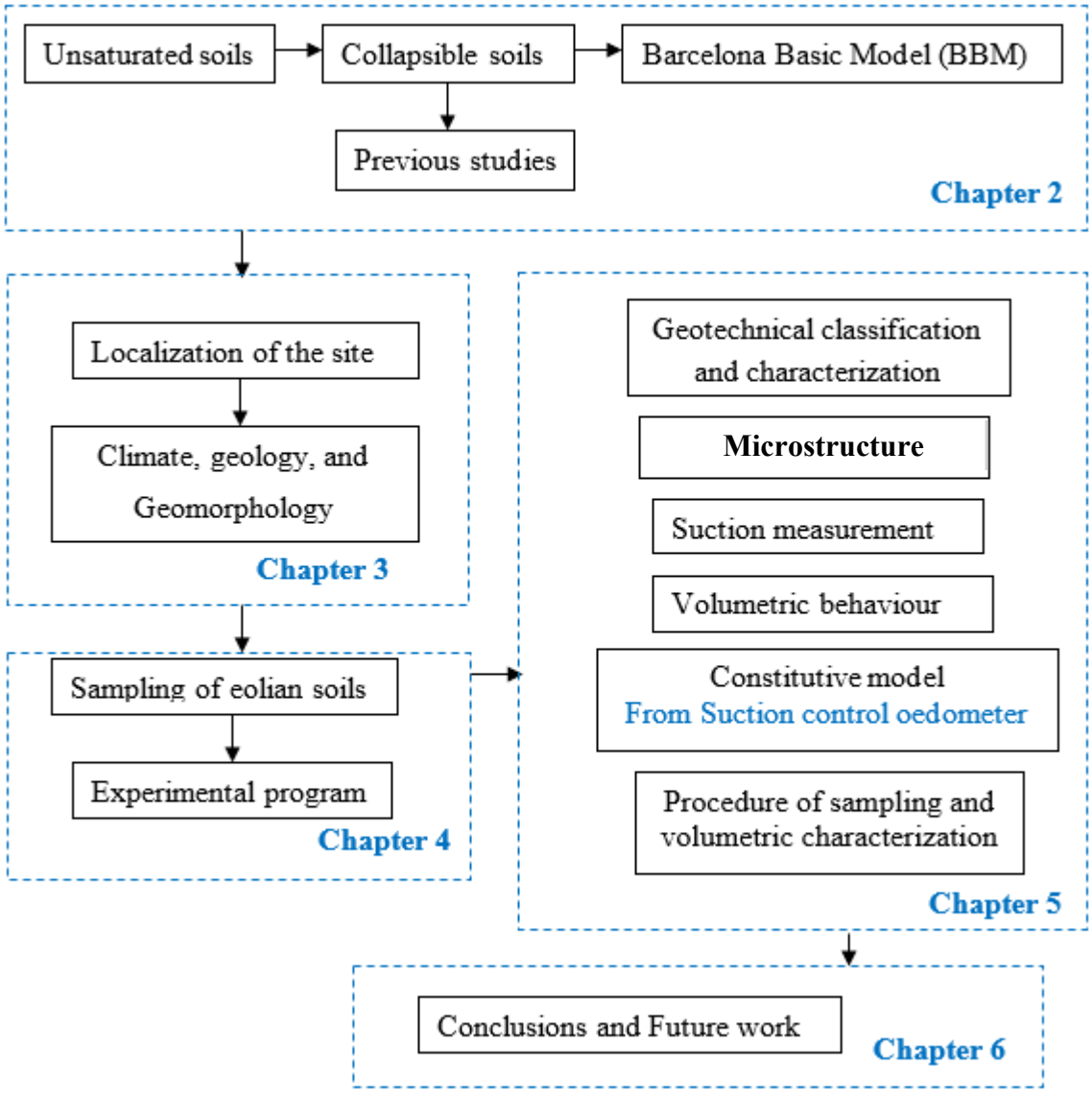

Figure 1-1. Thesis structure

1.6. References

Arango, C., Dorado, J., Guzmán, D., & Ruiz, J. . (2014). Climatología trimestral de Colombia. In *IDEAM*.

Camara de Comercio de La Guajira. (2017). *Informe Socio-Economico Sector Turismo de La Guajira*.

Delage, P., Cui, Y. J., & Pereira, J. M. (2005). Geotechnical problems related with loess deposits in Northern France. *Proceedings of International Conference on Problematic Soils*, *May*, 517–540.

FHWA. (2015). Soil Nail Walls Reference Manual. *Geotechnical Engineering Circular NO. 7*, *132085*, 425.

Gaaver, K. E. (2012). Geotechnical properties of Egyptian collapsible soils. *Alexandria Engineering Journal*, *51*(3), 205–210.

Jennings, J., & Knight, K. (1957). The Additional Settlement of Foundations due to a Collapse of Structure of Sandy Subsoils on Wetting. *Proceedings, 4th International Conference on Soil Mechanics and Foundation Engineering, London*, *1*, 316–319.

Leng, Y., Peng, J., Wang, Q., Meng, Z., & Huang, W. (2018). A fluidized landslide occurred in the Loess Plateau: A study on loess landslide in South Jingyang tableland. *Engineering Geology*, *236*(July 2016), 129–136.

Mejia, L., & Bolaño, L. (2014). La calidad de las ofertas turisticas en el departamento de la guajira Colombia. *Dimension Empresarial*, *12*, 139–149.

Yates, K., Fenton, C. H., & Bell, D. H. (2018). A review of the geotechnical characteristics of loess and loess-derived soils from Canterbury, South Island, New Zealand. *Engineering Geology*, *236*(July 2017), 11–21.

CHAPTER 2- STATE OF THE ART

2.1. Introduction

The collapsible soils are widely distributed in most parts of the world, particularly in arid and semi-arid regions. The collapse phenomenon is well understood as a sudden and significant volume change due to wetting, the additional presence of loading, or a combination of both (Jennings & Knight, 1957). Soil composition, mineralogy, structure, and suction are the factors responsible for the collapse behaviour of unsaturated soils.

The collapse behaviour gives rise to many geotechnical difficulties, including bearing capacity, the potential for unacceptable settlements, and slope stability. These problems are usually analyzed using saturated soil mechanics, and there is a lake of knowledge and applications of the unsaturated soil mechanics, of which collapsing sols are a part. It is necessary to understand the concepts that involve the unsaturated soils and collapse behaviour for this study.

This chapter is organized in the following way: First, a general overview of the unsaturated soil study in soil mechanics is present. Definition of collapse and the mechanics controlling this behavior. Also, it is shown a summary of the analysis and identification of collapsing soil used in this research, the axial translation technique for imposing and measuring suction, and the stress-strain behaviour of unsaturated soils.

Finally, an explanation of the constitutive model for the volumetric behaviour of unsaturated soils proposed by Alonso et al., 1987 Barcelona Basic Model (BBM), is presented. Also, the equations used in the Model is detailed.

2.2. Soil, a multiphase porous medium

“The porous medium of soils is composed of three species: mineral, water, and air. It is distributed in three phases: solid, liquid, and gas. And it is assumed that the mineral species is the solid phase. However, the liquid phase may contain dissolved air, and the gas phase is a mixture of water vapor and dry air” (Gens, 2010).

2.3. Unsaturated state of soils

2.3.1. Overview for saturated/ unsaturated soil mechanics

The importance of differentiating the saturated and unsaturated soils is the compressibility of the pore fluid in soils. The water in saturated soil is incompressible. In contrast, unsaturated soils have air bubbler into the water, and it makes water becomes “compressible” (Croney, 1952).

Gens, 2010 describes the variables to represent unsaturated soils: the liquid degree of saturation S_l, which is the proportion of the pores occupied by the liquid phase, and gas degree of saturation S_g is the proportion of the pores occupied by the gas phase”. Then $S_l = 1 - S_g$. However, it is difficult to measure the degree of saturation and use it to analyze unsaturated soil behaviour (Croney, 1952). Any soil in which pore water pressure is negative can be saturated or contain air bubbles in an occluded form. This behaviour is also presented in some soils with positive water pore pressures as soils with organic material, the gases (methane and carbon dioxide) are under pressure, the air bubbles decreases and the gas dissolves in the water, giving it the appearance of saturated soil.

Figure 2-1 shows an overview of the geotechnical world. A mid-level horizontal line symbolizing the water table is the soil level where the soil water is at atmospheric pressure. The saturated soil is localized below this water table, and usually, the pore water pressures are positive and increase linearly with depth. Also, the effective stress is the difference between total stress and pore pressure (Fredlund, 1999).

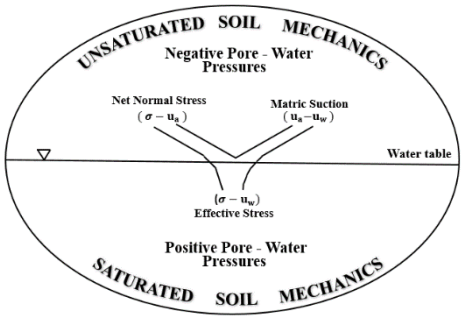

Figure 2-1. Scheme for the soil mechanics (Fredlund, 1999).

The unsaturated soils are above the water table, the pore space is occupied by more than a fluid, and a new component is added, the gas phase, see Figure 2-2. (Gens, 2010). In these, the pore water pressure (measured from atmospheric pressure as zero) is negative and increases to zero with the depth (Croney, 1952).

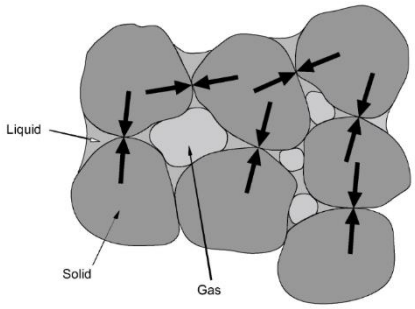

Figure 2-2. Scheme of an unsaturated soil (Gens, 2010).

The liquid phase is held in the soil above the water table because of surface tension and absorptive forces (Fredlund, 1999). For unsaturated soils, the effective stress concept is not enough to explain volumetric behaviour. Fredlund and Morgenstern, 1976 proposed two stress state variables, namely the net normal stress ($\sigma - u_a$) and the matric suction ($u_w - u_a$), which plays an important role in the volumetric behaviour of unsaturated soils.

The net normal stress and the suction changes influence the soil stiffness, triggering changes in the soil structure. The suction increment contributes to stiffening the soil against change in the applied stress. (Alonso et al., 1987). Also, the soil structure stiffness increases with an increase in net normal stress, regardless of the type of soil structure. (Fredlund & Rahardjo, 1993)

The phenomena caused by the change in the net normal stress and suction are swelling and collapse. The swelling phenomenon is typically associated with plastic clay rich in expansive clay minerals that attract and absorb water. When the expansive clays are in contact with water, the clay layers are forced further apart, increasing the soil pore pressure, and then the soil will expand in volume to a point when the pressures are in balances (Holtz & Kovacs, 1981).

In contrast, the collapsible soils are characterized by open structure and with low plasticity. The presence of water causes weakening of the structure, and consequently, a decreased soil volume. It has been demonstrated that more significant swelling and collapse occur at low suction (Alonso et al., 1987). Likewise, in collapsible and swelling soil, the stiffness increases with the increment of suction. The suction concept and collapse phenomenon are detailed in this chapter.

2.3.2. Definition of suction

Gens, 2010 defines suction as "the amount of work that must be done per unit mass of pure water to transport reversibly and isothermally an infinitesimal quantity of water from a reservoir of pure water at a specified elevation and gas pressure to the soil point under consideration". It can be defined as a total potential that controls the flow of water.

The total potential ψ is divided into four components: gravitational potential, ψ_m, gas pressure potential ψ_p; matric potential ψ_m, and osmotic potential ψ_o (Aitchison, 1965).

$$\Psi = \psi_g + \psi_p + \psi_m + \psi_o \qquad \text{Eq. 2-1}$$

However, the components of total potential have different effects on the mechanical behaviour of soil. The gravitational potential and gas pressure potential do not affect its behaviour. Thus, the principal components that affect the mechanical response of soil are the sum of matric and osmotic potential; each one with different magnitude depends on the type of soil. (Aitchison, 1965). The name potential is often replaced by suction if the work is done per unit volume, not per unit mass. The matric suction is the component with more attention by engineers due to this stress variable is strongly influenced by the environmental changes.

The suction is express in terms of pressure in negative values. Matric suction ψ_m is related to the interaction between liquid and solid (Gens, 2010). The osmotic suction π is a function of the amount of dissolved salt in the pore fluid in terms of pressure (Fredlund, 1999). Then, equation (1) can now be written below this concept:

$$\Psi = \psi_m + \pi \qquad \text{Eq. 2-2}$$

The matric suction is the component with more attention by engineers due to this stress variable is strongly influenced by the environmental changes (Fredlund, 1999). The matric suction is commonly related to the surface tension of water. This tension generates intermolecular forces between soil particles that tend to influence the soil skeleton, and this behaviour is associated with the capillary phenomenon. The pores soils with small radio act as capillary tubes called the meniscus that rise above the water table, see Figure 2-3.

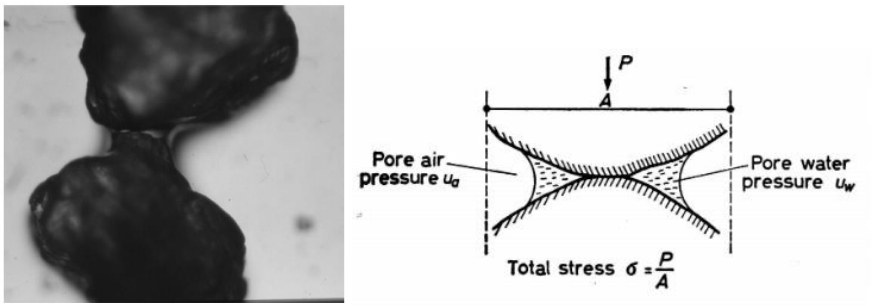

Figure 2-3. Meniscus between two sand particles (Gens, 2010).

The meniscus gives rise to a difference between the pore-air pressure, u_a, and the pore-water pressure u_w. The radius of the meniscus is inversely proportional to this difference, and it is called matric suction, ψ_m=u_a-u_w. (Fredlund & Rahardjo, 1993). In other words, the reduction of the meniscus area often causes an increase in suction.

On the other hand, the role of osmotic suction is related to the salt content in the pore-water, and its change can affect the mechanical behaviour of soil. However, most engineering problems related to the soil stability are primarily associated with matric suction component, and osmotic suction changes are less significant in soil behaviour (Fredlund & Rahardjo, 1993).

The soil suction can be expressed by the water retention curve, that define the relationship between the suction and the water in the pores in the soil. The relationship humidity-suction

is not-lineal and is specific for each soil. The shape of the water retention curve depends on the size and shape of the soil particles and the soil pores, the structure, and the stress history. Figure 2-4 shows a scheme of water retention curves for the soils (Fredlund & Rahardjo, 1993).

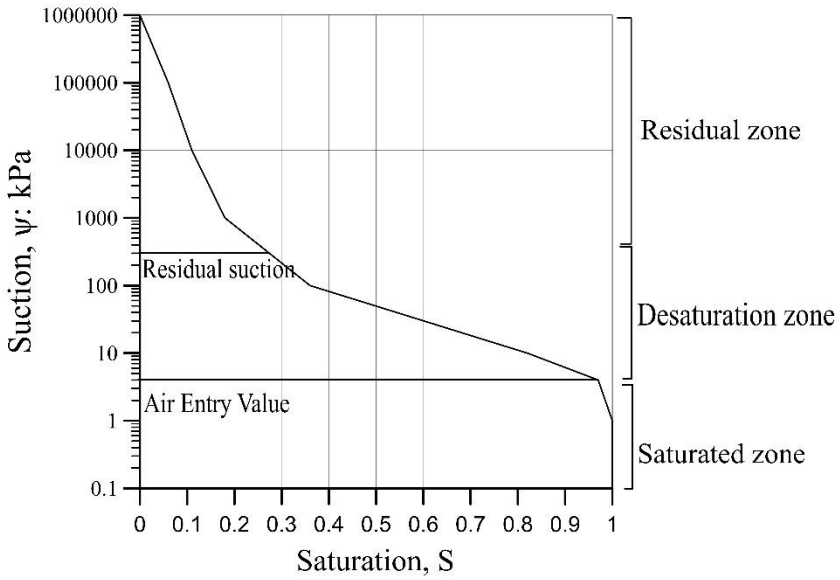

Figure 2-4. Scheme of water retention curve to represent the suction (Toll et al., 2015).

Several equations have been developed to adjust the water retention curve (Brooks & Corey, 1964; Gardner, 1957; van Genuchten, 1980), which include empiric parameters of adjusting relate to air entry value and residual water content. The water entry value represents the suction required for air to enter larger pores and begins the desaturation of the soil. Residual water content is the humidity in which the water in the pores begins to be discontinuous and these are mainly filled with air, observing a decrease in the rate of change of humidity with suction.

2.4. Collapsible soils

2.4.1. Definition

A collapsible soil is defined as an unsaturated soil that undergoes a sudden and significant volume change due to wetting, an additional presence of loading, or a combination of both. It causes a rearrangement of particles and consequently changes in structure (Jennings & Knight, 1957).

The collapse phenomenon takes place when the negative pore-water pressures at depth increase to zero due to an increment in water volume. The wetting of collapsing soil results in a volume decrease. A collapsible soil commonly has a metastable structure, affected by a gradual reduction in matric suction (Fredlund & Rahardjo, 1993).

The collapse phenomenon also can be understood by making a difference with the consolidation phenomenon. The collapse occurs due to the increment in moisture content because of the expulsion of air from the soil, and the consolidation implies water expulsion (Rogers, 1995). The consolidation is progressive soil densification, and the collapse is a sudden volume decreased due to radical particle rearrangement. There is a possibility that the consolidation can be present after the collapse.

2.4.2. Collapse mechanism

The collapse mechanism can be divided into three phases that, however, take place simultaneously (Klukanova & Frankovska, 1995). A graphic explanation of the collapse phases is shown in Figure 2-5.

In Phase 1, Soil particles are in contact with interparticle bondings. The destruction stage of the original microstructure of soil begins. This occurs due to an increase in water content and external pressure. Interparticle forces, clay films, and bridges begin to break, and the aggregates and microaggregates disintegrate.

In Phase 2, The destruction of the microstructure continues, the bonding material is dissolved and transported by water. Due to this, the particles are free to slide, and other fabric elements compress. Finally, the total volume of the soil decreases.

Finally, Phase 3 shows a new microstructure developed after the collapse. The bonding elements were removed or destroyed, and there are no interparticle forces. The soil porosity is reduced, and the soil structure becomes a heterogeneous structure in contrast with the homogenous structure original.

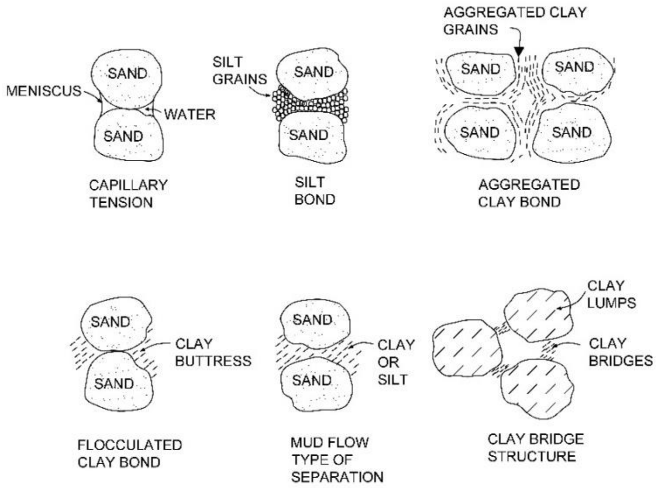

Figure 2-5. Mechanism of collapse (Gens, 2010).

According to studies, A soil potentially collapsible commonly possesses such features as high porosity, an open structure, a low dry density, a high porosity, sensitivity to water, geologically younger or recently altered deposits, and low interparticle bond strength. These features working together, play an important role in the volume loss of soil and rearrangement of structure (Rogers, 1995).

Particle shape also influences the soil structure. An angular particle will facilitate to soil with a loss packing structure maintains a vulnerable and metastable structure until cementation can resist stress involved or an external factor causes collapse. Unlike a soil formed by uniform spherical particles, the grains make up a denser soil (Rogers, 1995).

Collapsible soils must have a factor to avoid the particles make up a denser structure. Particle attraction plays an important role in the collapse behaviour. It can occur by chemical components, physical phenomena, cementation, or negative pore pressure (suction). The particle attraction can be represented in clay bridges, carbonates, gypsum, and capillary tension, and this last is a typical feature in arid soil (Rogers, 1995). Figure 2-6 presents the varieties of bonding agents in collapsible soils.

Figure 2-6. Varieties of bonding agents in collapsing soils (Rogers, 1995).

Although stiffness is considered a general characteristic in rock mechanics, the stiffness and strength can be controlled and increased by bonding agents in soils, not only stress history and porosity (Leroueil & Vaughan†, 1990).

2.4.3. Analysis and identification of collapsing soils

The Collapse phenomenon of soil is usually interpreted and studied into two main categories, micromechanical methods, relate to the analysis of the microstructure of soils, and macromechanical methods, the usual way to identify the collapse by measuring stresses and deformations. Thus, the study of collapsible soils should follow those two directions (Feda, 1995).

In micromechanical interpretation, the collapse involves the soil structure, interparticle force, bonding material, particle shape, pore size distribution, and mineralogy of collapsible soils. These studies have been performed using electronic microscopes and image processing tools (Derbyshire et al., 1995).

In Macromechanical interpretation, the collapse is triggered by the critical load, the most common in saturated soils. Another collapse trigger is to wetting, most common in unsaturated soils (Feda, 1995). Several criteria have been developed to identify whether a soil may exhibit collapsing tendency.

The first intends to quantify the volume change that occurs when a soil undergoes collapse was suggested by Abelev, 1948. Single oedometer tests were performed to measure the decrease in volume at constant load after flooding the soil sample. The collapse of potential Cp is defined as:

$$CP = \Delta\varepsilon = \frac{\Delta e}{1+e_0} \qquad \text{Eq. 2-3}$$

Where e_0 is the natural void ratio of the soil, Δe is the reduction of void ratio due to wetting and $\Delta\varepsilon$ is the vertical strain.

Although the collapse potential is not a design parameter, the results guide the researchers regarding the collapse situation and indicate whether there is a need for further investigations. Interpretation of the severity of collapse is based on the values of collapse potential given by Jennings & Knight, 1957. Table 2-1 shows this classification.

Table 2-1 Collapse Severity Classification (Jennings & Knight, 1957)

Collapse potential (%)	Severity of problem
0-1	No problem
1-5	A Moderate problem
5-10	Problem
10-20	Severe problem
> 20	Very severe problem

Researchers have developed empirical equations base on parameters that govern collapse behaviour are mainly the type of soil, dry density, water content, Atterberg limits, degree of saturation, and suction changes (Basma & Tuncer, 1993). However, none of these criteria directly measure the amount of deformation that could be expected. Besides, Most of these criteria are based on compacted or remolded soil properties, and the influence of natural soil fabric is not considered (Lutenegger & Saber, 1988).

2.4.4. Eolian soils

Eolian soils have been studied around the world because of the problems related with the collapse phenomenon. These soils include loess, dunes and other windblown deposits encountered in different parts of the world, covering about 17 % of the United States, about 17 % of Europe, 15 % of Russia and Siberia, and large areas of China. Loess and Dunes are also encountered in South America and southern Africa (Clemence & Finbarr, 1981).

The main features of the eolian soils are loose open metastructure, bonded by cementing agents, which upon wetting, become weak and may dissolve causing collapse. Related to the mineralogy, these soils are composed primarily of quartz with feldspar and clay minerals. The amount of clay mineral affects the collapse in the soil, with the increment in the clay mineral content decreases the likelihood of collapse (Bell & Bruyn, 1973).

Another feature plays an important role of the collapse of this kind of soils is spaced pores which are associated with spaced arrangement of the eolian deposits. They are also characterized by the size larger that surrounding particles poorly cemented and more likely in point-contact relation. Space pores contribute to favorable spatial conditions for collapse

to occur (Li et al., 2016). When the soil gets wet and bonding breaks, the particles fall into spaced pores and soil collapse.

2.5. Stress-strain behaviour of unsaturated soils

The stress-strain behaviour of the unsaturated soil has been studied considering a two-dimensional stress space: Net stress- suction. Net stress (p) is defined as the excess of total stress over gas pressure. Based on accumulated experiences on unsaturated soil behaviour, several tests with different stress paths in net stress and suction, Alonso et al., 1987, have summarized the following points to define the stress-strain behaviour in unsaturated soils:

1. The suction increased contributes to increment in the soil stiffness. Also, the apparent preconsolidation stress is increased. The suction increment also causes an increase in the yield stress for collapsing soils. These behaviour are demonstrated in experimental tests of Duddley, 1980, Aitchison, and Woodburn, 1969. However, the increase in stiffness is not indefinite, the relationship between stiffness and suction is non-linear, reaching a maximum stiffness value for suction that exceeds a specific value.
2. Applied mean stress controls the amount of swelling experienced by plastic and expansive clays soils when subjected to a decrease in suction. The more significant swelling takes place at low suction values. In expansive soils, cyclical wetting and drying processes cause a plastic expansion in the first wetting, and from it, the behaviour is practically elastic.
3. Soils with an open structure collapse when suction is decreased. The amount of collapse induced by a suction decrease increases with the intensity of stress (Duddley, 1980; Jennings & Knight, 1957). The value of the load or which maximum collapse occurs depends, among other factors, on the type of soil, the initial humidity, and the initial dry density.
4. Most soils with low plasticity silty clays can swell and collapse. With high loads, the soil collapses, but the soil expands at small loads. The net stress value that reverses volumetric behaviour from swelling to collapse is called “critical” stress. It is difficult to determine this value due to this double swelling-collapse character is depending

on the confining stress, density, the suction, and, in addition, the volume change associated with a decrease in suction, for a given applied stress, may change its sign along the suction path (Escario & Saez, 1973).

5. When the confining stress increases, the collapse in unsaturated soil increases to the maximum value, and then the value decreases to a negligible value. The vertical stress in test oedometers at which the maximum value of collapse occurs depends on depending on the type of soil. It is demonstrated in studies of Booth, 1975; Yudhbir, 1982.
6. For a given soil and a given applied load, the suction changes induce irreversible or plastic volumetric strains. The suction changes can produce irreversible strain volumetric. In terms of microstructure, these changes are explained as a change in the soil fabric induced by the increasing suction.

2.6. Technique of controlling suction. Axis translation technique.

Two main techniques of measuring and controlling the matric suction have been developed, the axis-translation technique (Richards, 1941) and the osmotic technique (P. Delage & Cui, 2008). For oedometer tests, the axis-translation technique has been used to control the matric suction for suction under 1.5 MPa in soil samples. Romero, 1999 used this technique to study the thermo-hydromechanical behaviour of compacted boom clay.

In an unsaturated soil, pore-air pressure is atmospheric, and pore water pressure is negative concerning the atmospheric pressure (Vanapalli et al., 2008). The objective of the axis translation technique is to reach a constant air pressure u_a to simulate an artificial increase in the atmospheric pressure in which the soil is immersed. This increase generates a negative pore water pressure, which is increased by an equal amount to a positive water pressure u_w to reach the matric suction required $u_a - u_w$ (Romero, 1999). The air pressure and water pressure were maintained a different value to generate the matric suction.

The axis translation technique allows us to measure and control the pore pressure in unsaturated soil. Figure 2-7 shows a scheme of the axis translation technique and its components. A High Air Entry Value (HAEV) ceramic disc is used as an interface permeable

to water but not to air. This interface maintains the pressure difference between extracted water and water in the soil (Richards, 1941). Also, HAEV ceramic disc separates air and water phases. The high air entry value is the maximum air value to which the disc can be subjected before free air passes through the disc (Vanapalli et al., 2008). For the Rowe and Barden oedometer, the air entry value of the HAEV ceramic disc is 500 kPa.

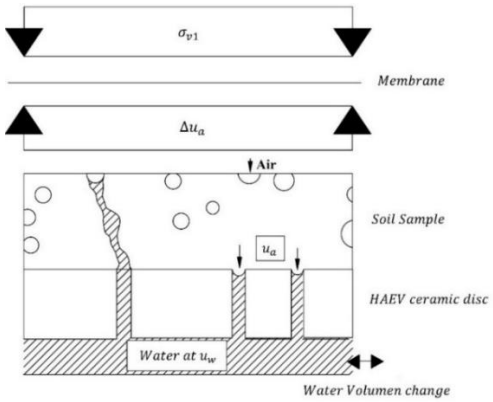

Figure 2-7. Axis translation (adapted of HILF, 1956; Richards, 1941).

The soil specimen is placed on the top of the HAEV ceramic disc, which is previously saturated. More details related to the saturation of HAEV ceramic disc is detailed in chapter 4. Figure 2-7 shows the tendency of the water to go into the soil. However, this is resisted by increasing the water pressure in the chamber until an equilibrium condition is reached (Vanapalli et al., 2008).

Net vertical stress also called overburden pressure is applied upper the sample and is the result of the equilibrium of vertical pressure (σ_{v1}) and applied air pressure u_a in the sample, $\sigma_{v1} - u_a$, these pressures are separated by a membrane.

2.7. Constitutive model for the behaviour of unsaturated soils

Typical constitutive models used in saturated soils usually are based on the relationship between stress and volume change. However, this relationship is generally limited when trying to model the general behaviour of unsaturated soils. This is due to considers partial aspects of behaviour without establishing consistent links between different features of behaviour.

In this context, Alonso et al., 1987, to explain the volumetric behaviour of unsaturated soil, have developed The Barcelona Basic Model (BBM), one of the most widely used elastoplastic models for unsaturated soils. This model expresses qualitatively the full behaviour of unsaturated soils and especially the volumetric collapse behaviour upon wetting. The BBM is used to model soils where the collapse potential increase with increasing stress. Alonso et al., 1990 also presented a mathematical formulation of an elastoplastic model validating the theoretical concept with experimental data.

One of the objectives of the model was to construct a complete and consistent framework capable of providing qualitative prediction by simple manipulation of the components of the model. The relevant stress state variables in the BBM are the net normal stress (σ-u_a), and matric suction (s), and the elastic changes are related to these (Gens, 2010).

The Barcelona basic model (BBM) is depicted schematically in Figure 2-8 (a), when the idealized results of consolidation tests under constant suction are shown. The yield point increases for suctions greater than 0 or saturated conditions. Suction allows the soil to keep the applied stress before the yield, the higher the suction, the higher is the yield. This yield point can be represented in the isotropic space of mean net stress-suction in Figure 2-8 (b). The points connected form the Loading Collapse (LC) curve. The Loading collapse curve represents the limit where the soil goes from elastic volumetric strains called elastic domain to irreversible plastic volumetric strains.

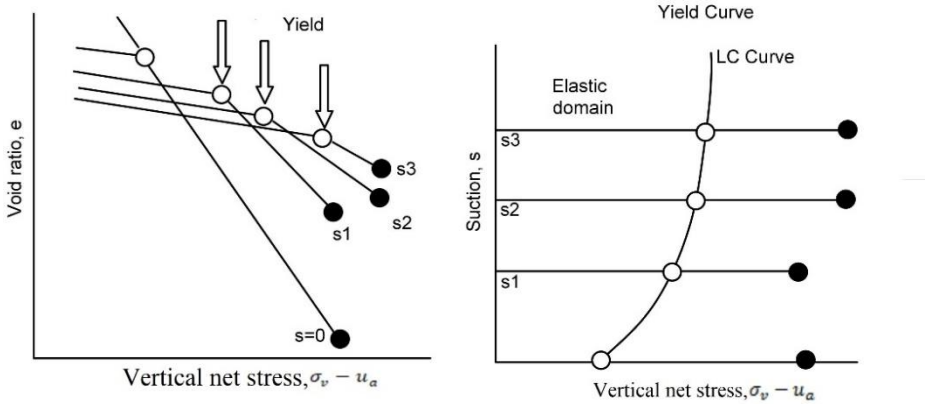

Figure 2-8. (a) Idealized scheme of consolidation lines at different suction values. (b) Definition of LC (Loading-collapse) yield curve (Alonso et al., 1990).

The loading collapse curve can predict irreversible plastic volumetric strain for any stress path which implied an increment in the stress (path L) or decrement in suction (Path C) or both, see Figure 2-9. The LC curve movement is related to the evolution of the soil structure. The loading and collapse at a structural level produce the same effect in the LC curve.

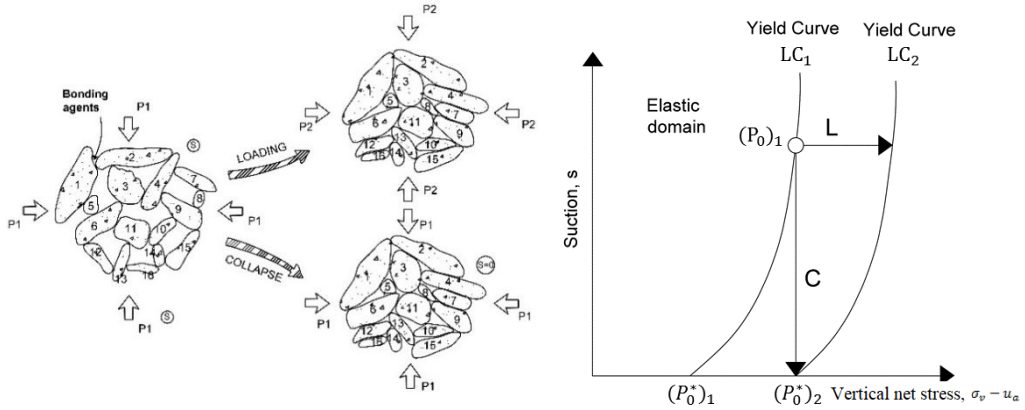

Figure 2-9. Displacement of the LC yield curve on loading at constant suction (path L) and wetting at constant applied stress (path C) (Gens, 2010).

The movement of the LC curve can be expressed as shown in Figure 2-9, the LC curve will move from position LC_1 to LC_2. The first path is related to increased loading L while the suction is maintained constant. The second path is wetting the soil (where the suction is reduced) under constant stress. The movement of LC yield curve is the same for both, and the same irreversible plastic volumetric strains will ensue. Therefore, the LC curve links together the compressive strains due to loading with the collapse strains due to wetting. (Gens, 2010).

2.7.1. Mathematical model

An appropriate stress space to describe the behaviour for unsaturated soils in an isotropic state is space (s,p), where p = $\frac{\sigma_1+2\sigma_3}{3} - u_a = \sigma_m - u_a$ (net mean stress), σ_m is the excess mean pressure over air pressure.

Parallel to the behaviour of saturated soils subjected to stress increment for a determined constant suction, the change in specific volume is given by:

$$v = N(s) - \lambda(s) ln \frac{p}{p^c} \qquad \text{Eq. 2-4}$$

p^c is a reference stress state for which $v = N(s)$ and $\lambda(s)$ are dependent on suction. Then, when suction increase the soil stiffness increase in the stress ranges used. On unloading and reloading curves with constant suction, the soil behaviour (consider elastic) was proposed based on the relationship:

$$dv = -\kappa \frac{dp}{p} \qquad \text{Eq. 2-5}$$

The slope κ of the unloading was considered as constant value and independent of the suction to ensure that the model was conservative.

Figure 2-10 shows the response of two samples of the same soil subjected to different suction (s=0 and s=constant), in isotropic stress paths in which p varies. For saturated soil, the preconsolidation pressure is p_0^* and for unsaturated soil the preconsolidation pressures is p_0.

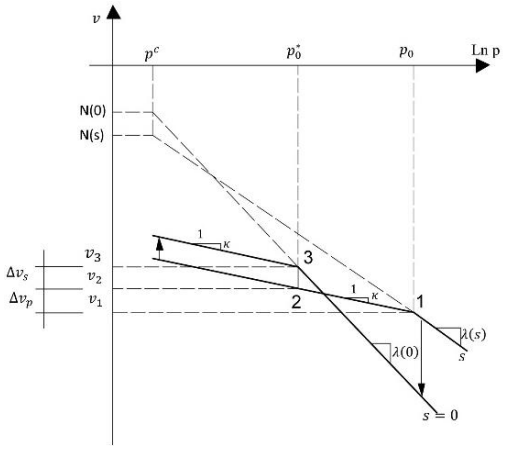

Figure 2-10. Compression curves for saturated and unsaturated soil (Alonso et al., 1990).

The generic relationship between p_0^* and $p_0$in the space (s,p) was obtained by relating the specific volume (v) at points 1 and 3, in a 1:2:3 paths such that:

$$v_1 + \Delta v_p + \Delta v_s = v_3 \qquad \text{Eq. 2-6}$$

The recoverable swelling that occurs in the 2:3 stretch was defined from the expression:

$$dv = -\kappa_s \frac{ds}{(s+p_{atm})} \qquad \text{Eq. 2-7}$$

κ_s is the slope of the line that relates v_s and ln(s+p_{atm}) in unloading line and reloading. Atmospheric pressure (p_{atm}) was incorporated to prevent that very low values of the suction dv or v tend to infinity.

From equations (4) (5) (7) is obtain:

$$N(s) - \lambda(s) ln \frac{p_0}{p^c} + \kappa \, ln \frac{p_0}{p_0^*} + \kappa_s \, ln \frac{s+p_{atm}}{p_{atm}} = N(0) - \lambda(0) ln \frac{p_0^*}{p^c} \quad \text{Eq. 2-8}$$

A convenient choice of p^c and N(s) in order to simplify the before equation is to assume:

$$\Delta v(p^c)_0^s = N(0) - N(s) = \kappa_s ln \frac{s+p_{atm}}{p_{atm}} \quad \text{Eq. 2-9}$$

Where $p^c$is the mean stress at which one may reach the saturated virgin state from an unsaturated condition, through wetting paths. If the equation (2-8) and (2-9) are joined the following relationship is obtained:

$$\frac{p_0}{p^c} = \frac{p_0^{*\frac{[\lambda(0)-\kappa]}{[\lambda(s)-\kappa]}}}{p^c} \quad \text{Eq. 2-10}$$

This equation defines the set of yield p_0 values for each associated suction in the space (s,p) in LC yield curve and the position is determined by the preconsolidation stress (p_0^*), which is a stiffness parameter of the model. Note that when $p_0^* = p^c$, the LC yield curve becomes a straight line $p_0 = p^c$. To consider possible changes in soil stiffness with increased suction is adopted the following expression:

$$\lambda(s) = \lambda(0)[(1-r)\exp(-\beta s) + r] \quad \text{Eq. 2-11}$$

r is a constant related to maximum soil stiffness for infinite suction, and β is a parameter that controls the rate of increase of soil stiffness with suction.

It was adopted a suction value s_0(p) considered the highest value of soil have been suggested in all the history for each spherical stress, so when the suction reaches this value, occur apparent deformations. s_0(p) is a new LC yield curve of the soil, consider constant in the first

approximation. It is also proposed a logarithm relationship between the specific volume v and the suction s in the unloading and reloading. The specific volume change dv is expressed as:

$$dv = -\lambda_s \frac{ds}{(s+p_{atm})} \quad \text{Eq. 2-12}$$

Hardening law

The evolution of the yield surface is controlled by hardening parameters ${p_0}^*$ and s_0 Hardening law is the change in the position of the surface, and it is considered dependent on the increment of plastic deformation ${d\varepsilon_v}^p$ of the microstructure and is express as follows:

$$\frac{d{p_0}^*}{{p_0}^*} = \frac{(1+e)}{\lambda(0)-\kappa} {d\varepsilon_v}^p \quad \text{Eq. 2-13}$$

2.8. Previous studies

Collapsible soils are found in several countries around the world, mainly in arid and semi-arid regions, and cover a wide variety of geological materials. Among the cases documented in the literature, include eolian, alluvial, residual, colluvial soils, volcanic flows, and mudflows.

Larges areas of the earth´s surface as the western United States, parts of Asia, and southern Africa, Francia, are covered with a type of eolian soils called Loess. Loess is a material consisting of well-selected particles of silt fraction, connected by clay films. It has a high load capacity without suffering major deformations, however, when flooded, it is susceptible to large decreases in volume. (Pier Delage et al., 2005; Howayek et al., 2011; Lutenegger & Saber, 1988; Nouaouria et al., 2008; Yates et al., 2018)

Some researchers as Gaaver, 2012, Olyansky, Kuzmenko, & Shchekochikhina, 2016 have studied the collapsibility phenomenon in eolian soils. These studies focus on the effect of wetting on geotechnical properties of eolian soils and predict wetting-induced collapse behaviour.

Suction is another factor that plays an important role in the collapse behaviour and has been studied by researchers as Muñoz-Casteblanco, Pereira, Delage, & Cui, 2012, Xie, Li, Vanapalli, & Wang, 2018. The researchers demonstrate the influence of the suction in the collapse behaviour of eolian soils due to sensitivity to change in moisture content.

On the other hand, researchers study the soil structure of a type of eolian soils, (Muñoz-Casteblanco et al., 2012;Assadi-Langroudi, Ng'ambi, & Smalley, 2018; Leroueil & Vaughan, 1990). The researchers show the influence of the form and the particle distribution of the soil in the collapse behaviour when is subjected to changes in the natural water content.

In Colombia, collapsible soils have been identified. Currently, several cases of occurrence, covering particularly a large area of central regions in Colombia. The collapsible soil studied consists of alluvial deposits, colluvial deposits in Florida Blanca, Santander (Quijano Arias & Tenjo Ramos, 2018), residual deposits in Barbosa, Antioquia (Orozco et al., 2010) y volcanic flows in Pereira (Molina & Alzate, 2018). However, there are no previous formal studies about the collapse behaviour in the eolian soils in Colombia.

2.9. Chapter conclusions

The collapse phenomenon has been studied into unsaturated soil mechanics. A soil potentially collapsible commonly possesses such features as high porosity, an open structure, a high porosity, sensitivity to water, geologically younger or recently altered deposits, and low interparticle bond strength.

The concept of collapse and the mechanism have been presented. The collapse phenomenon can be analyzed using micromechanical methods, relate to the analysis of the microstructure of soils, and macromechanical methods, the usual way to identify the collapse by measuring stresses and deformations in soils. A general explanation of the methods used in this research to measure the collapse has been present.

The suction plays a fundamental role in unsaturated soils. The increment of suction contributes to stiffening the soil. The general concept and suction components have been presented. The concept used to apply the matric suction in soil used in this research have been also presented.

The collapsible soils present the stress-strain behaviour typical of unsaturated soils, and it is summarized in the following statements: The suction increased contributes to increment in the soil stiffness, soils with an open structure collapse with decreased of suction, When the confining stress increases the collapse increases to the maximum value and the value decreases to a negligible value.

The general explanation of the Barcelona Basic Model (BBM) and the equations applied have been presented. The model expresses qualitatively the full behaviour of unsaturated soils and especially the volumetric collapse behaviour upon wetting. With this model was constructed a complete and consistent framework capable of providing qualitative prediction by simple manipulation of the components of the model.

Several researchers have studied and analyses the deformational behaviour of collapsible soils. These studies are focus on the influence of the suction in the soil, the structure, particle distribution, change in the saturation and stress, in the Collapse behaviour of soils. In Colombia, collapse phenomenon has been found and analyzed in residual soil, alluvial and colluvial deposits and volcanic flows. However, there is no formal studied about the collapse behaviour in the eolian soil in Colombia.

2.10. References

Abelev, Y. M. (1948). The essentials of Designing and Building on Microporous Soils. *Stroital Naya Promyshlemast*, *10*, 127–130.

Aitchison, G. D. (1965). Soil properties, shear strength and consolidation. *6th Int Cong. Soil Mechanics Found.*, 318–321.

Aitchison, G. D., & Woodburn, J. A. (1969). Soil suction in foundation design. *7th ICSMFE*.

Alonso, E. E., Gens, A., & D., W. (1987). Groundwater Effects in Geotechnical Engineering. *The Ninth European Conference on Soil Mechanics and Foundation Engineering*, *3*.

Alonso, E. E., Gens, A., & Josa, A. (1990). A constitutive model for partially saturated soils G ”. *Géotechnique*, *40*(3), 405–430.

Assadi-Langroudi, A., Ng’ambi, S., & Smalley, I. (2018). Loess as a collapsible soil: Some basic particle packing aspects. *Quaternary International*, *469*, 20–29.

Basma, A. A., & Tuncer, E. R. (1993). Evaluation and control of collapaible soils. *Journal of Geotechnical Engineering*, *118*(10), 1491–1504.

Bell, F., & Bruyn, I. (1973). Sensitive, expansive, dispersive and collapsive soils. *Bull Int Assoc Eng Geol*.

Booth, A. R. (1975). The factors influencing collapse settlement in compacted soils. *6th. Reg. Conf. for Africa on SMFE*, 57–63.

Brooks, R. H., & Corey, A. T. (1964). *Hydraulic properties of porous media*. Colorado state university.

Clemence, S., & Finbarr, A. (1981). Considerations for collapsible soils. *Geotechnical Engineering Division*.

Croney, D. (1952). The movement and distribution of water in soils. *Geotechnique*, *3*(1), 1–16.

Delage, P., & Cui, Y. J. (2008). An evaluation of the Osmotic Method of Controlling Suction. *Geomechanics and Geoengineering*, *3*(1), 1–11.

Delage, Pier, Cui, Y. J., & Pereira, J. M. (2005). Geotechnical problems related with loess deposits in Northern France. *Proceedings of International Conference on Problematic Soils*, *May*, 517–540.

Derbyshire, E., Dijkstra, T., & Lan, S. (1995). Genesis and Properties of Collapsible Soils. *Proceedings of the NATO Advanced Research*.

Duddley, J. H. (1980). Review of collapsing soils. *ASCE*, 925–947.

Escario, V., & Saez, J. (1973). Measurement of the properties of swelling and collapsing soils under controlled suction. *3rd Int. Conf. Expansive Soils*, 195–200.

Feda, J. (1995). Mechanisms of Collapse of Soil Structure. *Genesis and Properties of Collapsible Soils*, 149–172.

Fredlund, D. G. (1999). The emergence of unsaturated soils mechanics. Fredlund volume. In A. W. Clifton, G. W. Wilson, & S. L. Barbour (Eds.), *NRC Research Press*.

Fredlund, D. G., & Morgenstern, N. R. (1976). Constitutive Relations for Volume Change in Unsaturated Soils. *Canadian Geotechnical Journal*, *13*(3), 261–276.

Fredlund, D. G., & Rahardjo, H. (1993). Soil Mechanics for Unsaturated Soils. *John Wiley & Sons, Inc.*, *30*(2), 113–123.

Gaaver, K. E. (2012). Geotechnical properties of Egyptian collapsible soils. *Alexandria Engineering Journal*, *51*(3), 205–210.

Gardner, W. R. (1957). Some steady-state solutions of the unsaturated moisture flow eqaution with application to evaporation from a water table. *Soil Science*.

Gens, A. (2010). Soil Environment Interactions in Geotechnical Engineering. *Geotechnique*, *60*(1), 3–74.

HILF, J. W. (1956). *An investigation of pore-water pressure in compacted cohesive soils.* United States Bureau of Reclamation.

Holtz, R., & Kovacs, W. (1981). *An Introduction to Geotehcnical Engineering*. Prentice Hall.

Howayek, A. El, Huang, P., Bisnett, R., & Santagata, M. C. (2011). *Identification and Behavior of Collapsible Soils*.

Jennings, J., & Knight, K. (1957). The Additional Settlement of Foundations due to a Collapse of Structure of Sandy Subsoils on Wetting. *Proceedings, 4th International Conference on Soil Mechanics and Foundation Engineering, London*, *1*, 316–319.

Klukanova, A., & Frankovska, J. (1995). The Slovak Carpathians Loess Sediments, their Fabric and Properties. *Genesis and Porperties of Collpasible Soils*, 129–147.

Leroueil, S., & Vaughan†, P. R. (1990). The general and congruent effects of structure in

natural soils and weak rocks. *Geotechnique*, *40*(3), 467–488.

Leroueil, S., & Vaughan, P. R. (1990). The general and congruent effects of structure in natural soils and weak rocks. *Géotechnique*, *40*(3), 467–488.

Li, P., Vanapalli, S., & Li, T. (2016). Review of collapse triggering mechanism of collapsible soils due to wetting. *Journal of Rock Mechanics and Geotechnical Engineering*, *8*(2), 256–274. https://doi.org/https://doi.org/10.1016/j.jrmge.2015.12.002

Lutenegger, A. J., & Saber, R. T. (1988). Determination of Collapse Potential of Soils. *Geotechnical Testing Journal*, *11*(3), 173–178.

Molina, G., & Alzate, A. (2018). *Potencial de Colapso de Suelos Derivados de Cenizas Volcánicas de la Zona de Expansión Urbana de Pereira*. Universidad Libre Seccional Pereira.

Muñoz-Casteblanco, J. A., Pereira, J. M., Delage, P., & Cui, Y. J. (2012). The water retention properties of a natural unsaturated loess from northern France. *Géotechnique*, *62*(2), 95–106.

Nouaouria, M. S., Guenfoud, M., & Lafifi, B. (2008). Engineering properties of loess in Algeria. *Engineering Geology*, *99*(1–2), 85–90.

Olyansky, Y. I., Kuzmenko, I. Y., & Shchekochikhina, E. V. (2016). Features of Construction Buildings on the Loessial Soil of Central Moldova. *Procedia Engineering*, *150*, 2208–2212.

Orozco, J. M., Ramos, J., & Valencia, Y. (2010). Evaluación de la colapsabilidad de los suelos en la doble calzada Hatillo-Barbosa. *XIII Congreso Colombiano de Geotecnia - VII Seminario Colombiano de Geotecnia*, *1*(March 2014), 101–107.

Quijano Arias, D. A., & Tenjo Ramos, E. A. (2018). *Análisis de efectividad en la estabilización de suelos colapsables en el tramo II de la transversal el bosque en el municipio de floridablanca, santander*. 88.

Richards, L. A. (1941). A Pressure-Membrane Extraction Apparatus for Soil Solution. *Soil Science*, *51*(5), 377–386.

Rogers, C. D. F. (1995). *Types and Distribution of Collapsible Soils*. 1–17.

Romero, E. (1999). *Characterisation and thermo-hydromechanical behaviour of unsaturated boom clay: an experimental study*. Univesitad Politecnica de Cataluna.

Toll, D. G., Asquith, J. D., Fraser, A., Hassan, A. A., Liu, G., Lourenço, S. D. N., Mendes, J., Noguchi, T., Osinski, P., & Stirling, R. (2015). Tensiometer techniques for determining soil water retention curves. *Unsaturated Soil Mechanics from Theory to Practice - Proceedings of the 6th Asia-Pacific Conference on Unsaturated Soils*, *October*, 15–22.

van Genuchten, M. T. (1980). A Closed-form Equation for Predicting the Hydraulic Conductivity of Unsaturated Soils. *Soil Science Society of America Journal*, *44*(5), 892–898.

Vanapalli, S., Nicotera, M. V., & Sharma, R. (2008). Axis translation and Negative Water Column Techniques for Suction Control. *Geotechnical and Geological Engineering*, *26*(6), 645–660.

Xie, W. L., Li, P., Vanapalli, S. K., & Wang, J. D. (2018). Prediction of the wetting-induced collapse behaviour using the soil-water characteristic. *Journal of Asian Earth Sciences*, *151*(October 2017), 259–268.

Yates, K., Fenton, C. H., & Bell, D. H. (2018). A review of the geotechnical characteristics of loess and loess-derived soils from Canterbury, South Island, New Zealand. *Engineering Geology*, *236*(July 2017), 11–21.

Yudhbir, Y. (1982). Collapsing behavior of collapsing soils. *7th Southeast Asia Geotechnical Conference*, 915–930.

CHAPTER 3 – EOLIAN SOILS OF MAYAPO

3.1. Introduction

To carry out a better comprehension of the volumetric behaviour of the eolian soils, the processes that originated the soil must be considered in the first instance, due to the environmental factors are determining in the formation and evolution of the soil and as a consequence in the properties and the volumetric behaviour.

This research intends to characterize the volumetric deformation of eolian soils. This characterization is carried out in the eolian soil of Mayapo, a town located in the north of Colombia. The choice of sampling site was made considering the materials that could be potentially collapsible.

The soil of this research has been originated by physical alteration of igneous rocks. The process the soil formation includes the weathering of the parental rock, transport by wind and deposition. These processes influence the mineral composition, soil structure, the shape and size particle, and the porosity. Its influence is controlled by weather conditions and time.

In this chapter, the information of the eolian soil from Mayapo is presented, begins with a description of the localization of the site, the climate, the geology description, and geomorphology of the eolian soils. The information presented in this chapter is obtained through field studies and bibliographic research presented by Lockwood, 1984; Alcaldía de Riohacha, 2001; IDEAM, 2005; Ingeominas, 2009,.

3.2. Localization of the site

The research area involves eolian soils of the north of Colombia, particularly, is placed in the small town called Mayapo in the Department of La Guajira. Figure 3-1 shows the extension of the eolian deposits in Mayapo. The area studied is next to the Caribbean Sea. The choice of site was made considering the materials that could presents geotechnical problems.

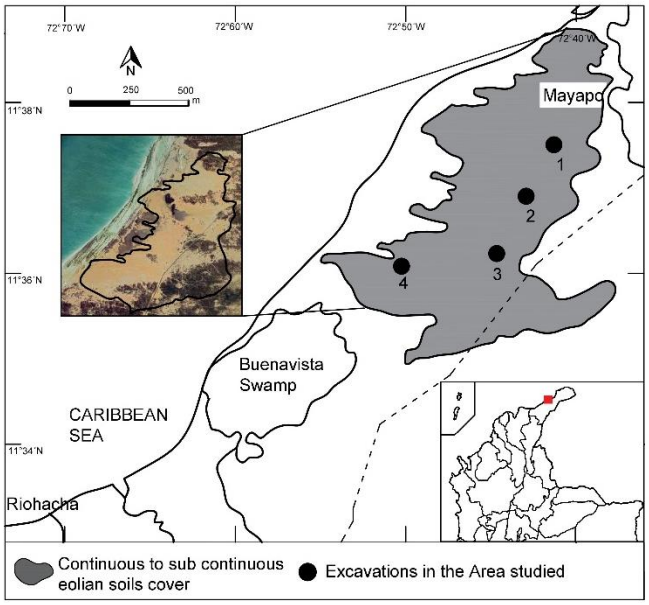

Figure 3-1. Localization and extension of eolian deposits in Mayapo, Colombia.

Figure 3-1 also shows the localization of the excavations to study the properties and collapse behaviour of these eolian soils in the region. The sampling sites are specifically located in the coordinates shown in Table 3-1.

Table 3-1. Site coordinates of the excavations in the area studied

Dune	Latitude	Longitude	m.s.n.m
1	11°36'45.84"N	72°49'54.08"O	1
2	11°36'30.30"N	72°50'3.16"O	3
3	11°36'19.08"N	72°50'11.80"O	1
4	11°36'28.03"N	72°50'35.14"O	1

The area is characterized by large extensions of eolian soils and dunes, see Figure 3-2. These deposits have approximately 4 meters high. The area of study has an approximate elevation of 1 meter above sea level. This area is distinguished in the region for its tourist attraction due to the coastal location and the desert landscapes.

Figure 3-2. Eolian soils in Mayapo, Colombia.

3.3. Climate

La Guajira is the region with the least precipitation in Colombia, and the climate is arid with temperatures ranges from 27° to 34° and maximum up to 45°. The average precipitation of 0 to 250 mm for the first three trimesters. However, La Guajira lost its marked drought during September, October, and November reaching ranges of 250 to 750 mm during this trimester (Arango et al., 2014) .

The region has quite marked seasons. A rainy season is manifested for three months. Precipitation is concentrated in September to November. In this season, precipitation exceeds evaporation, and it causes flooding in some regions. Figure 3-3 shows a flooding present in the area of eolian soils it the rainy season. These events could trigger collapse phenomena in the region and in the soils studied (IDEAM, 2005).

Figure 3-3. Flooding in the eolian soils area during the wet season.

Subsequently, a season of drought and night cold, from January to April, with wind blow with strong intensity prevailing from the northeast. Following this period, a long dry period continues, from May to September, characterized by a continuous wind that comes from the northeast with increasing force and very hot. These marked seasons influenced the geology and geomorphology of La Guajira Department, and the area studied.

3.4. Geology

The geology in the area is recent, formed in the quaternary period. Figure 3-4 shows the formations of the site, Recent Alluvial Deposits (Qale), Sand Dune Deposits (Qe), Evaporitic Deposits and Recent Lagoons (Qes), Recent Alluvial Deposits (Qal), which share some sediments due to receive contributions from eolian currents and fluvial systems present in the area.

The Sand Dune deposits (Qe), where the area of interest is located, were deposited during one or more periods in the Pleistocene when the sea level was lower than the current one, this generated an extended plain to the east and northeast of the peninsula, which would have been the source for the large volumes of sand deposited in the area Lockwood, 1984.

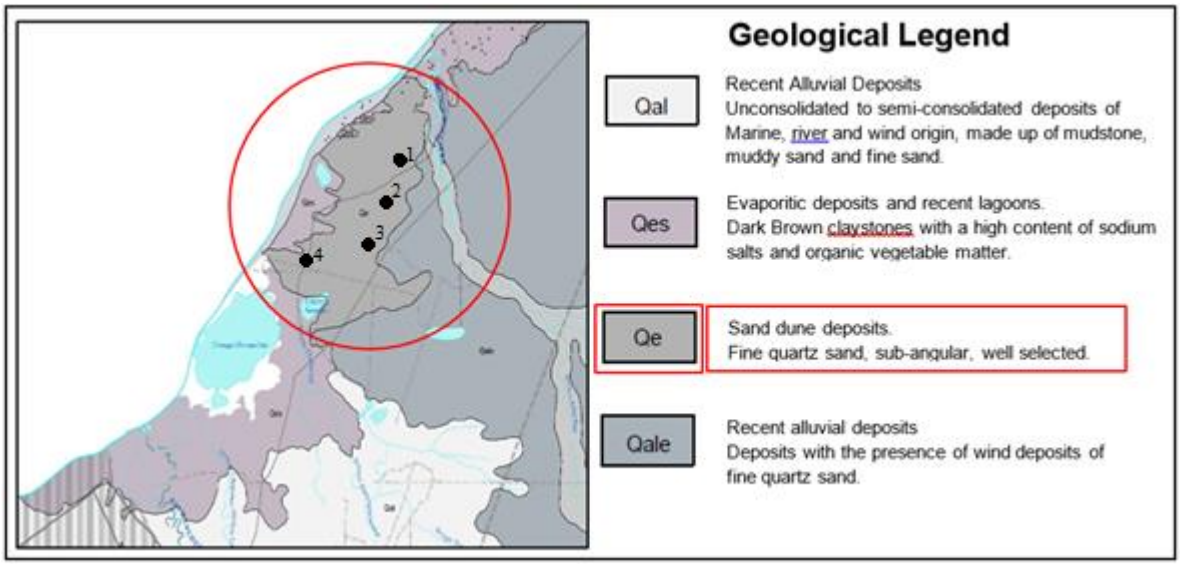

Figure 3-4. Geological map of site of eolian soils (Adapted from Ingeominas, 2009).

Sand Dunes deposits Formation (Qe) is predominantly composed of quartz of medium size and rounded well selected, potassium feldspar, red lithic grains with medium size and rounded. There is no trace of calcareous material in the dunes. This indicates that the dunes are derived primarily from silicate rocks localized distant from the marine platforms. The dunes are deposited above recent alluvial deposits.

Ingeominas, 2009 recognized the main two types of these sediments: Active dunes and stabilized dunes. Active dunes are formed from eolian deposition and are around three meters high and are generally loose deposits with little vegetation, and particles are transported on a seasonal to daily basis. In contrast, stabilized dunes have a stabilizing vegetation cover allowed by a positive moisture balance. Inactive dunes usually present little or no movement, these dunes reach heights of approximately five meters.

Transported soil type determines its corresponding engineering problem. The eolian soils are transported by wind, and usually, the grains are sand size. The problems to anticipate are collapsible grain structure and compressibility (Yaw, 2015).

3.5. Geomorphology

The geomorphology depends on geological material and the predominant geomorphologic processes. In the area, eolian and fluvial processes govern the shapes of the surface of the geological formations, and it helps to understand their genesis and their current behaviour.

Sand Dunes Formation (Qe) has deposits in which the thicknesses vary geographically, from 1 to 3 meters high. Based on Davies, 1980 classification, these deposits are Impeded Primary, in which vegetation plays a major role, impeding the downwind transport and the development of the dune (Figure 3-2). These kinds of dunes are significantly influenced by wave action, generating erosional forces. Based on the shape and orientation of dunes, the predominant wind direction is East-West.

Figure 3-5 shows some sedimentation structures present in the eolian soils. Gullied are created by running water eroding sharply into soil, see (a). The soil is more prone to gully erosion where there is less vegetation, the dunes have been reworked by the water currents that drain the area. Also, there is a Flaser bedding observed in the block samples. These are presents by isolate thin layers of mud amongst the cross-laminate of the sand, see (b and c).

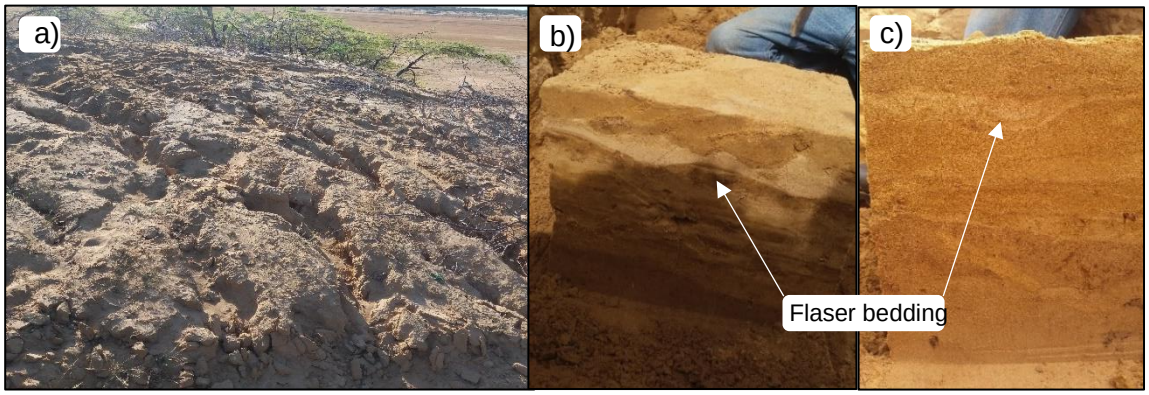

Figure 3-5.a) Gullied in eolian deposit formation. b & c) Flaser bedding.

The shapes caused by the geomorphological processes and sedimentation that, together with the geology and soil loose structure, demonstrate the strong material heterogeneity and the poor mechanical properties of the material.

3.6. Chapter conclusions

The information of the Eolian soil of Mayapo presented includes the climate, geology geomorphology, and it is determining to know the evolution the soil and have a better comprehension of the volumetric behaviour of the eolian soils.

The climate in this region is arid with high temperatures from 27° to 34° and maximum up to 45°. The average precipitation of 250 mm for the first three trimesters, reaching the higher value of precipitation of 700 mm in September to December. In this season, precipitation exceeds evaporation, and it causes flooding in some regions.

The eolian soils are predominantly composed by quartz of medium size and rounded well selected, potassium feldspar, red lithic grains with medium size and rounded. There is no trace of calcareous material in the dunes. This indicates that the dunes are derived primarily from silicate rocks localized distant from the marine platforms.

According to the geomorphologic analysis, dunes are classified as active dunes and stabilized dunes. Active dunes are generally loose deposits with little vegetation, and particles are transported on a seasonal to daily basis. In contrast, stabilized dunes have a stabilizing vegetation cover allowed by a positive moisture balance. Inactive dunes usually present little or no movement. The problems to anticipate consider these kinds of soils are collapsible grain structure and compressibility.

The geoforms presented in the eolian soils includes gullied, formed due to soil reworked by the water currents that drain the area, and Flaser bedding, composed by mud amongst the cross-laminate of the sand. The shapes caused by the geomorphological processes and sedimentation that, together with the geology and soil loose structure, demonstrate the strong material heterogeneity and the poor mechanical properties of the material.

3.7. References

Alcaldía de Riohacha. (2001). Plan De Ordenamiento Territorial Del Municipio De Riohacha, Guajira. *Alcaldia Municipal de Riohacha*.

Arango, C., Dorado, J., Guzmán, D., & Ruiz, J. . (2014). Climatología trimestral de Colombia. *Ideam*, 19.

Davies, J. L. (1980). *Geographical variation in coastal development*.

IDEAM. (2005). *Atlas climatológico de Colombia*.

Ingeominas. (2009a). *Geología de las Planchas 7-8 Ranchería y Riohacha*.

Ingeominas, A. M. (2009b). *Cartogafría Geológica de las Planchas 7-Rancheria 8-Riohacha, 9-Uribia- Dibulla, 14- 4- Albania y 15-15 bis Maicao*.

Lockwood, J. P. (1984). *Geology of the serranía de Jarara Area. Guajira Peninsula, Colombia.* Princeton University.

Yaw, A. S. (2015). *Alternate Methods To Determine the Microstructure of potentailly collapsible soils*.

CHAPTER 4- EXPERIMENTAL PROGRAM

4.1 Introduction

This research is mainly focused on the characterization of volumetric behaviour of eolian soils from an experimental point of view. In order to study and understand this soil behaviour, the designed experimental program is presented in this chapter.

The experimental program includes tests to characterize the volumetric behaviour, analyzing the soil properties as mineralogy and its distribution, the soil structure, bonding, the suction behaviour, and the volumetric behaviour under different stress and suction paths. In this way, the objective and standards used for each test are described.

In this chapter, the methods of eolian soils sampling and preparing the samples are present, as well as the equipment and procedures adopted during the realization of the experimental program. This program includes the soil classification tests, the microstructure tests with X-ray diffraction, the optical microscopic, and Scanning Electronic Microscopic, also the suction measurement tests to determine the water retention curve by the paper filter method and electrical conductivity method to determine the osmotic suction. Finally, oedometer tests were carried out to know the volumetric behaviour of the eolian soils. For that, the equipment, and procedures of simple oedometer test, double oedometer tests, and oedometer with suction-controlled tests are described.

It is worth noting that, the tests of geotechnical classification, microstructure, suction measurement and classical oedometers were carried out in Universidad Nacional de Colombia, in Medellín. The soil classification with laser method and blue the methylene, and the oedometer tests with suction-controlled was carried out in the geotechnical laboratory of CEREMA in Toulouse, France.

4.2 General scheme of the experimental program

The experimental program was design to reach each objective raised in this research. Figure 4-1 summarized the experimental program of this research. The microstructure tests are carried out to know the minerals, the soil structure and elemental distribution, suction measurement test in order to know the principal component of suction, total, matric and osmotic suction, and the end the oedometer test to know the volumetric behaviour of eolian soil. The target is to characterize the volumetric behaviour of the eolian soils.

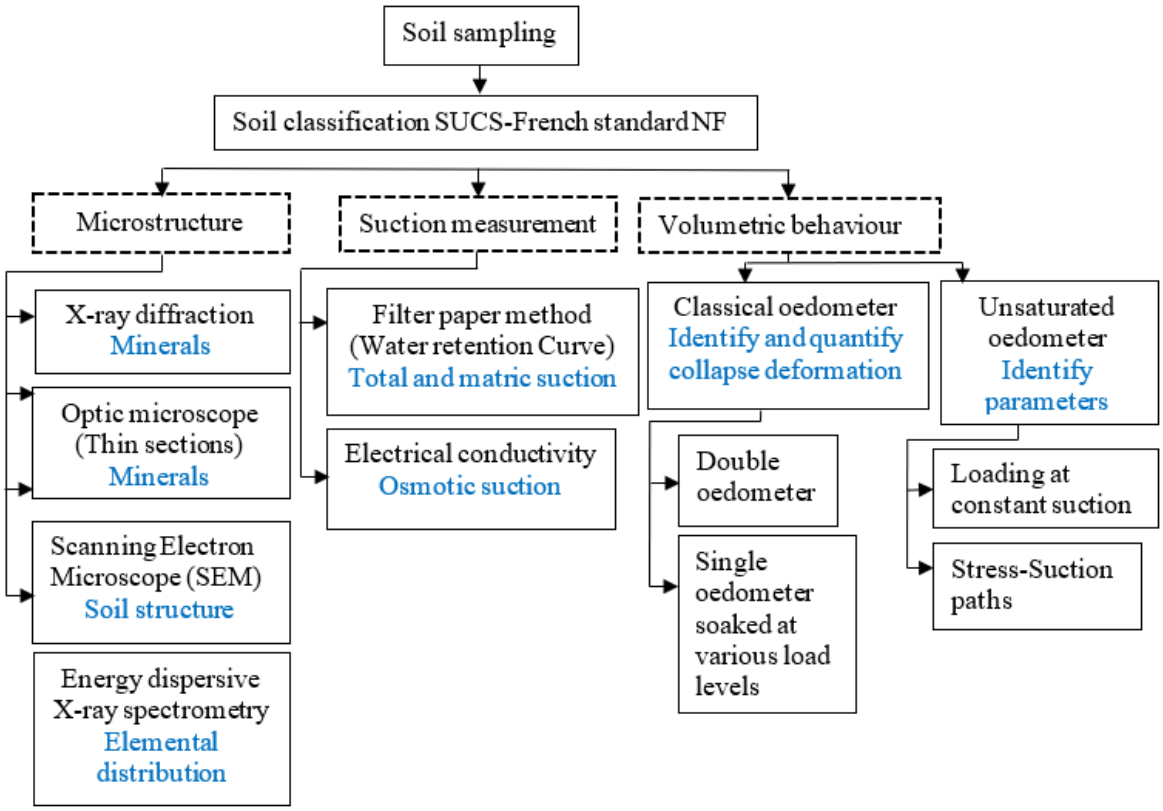

Figure 4-1. Experimental program.

4.3 Sampling of the eolian soils.

The sampling procedure in the soil was performed according to the guidelines of Standard practices for obtaining intact block (Cubical and Cylindrical) samples of soils described in ASTM D7015, 2018. This method was applied in order to maintain the soil structure and evaluate the volumetric behaviour with the “in situ” conditions of the eolian soil.

Eleven undisturbed samples that are expected to exhibit collapse behaviour are collected from the bottom of twelve pits that were dug at four sites in the area of eolian soils in Mayapo.

Figure 4-2 shows the process of sampling of undisturbed samples. The exposed faces were covered with several layers of plastic wrap in order to preserve the natural moisture. The initial water content of the sample was measured in situ. The samples were transferred to the laboratory and covered using melted paraffin instead of melted wax.

Figure 4-2. Procedure for cubical block sampling of eolian soils.

Figure 4-3 shows the samples of eolian soil extracted at each point. Samples were obtained from depths of between 0.8 to 1 m. The size of the undisturbed block samples was 15 cm per side approximately.

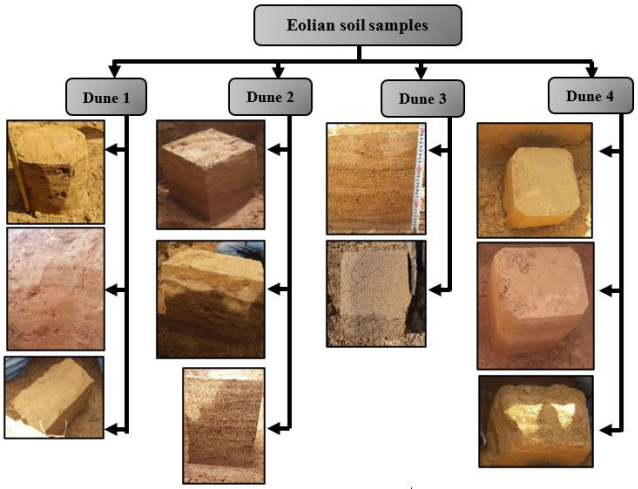

Figure 4-3. Cubical samples of the eolian soils.

4.4 Soil classification

General geotechnical tests were realized to classify the eolian soils from Mayapo. These tests were carried out in order to obtain the geotechnical characterization of the eolian soils and group the samples with similar characteristics according to their volumetric behaviour.

The water content of the soil in the natural state was realized based on ASTM D2216, 2019. The Specific gravity tests of soil particles were realized based on ASTM D854, 2014, the tests were realized twice in order to verify the results. The consistency limits tests were realized based on ASTM D4318, 2017.

4.4.1 Sedimentation hydrometer analysis

The particle size distribution analysis was realized using sedimentation hydrometer analysis (ASTM D7928, 2017). The tests were carried out in the geotechnical laboratory of Universidad Nacional de Colombia, Medellín, see Figure 4-4. The objective was to know the distribution of soil particles from a diameter of 4.75 mm to particles of 1µ. Eleven samples were tested with a dispersing agent to cause the breakdown of the aggregates as standard procedure suggests. The tests were also realized without the dispersing agent to obtain the flocculation percent due to it can affect volumetric behaviour of the eolian soil.

Figure 4-4. Hydrometer test.

4.4.2 Granulometric analysis of soils. Laser diffraction method

These tests were carried out to analyze the fines particles in the sample soil and compare with the hydrometer tests. The analysis of granulometry of the eolian soil using the laser diffraction method was based on the Frances standard NF ISO 13320-1, 2000. The tests were carried out in the geotechnical laboratory of CEREMA in Toulouse, France. The method consists of determinate the weight distribution of the size of fine particles of the soil.

Figure 4-5. Left: Magnetic stirrer. Right: Laser particle size analyzer.

The laser granulometry calculates the particle size form the diffraction of laser radiation: any particle of the same size diffracts at the same angle and the diffracted ray, therefore, illuminates the same detector. Four tests were carried out, one for each Dune. Five grams of the sample was separated and suspended in water. The whole of the solution is homogenized using a magnetic stirrer. Then the particle concentration of the solutions is measured by the laser particle size analyzer, see Figure 4-5. The weight distribution of the particle size is calculated from these data.

4.4.3 Blue of methylene absorption capacity

The test allows classifying the soil based on the French standard and comparing the results with the obtained by sedimentation hydrometer test. Measuring the adsorption capacity of methylene blue from the soil was based on the Norme française, 1998. The tests were carried out in the geotechnical laboratory of CEREMA in Toulouse, France. The test consists of measuring by dosage the amount of methylene blue can be adsorbed by the material

suspended in water, see Figure 4-6. The blue value of the soil was directly related to the specific surface of the particles constituting the soil.

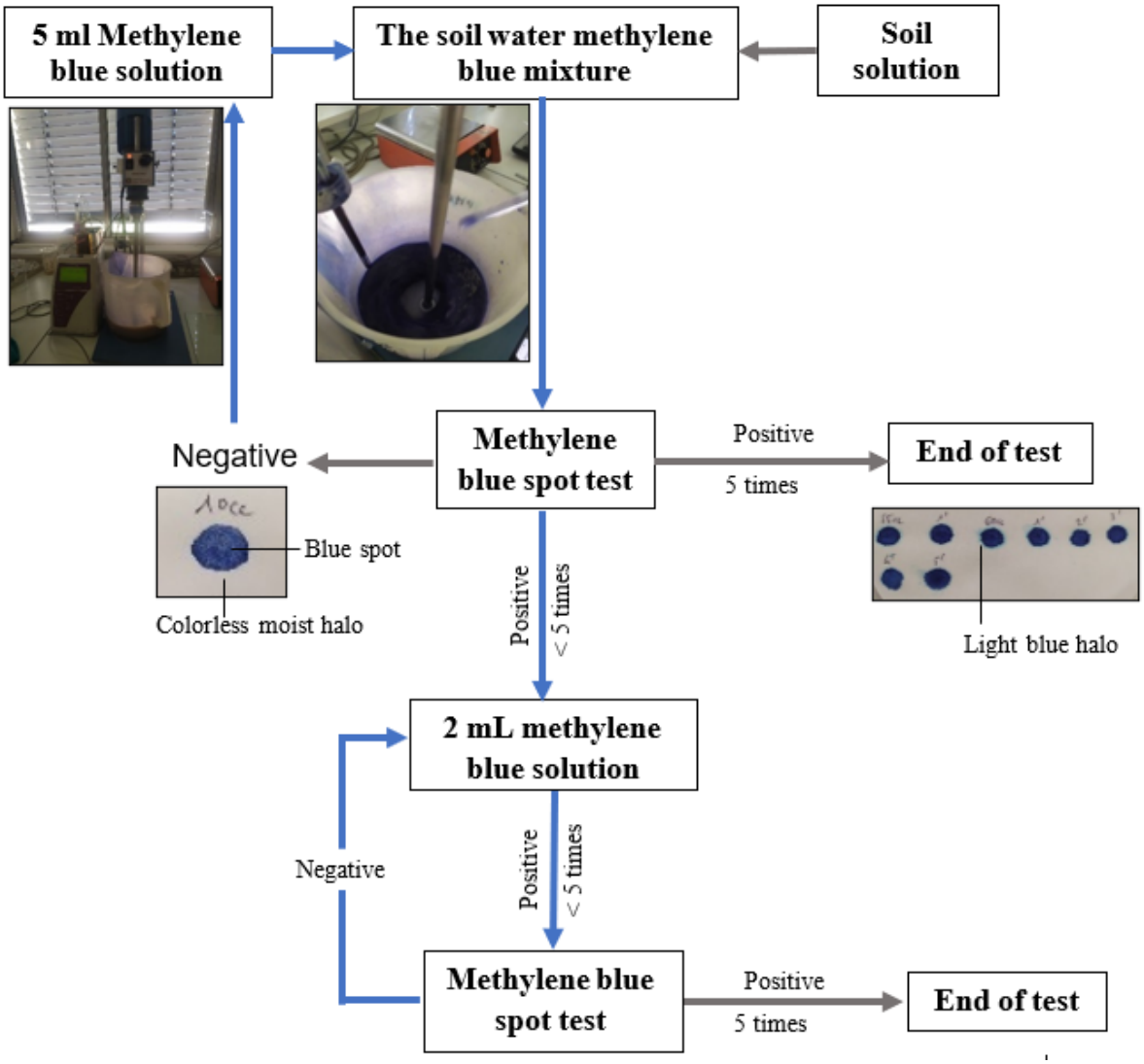

Figure 4-6. Blue of methylene absorption capacity procedure.

The test was carried out by successively adding different methylene blue quantities and controlling the adsorption after each addition. To do this, we take a drop of the suspension, which was deposited on a filter paper, creating a spot. The maximum adsorption was reached when a persistent light blue aureole appears at the periphery of the spot, see Figure 4-6.

To calculate the methylene blue value of the sample, the following expression was used:

$$VBS = \frac{B}{m_0}$$

Where:

VBS = Soil Blue of methylene Value

B = mass of blue of methylene introduced

m_0 = dry mass of the test sample

4.5 Microstructure

These tests allow realizing the geological characterization of the eolian soil, correlating the current properties with the geological history of this area, including the chemical composition, mineralogy, structure, and bonding material. Also, it allows evaluating the collapse behaviour focusing on the micro-scale level, having a better understanding of the relationship between the geological features and volumetric behaviour of the soil.

4.5.1 X-ray diffraction

The main objective is to identify the minerals in the silt and clay fraction of the sample and to obtain a semi-quantitative analysis. The tests were carried out in the Chemical laboratory of Universidad de Antioquia, Medellín. For this test, a sample of eolian soil was selected and dried in the oven. The sample was sieved using sieve N° 200 to separate the soil fraction less than 76 µm. The sample was powdered in order to make pass all the material through the sieve. The X-ray diffraction was carried out in an EMPYREAN diffractometer Model 2012. The incident radiation wavelength was of l= 1.7903 Å and a step size of 0.026°. The platform configuration used was spinner transmission reflection. The diffractogram was refined using the Rietveld method.

4.5.2 Optical microscope analysis from thin sections

The samples were also subjected to optical microscope analysis to know the grain structure, mineralogy, and bonding material between grains, which can affect the volumetric behaviour of the eolian soil. The tests were carried out in the optical laboratory of Universidad Nacional de Colombia in Medellín.

Four thin sections representing each dune studied were prepared using resin in order to keep the natural fabric. The preparation consists of cut the sample into a thin tabular form. Then,

the sample is placed into an activated polylite resin. The soaked sample is placed into a vacuum desiccator to evacuate the air bubbles. The sample gets hard in 1-2 hours. After that, the sections were polished to a thickness of approximately 20 μm. By last, the slice is put in a cover slip and fixed with a cover slip. The thin sections were analyzed using a petrographic microscope, see Figure 4-7. The samples were examined under plane-polarized light (PPL) and cross-polarized light (XPL).

Figure 4-7. Optical microscope for thin sections.

4.5.3 Scanning electronic microscopy analysis (SEM)

The test target was to know the soil structure, describe the porosity, the shape of grains of the eolian soils to relate these features with the soil response. The tests were carried out in the biomaterials laboratory of Universidad Nacional de Colombia, Medellín.

Four undisturbed samples of eolian soils were studied for the test, as shown in Figure 4-8. The volume of each sample was around 1 cm^3. The specimen was fractured without carving them to preserve the fracture preference that was considered representative of the undisturbed fabric. For the eolian soils, the preparation process could be difficult because soil particles were removable. The equipment used to analyze the specimens was the scanning electron microscope SEM Carl Zeiss EVO MA10. This equipment uses a vacuum sample chamber. For this reason, samples were dried in the oven at 105° Celsius, to the vacuum process was faster. The thin sections were analyzed by scanning electronic microscope using the same process.

Figure 4-8. Sample preparation for SEM. Left: Geometry samples and putting the sample in the slides. Right: Sputter coating process.

SEMs were capable of imaging from conductive or semi-conductive materials. Due to the soil was a non-conductive material, SEMs could present difficulty in imaging. The soils can behave as an electron trap and gather them on its surface. This phenomenon is known as charging and create white regions in the images. For this reason, samples must be prepared before the tests to prevent surface charging and loss of resolution (Mitchell & Sangrey, 1975). The process is called sputter coating and consists of covering the soil with a thin layer of a conductive metal in a closed recipient, which is pumped down to a vacuum base (Constantin et al., 2011). In this case, the samples were covered by 5 nanometers of gold to enhance the SEM images. To enable the ignition of plasma was used argon gas in the chamber up to a pressure of 0.5 Pa.

The processing and analyzing the SEM photomicrographic was made by ImageJ, an open source image analysis tool (Ferreira & Rasband, 2012). Images obtained from SEM were converted to grayscale. Then, the images were converted to binary (black and white) following the image analysis steps through the transformation of the micrograph.

4.5.4 Energy dispersive X-ray spectrometry (EDS)

The energy dispersive X-ray spectrometry (EDS) tests were realized to know the distribution of the elements in a section of the dune. The tests were carried out in the biomaterials laboratory of Universidad Nacional de Colombia, Medellín. The main objective was to determine if a bonding material between grains would provide higher stiffness to the soil. Due to the soil being exposed to marine environments, it could have carbonates and salts in the contacts between the grains acting as bonding material affecting the volumetric behaviour of the soil. EDS tests also could give a response to this hypothesis.

For the energy dispersive x-ray spectrometry EDS tests, four thin sections of the eolian soils were used. The same process described for the SEM was made for preparing and analyzing the samples in the EDS tests.

4.6 Suction measurement

These tests were carried out to know the suction range of the soil due to the unsaturated soil that can have higher suctions and affect the collapse behaviour. The test target is to know the range of suction of the eolian soil, likewise, to design the suction paths to the unsaturated tests.

4.6.1 Water retention curve (WRC) by filter paper method

The filter paper method was applied to measure the total and matric suction of the eolian soils to obtain the water retention curves. The tests were realized following the procedure described in ASTM D5298, 2016. The tests were carried out in the geotechnical laboratory of Universidad Nacional de Colombia in Medellín.

Eighteen soil specimens with 56 mm of diameters and 20 mm of high to obtain two water retention curves. For these tests, the saturated path was analyzed. The soil specimens were carved and then air-dried, and saturated to different degrees to get proper distribution in the water retention curves, see Figure 4-9. The test procedure involves placing pieces of filter paper against the soil specimen, as shown in Figure 4-10, and sealing the whole to prevent evaporation. The Whatman 42 filter paper was used in all tests.

Figure 4-9. Left: Sample drying. Right: Saturation process.

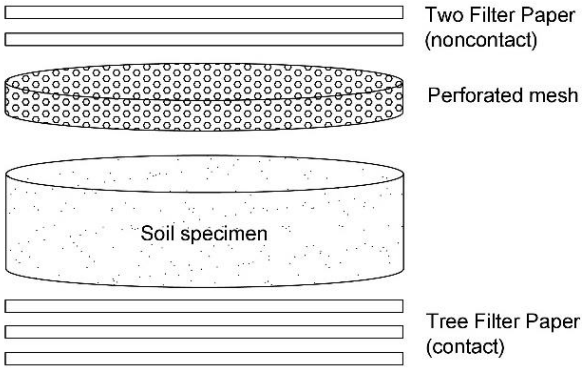

Figure 4-10. Contact and noncontact filter paper methods for measuring matric and total suction, respectively (adapted of Fredlund & Rahardjo, 1993).

For 15 days, the filter paper wets up to reach a water content in equilibrium with the magnitude of matric and total suction. Then, the water content of the filter paper was measured, which allows us to obtain the soil suction from a previously established correlation.

4.6.2 Pore water extraction by squeezing method. Osmotic suction measurement

The eolian soils of this research were exposed to marine environments, and the salt content is present and evidenced in the microstructure tests. The test target is evaluating the osmotic suction related to salt content in the soil. The osmotic suction has effect in the hydraulic conditions of the eolian soils. The water flow is governed not only by the matric suction but also osmotic suction and can attract more water increasing the saturation, and then affecting the volumetric behaviour of soil. This test was also carried out in order to do a chemical analysis of the water pore of the eolian soils of Mayapo to understand its influence in the possible collapse behaviour.

There are several techniques to measure the osmotic suction based on the extraction of pore water from the soil sample: immiscible liquid displacement, gas extraction method, centrifuging method, saturation extract method, and mechanical squeezing method, and others (Iyer, 1990). In these, the osmotic suction is indirectly estimated by measuring the electrical conductivity of the pore-water from the soil (Fredlund & Rahardjo, 1993). The pore water of the soil contains dissolved salts with high and electrical conductivity compared to

pure water. The concentration of dissolved salts can be indicated by the electrical conductivity, which was related to the osmotic suction of the soil. The salinity of soil is not dependent on the quantity of water (Romero, 1999).

In this research, the centrifuging method was employed for pore water extraction of soil. This method is reported to be satisfactory with sand and silts (Iyer, 1990). The test was carried out in the chemical laboratory of Universidad Nacional de Colombia in Medellín. A centrifuge Thermo electron, IEC CL31R Multispeed, was used to extract soil water with a limit rotation of 10000 rpm. Six soil samples of a total volume of 300 mL were employed in the test. Water was added to the sample up to reach 100% of saturation in order to obtain the electrical conductivity in the saturated state of the soil.

Once saturated, the samples were placed in the centrifugation device and were centrifuged up to obtain 10 ml of pore water. After that, the pore water in the soil was extracted, and electrical conductivity was then measured using a portable conductometer CRISON, see Figure 4-11.

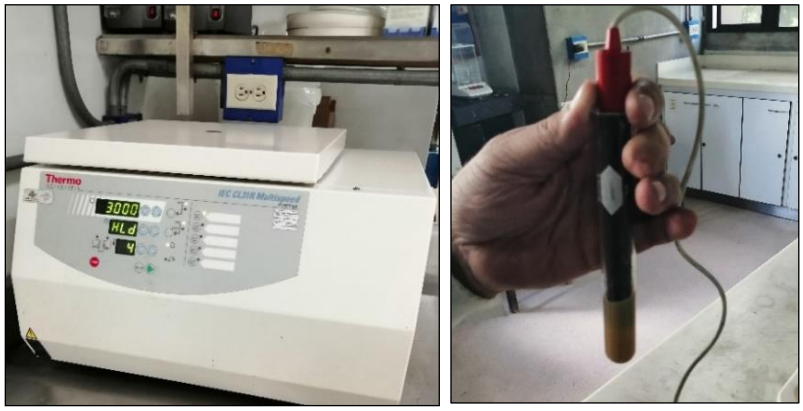

Figure 4-11. Left: Centrifuged process in eolian soils. Right: Measurement of electrical conductivity in pore water extracted.

Osmotic suction was estimated from electrical conductivity using empirical relationships of equation 1 and 2, based on exponential correlations between electrical conductivity and osmotic suction. The first expression was proposed by the USDA, agricultural Handbook N.60 1954; after Fredlund & Rahardjo, 1993, and was obtained with a mixture of dissolved salts in water. The second one were determined with homoionic NaCl solutions by Romero,

1999. The difference between the two curves were of 15% for osmotic suction greater than 40 kPa.

$$\pi = 0.0191\ EC^{1.074} \quad \text{(U.S.D.A, 1950)} \qquad (1)$$

$$\pi = 0.0240\ EC^{1.065} \quad \text{((Romero, 1999)} \qquad (2)$$

Where,

π = Osmotic pressure (kPa).

EC = Electrical conductivity (µS/cm).

4.7 Volumetric behaviour

These tests were focused on studying the volume change behaviour of the eolian soils due to loading and wetting. The test results and analysis are correlated with the microstructure analysis to have a better understanding of volumetric behaviour of the eolian soil.

4.7.1 Experimental design

The experimental design was realized based on the design of experiments proposed by Fisher, 1947. The design of experiments consists of determining what test should be made and how to obtain data, which will statistically provide evidence to allow answers to questions raised. An explaining each step of planning experimental design and associating them with the oedometer tests experimental design is presented in this section.

4.7.1.1 Hypothesis definition

Recognition of the hypothesis of the research gives a clear statement of the problem. It contributes to a better understanding of the phenomenon being studied and the final solution to the problem. For these tests, the following hypothesis is proposed: “Changes in suction and stress paths influence the volumetric behaviour of the eolian soil”.

4.7.1.2 Choice of factors and levels

A factor is an independent and controllable variable, and the levels are the measures which the factor will be evaluated. The factors and levels influence the performance of the system, and its combination or treatments helps to answer the hypothesis. How these factors are

controlled to keep them at the desired levels should be considered. Table 4-1 presents the factor and levels selected to evaluate the volumetric behaviour of the eolian soils.

Table 4-1. Factors and levels of the factor for each oedometer tests

Test type	Factor	Levels
Double oedometer	A: Void ratio	0.6 0.65 0.81 0.82
Oedometer at different loads	A: Void ratio	0.69 0.71 0.72 0.77
	B: Soaking load (kPa)	80 200 400 800
Loading at constant suction	A: Suction (kPa)	0 30 100 200 300
Stress-suction paths	A: Vertical net stress (kPa) for collapse 30 kPa	10 300

4.7.1.3 Experimental Unit

Also called the measurement object, it is the place or context used to produce in a condition to obtain a representative measurement. For each unit is applied a single treatment (which is a combination of many factors. For oedometer tests, the eolian soils of Mayapo was selected to evaluate volumetric behaviour.

4.7.1.4 Selection of response variable

The response variable is the value of the product of interest. The experimenter should be certain that this variable really provides useful information about the process under study.

Table 4-2 shows the four types of experimental tests were carried out in order to answer the hypothesis proposed.

Table 4-2. Response variable for each test

Test type	Response variable
Double oedometer	Collapse potential
Oedometer at different loads	Collapse potential
Loading at constant suction	Yield stress to LC curve
Stress-suction paths	Yield stress

4.7.1.5 Choice of experimental design

Two experimental designs were selected to obtain the response variable of each test type and to analysis the volumetric behaviour of the eolian soils. Table 4-3 show the experimental design for each test.

Table 4-3. Experimental design of each oedometer tests

Test type	Response variable
Double oedometer	Experiment with a single factor
Oedometer at different loads	Full factorial General
Loading at constant suction	Experiment with a single factor
Stress-suction paths	Experiment with a single factor

For the tests using the “experimental with a single factor”, it will evaluate the influence of the factor levels in the response variable. The tests analyzed with “Full Factorial Design”; it will evaluate all possible combinations of the levels of the factors.

Figure 4-12 shows the experimental design with the treatments or combinations of the level of the factors, showing the variation of levels of factors. Twenty-seven response variables were obtained to characterize the volumetric behaviour of the eolian soils.

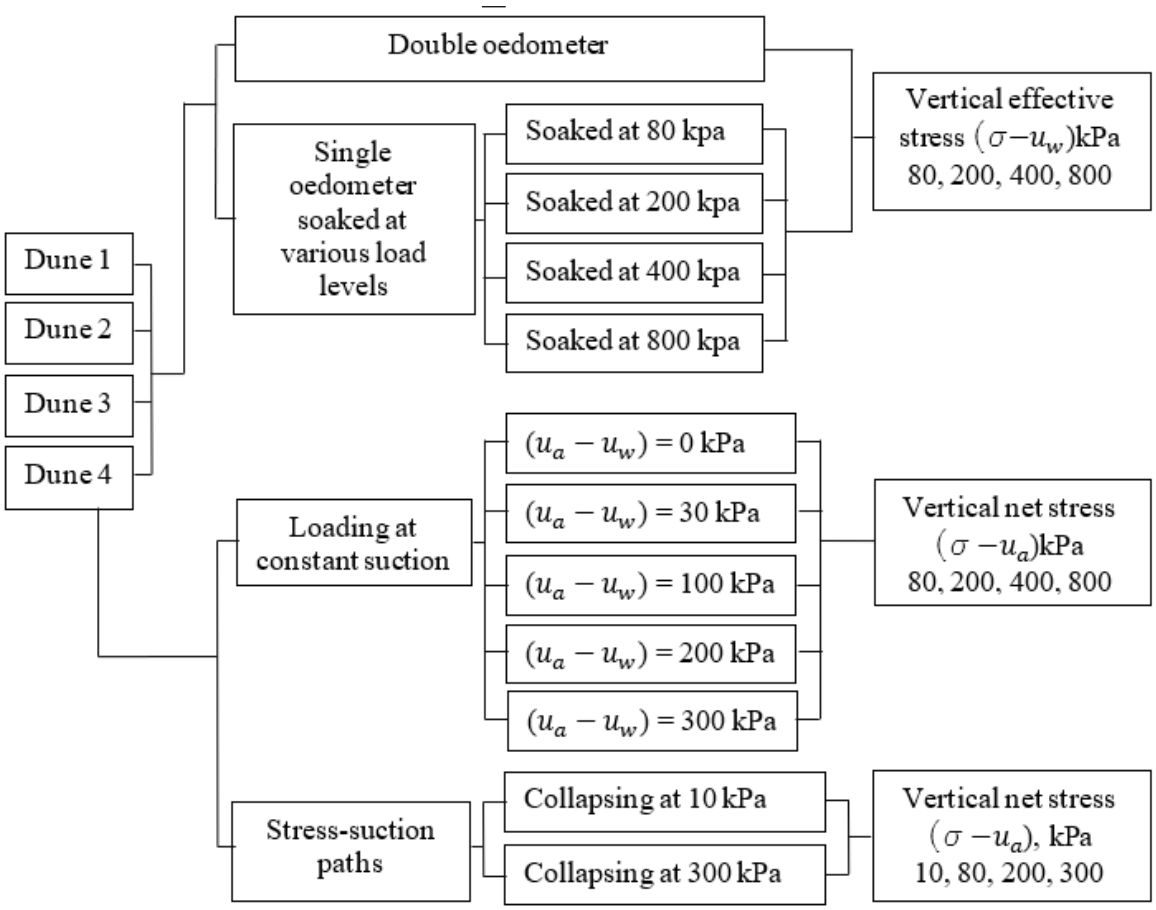

Figure 4-12. Experimental design of the oedometer tests.

High levels of soaking load were selected to know the complete paths of the compressive curves of the eolian soils, knowing the load in which the soil experiment the highest collapse and determinate if the collapse increment with the load. On the other hand, the level suction paths were selected based on the results obtained in the double water retention curves.

Oedometer tests were conducted randomly to neutralize the effects of strange factors that may be present. With the randomization, the observations (or errors) be independently distributed random variable. It is necessary to obtain valid significance tests.

4.7.1.6 Results analysis

Statistical methods should be used to analyze the data so that the results and conclusions are objective rather than operational. The principal effects of the levels of the factors and the influence of interaction between factors in the variable response. The software of statistical analysis Minitab was used for the analysis.

4.7.2 Classical oedometers

Classical oedometers were performed to identify the collapse of the soil. From these tests results the magnitude of collapse of the eolian soils is calculated. The oedometer tests were realized based on the procedure indicated in ASTM D2435, 2011. Some modifications were made to understand the volumetric behaviour of the eolian soil under different stresses and wetting paths. The methods are described below.

4.7.2.1 Simple oedometer

This test was realized base in Norme Française, 2017. The tests were carried out in the geotechnical laboratory of CEREMA in Toulouse, France. This test was made in order to obtain the consolidation curve at 0 kPa of suction to complete the Loading Collapse (LC) curve in the results of the unsaturated tests. Figure 4-13 shows the equipment used for the test. The apparatus consists of a consolidation cell, a smart keypath, a 10 kN load cell, a 10 mm LVDT. It was not needed manually placed weights.

Figure 4-13. Oedometer test in Automatic oedometer system of Global Digital Systems GDS.

One undisturbed specimen was soaked and then loaded at the following stresses: 30, 80, 200, 400, and 800 kPa.

4.7.2.2 Double oedometer test

The tests were carried out in the geotechnical laboratory of Universidad Nacional de Colombia in Medellín. The test target was to know the magnitude of the collapse in the eolian

soils. Four double oedometer tests were realized from each sample point. Two specimens of each sample were testing at the same time, see Figure 4-14. One sample keeps the natural moisture content, and the other was soaked at the beginning of the test. The specimens were loaded by stages of 30, 80, 200, 400, and 800 kPa.

Figure 4-14. Left: Oedometers for the tests. Right: Soil specimens for the tests.

4.7.2.3 Oedometer tests under different vertical effective stresses

These tests were focusing on knowing the stress in which the eolian soil presents the maximum collapse percentage. For this reason, four undisturbed specimens were loaded at natural moisture content up to the following stresses: 30, 80, 200, 400, and 800 kPa. After the equilibrium in each load, the specimen was soaked. Figure 4-15 shows the point where the soil is soaked, and the deformation measured at this point is the collapse. Once the stabilization was complete, the soil was loaded progressively up to 800 kPa under saturated conditions, to obtain the curve in the saturated state. The equipment used in this test is shown in Figure 4-14.

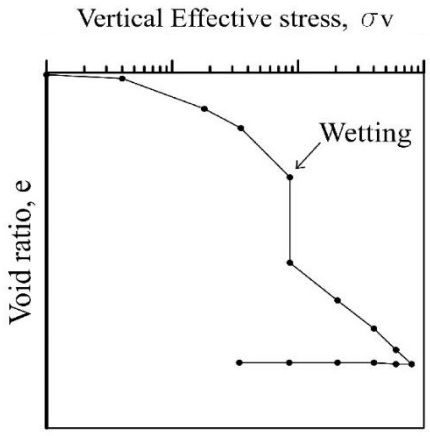

Figure 4-15. Scheme of single oedometer test result.

4.7.3 Unsaturated oedometers

The collapse phenomenon is attributed to the loss of stiffness associate with suction decrease because of wetting. For this reason, with the unsaturated oedometer tests using suction-controlled, the collapse behaviour of eolian soils at different stresses and suction paths is investigated. As well as it was performed to the identification of the parameters to model the soil using the Barcelona Basic Model (BBM). The tests were carried out in the geotechnical laboratory of CEREMA in Toulouse, France.

4.7.3.1 Description of the oedometer cell

The features and procedures described in these items are based on the GDS handbook for the GDS Consolidation testing system (GDS, n.d.). The suction controller oedometer cells have been utilized by many researchers to study the influence of suction on compressibility and swelling properties of soils (Delage et al., 2008). Figure 4-16 shows a scheme and picture of the suction controller oedometer cell Rowe and Barden type. The equipment provides a test chamber in which the pressure conditions can be controlled. The parameters that can be controlled and measured are water back pressure, air pressure, specimen volume change, pore pressure, axial displacement, axial stress (GDS, n.d.).

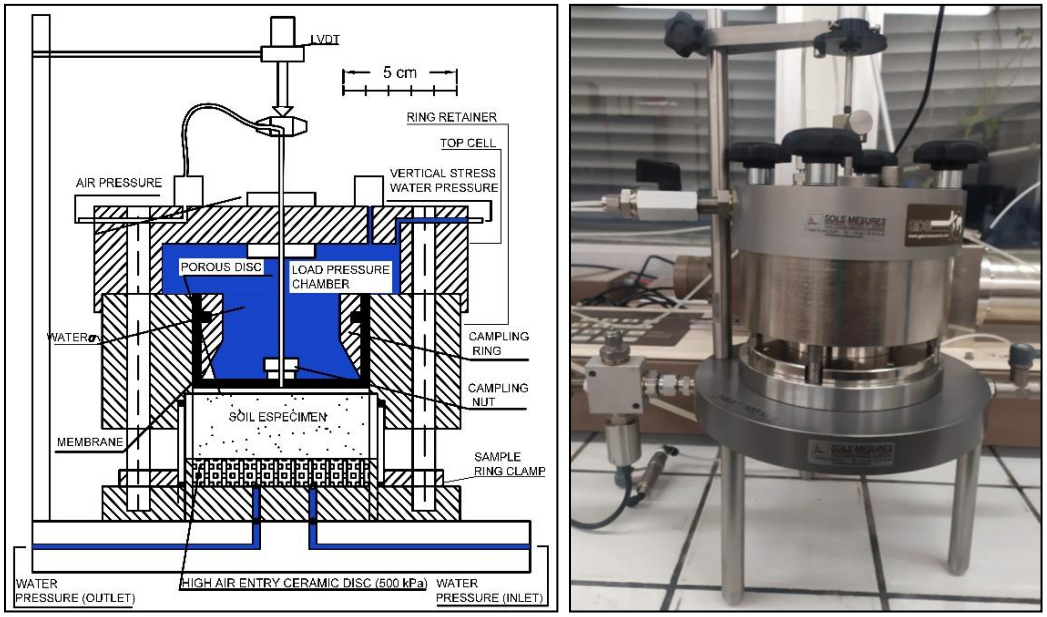

Figure 4-16. Scheme and picture of the suction controlled oedometer cell.

The cell consists of three main parts join by o-rings and screws to ensure closure of the system. The superior part connected to the air pressure, the cell base connected to

backpressure and rings to place the sample. All parts of the equipment are detailed in Figure 4-17. The thickness of the chamber wall is sufficiently thick for maintaining the pressure in the equipment (Vanapalli et al., 2008).

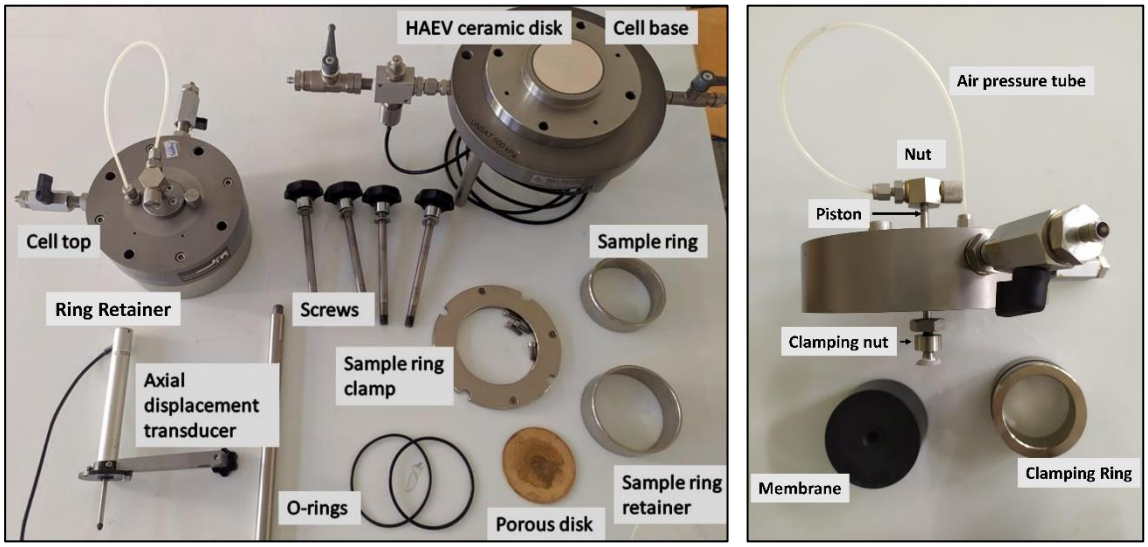

Figure 4-17. Parts of the equipment.

4.7.3.2 Auxiliary devices

The suction oedometer cell requires auxiliary devices in order to control and measure the pressure, volume, and deformation during the test. Figure 4-18 shows a scheme of the Rowe and Barden cell and the auxiliary devices used with Rowe and Barden Cell. Each device is described below.

GDS pressure/volume controllers: The equipment requires GDS pressure/volume controllers. The controllers measure the water volume changes, air volume changes, and control the supply pressures.

Two water pressure/volume controllers are used to supply the backpressure in the sample and supply the vertical pressure upper soil sample. The volume change is measured in cubic millimeters. The axial displacement can be measured indirectly using the values of air volume change and water volume change.

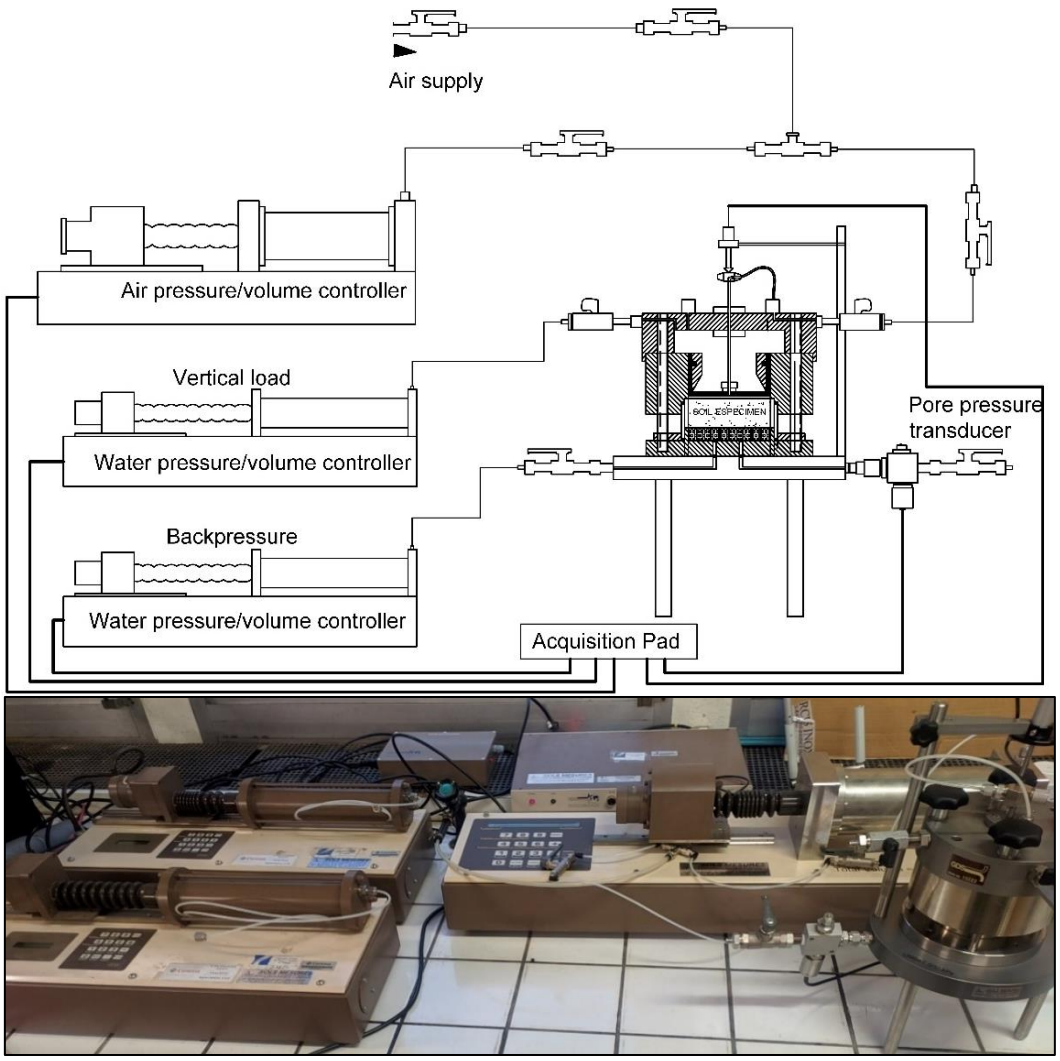

Figure 4-18. Scheme oedometer with auxiliary devices.

One air pressure/volume controller is connected to the top of the test specimen to impose the air backpressure. The air pressure/volume controller is pre-pressurized at using a compressed air source to save volumetric capacity used up in pressurizing itself. The air pressure is connected to the top of the test specimen.

Axial displacement transducer: An axial displacement transducer is used to measure directly axial deformation in the sample using an LVDT transducer. The LVDT is placed over the piston.

Pore pressure transducer: The pore pressure transducer is connected to the sample base using a rigid pore pressure sensor to measure the pore pressure. This transducer does not control the pore pressure. Naturally, there will have a small difference between measurement by the

transducer and the same pressure applied by the GDS controller. This difference is normal and should be considered when interpreting the results because this inherent discrepancy is not controllable. However, pore water measurement is not essential. (GDS, n.d.)

Acquisition pad: The acquisition pad is used for the data acquisition of axial displacement and pore water pressure. Simultaneously, it is connected to the water and air pressure/volume controllers to program the imposed pressures during the test.

4.7.3.3 Assembly of suction-controlled cell

The first step is to assembly the superior part of the Rowe and Barden cell. This step should be made carefully to avoid leakages of water and air during the tests. The procedure is realized once, and the superior part is maintaining assembled between tests. The steps to assemble the superior part of the equipment is described below:

1. The membrane and all the o-rings are lightly lubricated with silicone grease before the assembly.
2. The piston is joined with the top cell feeding the piston up carefully through the cell top.
3. The clamping nut and the piston are screwed to the membrane using a flat screwdriver to stop the piston rotating.
4. The clamping ring is placed inside the membrane and after inside the ring retainer.
5. The cell top and the ring retainer are attached using the four bolts on the top of the equipment.
6. The nut (which has the air pressure connector) at the top of the piston is screwed to the main part of the piston while a flat screwdriver is used to stop the piston rotating.
7. The air pressure tube is screwed to the top of the main body of the cell. This process is realized just once to ensemble the membrane in the superior part of the equipment and when the membrane is lubricated or changed.

Disassembly the part superior is carried out by reversing the process described above. Between essays, the part superior never is separated. (GDS, n.d.)

The procedure to assemble the equipment is shown in Figure 4-19. The sample base with the HAEV ceramic disc is attached up the cell base with screws, see Figure 4-19 (a). Care must be taken to the drainage holes are aligned, and the o-rings between them are put correctly and

then insert and tighten the retaining bolts. This step does not need to be repeated between essays, except for cleaning. One O-ring is placed around the pedestal on the cell base and attached the cell ring clamp to the cell base with screws, see Figure 4-19 (b).

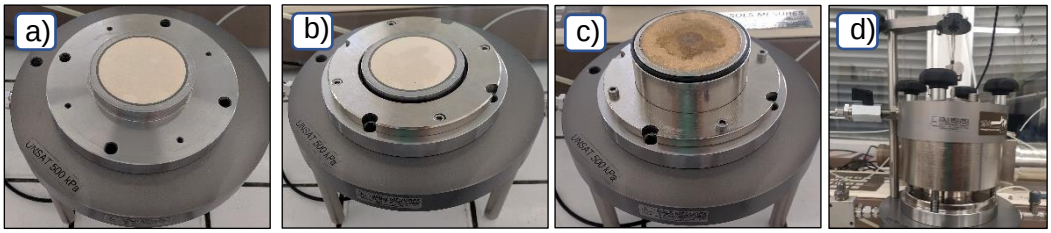

Figure 4-19. Procedure to assemble the equipment a) sample base b) sample base and ring clamp c) assemble the sample d) assemble the part superior to the cell.

Water upper the ceramic is removed almost completely, leaving a thin film of water to avoid desaturation and guaranty adequate contact with soil water. The specimen is weighted and is placed upper the pedestal, covering it with a plastic paper to prevent drying due to evaporation.

The sample ring retainer is placed around the pedestal and the sample. A second O-ring is attached to the top edge to avoid part of the cell in contact with the piston (GDS, n.d.). The axial stress is generated by the pressure in the top chamber and is constant during each test stage.

4.7.3.4 Saturation stage

Before the tests, the HAEV ceramic disc should be saturated to apply the pore pressure. The saturation process consists mainly of dissolving air bubbles under high water pressures (Romero, 1999). The direct contact between the sample and the HAEV ceramic disc could result in cavitation of the meta-stable water in a closed system. Air is entrapped in microscopic crevices, resulting in erroneous estimation of the imposed matric suction. Therefore, it is recommended to realize the saturation process in the HAEV ceramic disc (Ridley & Wray, 1996). The procedure is realized based on the procedure of Romero, 1999, and the Rowe and Barden cell handbook GDS, n.d.

For speeding up the saturation process, the HAEV ceramic disc is dipped in distilled water for one week. Air is purged from individual pipes before connecting to the pedestal base, and

the base pedestal is put in place. For removing air from connectors, these are pressurized under 25 kPa. The non-pressurized connector is dipped in water until no further visible bubbles come out of the pipework. This process is realized in both directions. Usually, the pressure under the HAEV ceramic disc should not exceed 50 kPa. Positive water pressure of 30 kPa is applied to the ceramic disc until water pooled on the top surface of the disc. For 500 kPa air entry value disc used in this research, the process to remove air is completed in 2 hours.

The cell is pressurized to make water flow through the HAEV ceramic disc to atmospheric pressure. The sample ring is filled with water, and the odometer is pressurized under 520 kPa. For water to flow through the HAEV, pressure in the odometer should exceed the high air entry value. The pore-pressure connectors are opened to the atmosphere, and the pipework dipped in de-aired water. The water flows through the HAEV in the opposite direction, and burbles come out. This process is completed when no air remained in the pipework. The valve connected to the atmosphere is closed, and the cell pressure is kept in 520 kPa. This process is made in order to dissolve air entrapped in a microscopic crevice (Romero, 1999). For applying the chamber pressure is used water instead of air. The water is used to visualize any leakages in the vertical pressure more easily.

It is essential to maintain the test under low-temperature conditions. The desaturation of the HAEV ceramic disc could occur at high temperatures with relative humidity around 50% (Romero, 1999).

The hydraulic conductivity of the HAEV ceramic disc is measured to verify the ceramic disc is not cracked. After the saturation process, a thin film of water is left over the disc, and the test is started rapidly in order to avoid the desaturated.

4.7.3.5 Equalization stages

The equalization time is dependent on the type of soil, size of the specimen, and air-entry value of the disk, hydraulic conductivity of the specimen tested, and the hydraulic conductivity of the HAEV ceramic discs.

When net vertical stress is applied, an excess of pore air and water pressure is generated within the sample. The excess pore air is dissipated rapidly up to reach the backpressure due

to the air permeability. However, excess of pore water pressure takes more time to dissipate to the target water backpressure. It is mainly caused by the low permeability of the HAEV ceramic disc.

Figure 4-20 shows an example of the time evolution of the water volume change in the equalization stage of the application of a loading step and during the subsequent consolidation period at select nodes of the eolian soils. Time load increment was selected according to the previous values in order not to have significant creep. This way, the equalization period was around 0,4 week and the primary consolidation was completed within 24 hours. The time evolution of air volume change was not measured.

Two stages are evidenced in the volumetric strain evolution. The primary consolidation denoted in the curve of volume change. It usually occurs cause of air voids interconnected and the compression of burbles. The secondary consolidation is dependent on time, and it happens due to the water mass movement in air void space and the gradual dissolution of bubbles during the evolution of vertical net stress (Romero, 1999). Volumetric deformation is maintained, with 83 % of the total volume change.

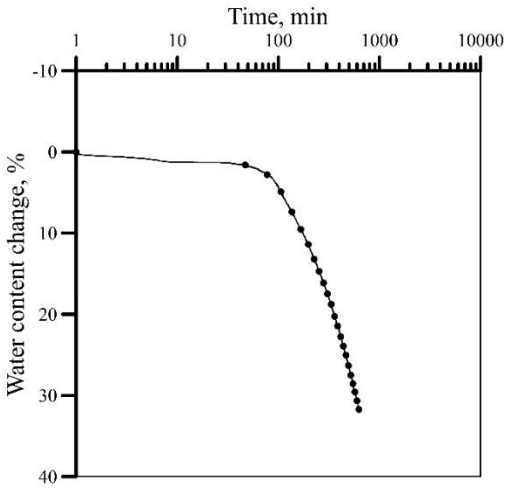

Figure 4-20. Time evolution of equalization stage of water content change under controlled matric suction tests.

4.7.3.6 Test Procedure and paths

The test program is intended to analyses the volumetric behavior of the eolian soil associated with suction and stress changes. Also, it intent to obtain the shape of Loading-Collapse LC curve. The planned laboratory testing program includes, in consequence, different stress

paths to follow to reveal different aspects of constitutive models. Two types of controlled suction test are performed:

- Controlled suction oedometer tests with constant suction (Tests 1-2-3-4)
- Controlled suction oedometer tests with soak at different loads (Tests 5-6)

Table 4-4 Show the data of the initial conditions of each sample for the tests. The tests are realized with different water and air pressures values to generate the matric suction required for the test.

Table 4-4. Initial conditions of controlled suction oedometer tests.

Test	e_o	Suction, kPa	Air pressure (U_a), kPa	Water pressure (U_w), kPa	Time (days)
1	0,7508	300	330	30	30
2	0,7525	200	220	20	30
3	0,7534	100	80	20	30
4	0,7631	30	50	20	30
5	0,7335	200	220	20	30
6	0,7436	200	220	20	30

The stresses and suction paths for the Controlled suction oedometer tests with constant suction and soak at different loads are shown in Figure 4-21.

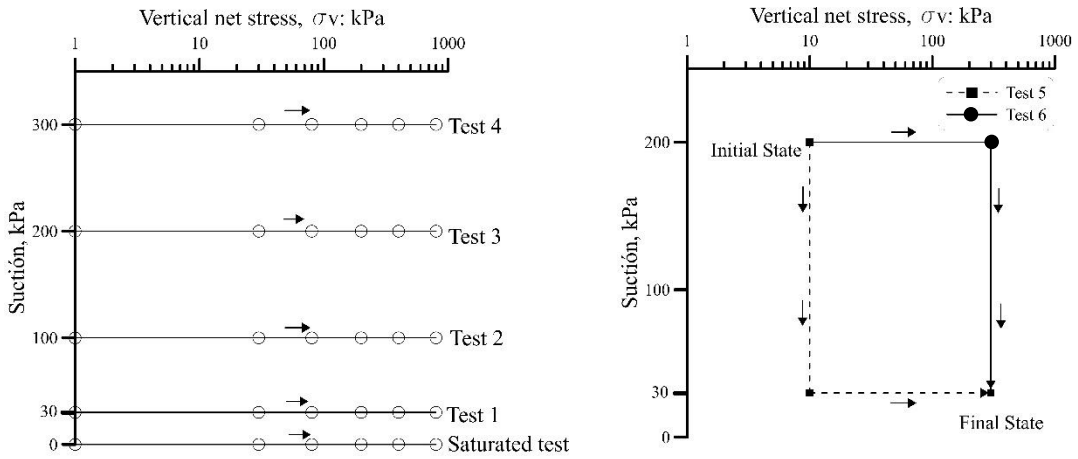

Figure 4-21. Left: Paths for controlled suction oedometer tests, loading at constant suction. Right: Paths for controlled suction oedometer tests with soak at different loads.

The stress path planning procedure is based on the process of the oedometer tests by Romero, 1999. The process is detailed below:

- The HAEV ceramic disc is pressurized to 15 kPa before the test in order to keep it saturated and minimize the application of suction time.
- Before putting the sample in the HAEV ceramic, water upper the ceramic is removed with an absorbent paper, leaving a thin layer of water to avoid any desaturation of the ceramic disc.
- When the equipment is assembled, a pressure of 5 kPa is applied to adjust the membrane with the upper porous disc. This can be noticed when the axial displacement transducer registered movement.
- To reach the suction required in the soil is necessary to increase the air pressure before the water backpressure. The air pressure must be imposed at the same time as vertical stress in steps of 50 kPa. During pressures increased, the difference between pressures should keep in 25 kPa.
- Once the air pressure is reached, the HAEV ceramic disc is pressurized with water to the desired value to achieve the suction required. The equilibrium of the pore pressure can be measured with the water volume change in GDS.
- When the water pressure needed is reached, the vertical pressure is raised to the desired value, and the compressive strain is measured and monitored. The equilibrium of the pore pressure should be reached before the next vertical stress.
- For the tests at constant suction, four tests at constant suction of 30, 100, 200, and 300 kPa are carried out, see Figure 4-21. Each soil specimen is loaded with the following vertical net stresses: 30, 80, 200, 400, and 800 kPa, to compare the behaviour with the classic oedometers results.
- For the tests soaked at different loads, two tests at different suction and stress paths are carried out, see Figure 4-21. the initial test conditions are 10 kPa of stress and 200 kPa of suction. For test 5, the soil specimen is wetting at the initial condition to reach 30 kPa of suction. After, the soil specimen is loaded at 300 kPa. For test 6, the soil specimen is subjected to a load of 300 kPa under constant

suction. Subsequently, the sample is wetting under a constant load to reach 30 kPa of suction.

- By last, the samples are weight, and the water content is calculated to determine the relation of suction imposed and water content.

Many of the test failed by different causes: electrical power interruption, desaturation of the HAEV ceramic disc due to diffused air accumulation, water, and air pressures leaks during the tests. however, these failed tests were used to state the repeatability. In general, repeatability and consistency in the results were observed in terms of volumetric strains.

4.8 Chapter conclusions

The experimental program was realized to characterize the volumetric behaviour of the eolian soils. The objective and procedure for each test were presented.

To maintain the soil structure and evaluate the volumetric behaviour with the “in situ” conditions, the soil was sampling using the block sampling method. Soil classification of the eolian soil was realized to obtain the geotechnical characterization of the eolian soils and group the samples with similar geotechnical properties.

Also, microstructure tests were carried out to realize a geological characterization of the eolian soil, correlating the current properties with the geological history of this area, including the chemical composition, mineralogy, structure, and bonding material. Also, it allows evaluating the collapse behaviour focusing on the micro-scale level, having a better understanding of the relationship between the geological features and volumetric behaviour of the soil. The microstructure tests are x-ray diffraction, microscope analysis, scanning electronic microscope and x-ray spectrometry.

On the other hand, the suction behaviour of the soil was also studied. The procedure to obtain total and matric suction of the eolian soil and the water retention curves is detailed. The squeezing method to obtain the osmotic suction is also described, and the target is to evaluate the influence of the osmotic suction related to the salt content in the soil and the effect in the hydraulic conditions of the eolian soils.

Finally, the tests to understand the volumetric behaviour is also explained. Classical oedometer and unsaturated oedometer tests were focused on studying the volume change behaviour of the eolian soils due to loading and wetting, on identifying the collapse of the soil, and know volumetric behaviour at different stress and suction paths.

4.9 References

ASTM D2216. (2019). Standard Test Method for Laboratory Determination of Water (Moisture) Content of Soil and Rock by Mass. *ASTM International*, *January*, 1–5.

ASTM D2435. (2011). Standard Test Methods for One-Dimensional Consolidation Properties of Soils Using. *ASTM Standards*, *04*(June), 1–10.

ASTM D4318. (2017). Standard Test Methods for Liquid Limit, Plastic Limit, and Plasticity Index of Soils. *Report*, *04*(March 2010), 1–14.

ASTM D5298. (2016). *Standard Test Method for Measurement of Soil Potential (Suction) using filter paper*. 1–6.

ASTM D7015. (2018). *Standard Practices for Obtaining Intact Block (Cubical and Cylindrical) Samples of Soil*. 1–7.

ASTM D7928. (2017). Standard Test Method for Particle-Size Distribution (Gradation) of Fine-Grained Soils Using the Sedimentation (Hydrometer) Analysis. *ASTM International, West Conshohocken, PA.*, 1–25.

ASTM D854. (2014). Standard Test Methods for Specific Gravity of Soil Solids by Water Pycnometer. *Astm D854*, 1–7.

Constantin, D. g, Apreutesei, M., Arvinte, R., Marin, A., Andrei, O. C., & Munteanu, D. (2011). Magnetron Sputtering Technique Used for Coatings Deposition ; Technologies and Applications. *7 International Conference on Materials Science and Enginering*, *12*(March), 24–26.

Delage, P., Romero, E., & Tarantino, A. (2008). Recent Developments in the Techniques of Controlling and Measuring Suction in Unsaturated Soils. *Unsaturated Soils: Advances in Geo-Engineering - Proceedings of the 1st European Conference on Unsaturated Soils, E-UNSAT 2008*, *November*, 33–52.

Ferreira, T., & Rasband, W. (2012). ImageJ User Guide. *XXVI Focus on Bioimage Informatics*.

Fisher, R. A. (1947). Design of experiments. In *Society for Industrial and Applied Mathematics*.

Fredlund, D. G., & Rahardjo, H. (1993). Soil Mechanics for Unsaturated Soils. *John Wiley & Sons, Inc.*, *30*(2), 113–123.

GDS. (n.d.-a). *164 Helpsheet Hardware Rowen and Barden Cell Removing the Old Top-*

Bag.

GDS. (n.d.-b). *The GDS Consolidation Testing System and Constant Rate of Strain Harware Handbook.*

Iyer, B. (1990). Pore water extraction. Comparison of saturation extract and high-pressure squeezing. *ASTM Special Technical Publication*, *1095*, 159–170.

Mitchell, R. J., & Sangrey, D. A. (1975). *Soil Specimen Preparation for Laboratory testing*. ASTM.

Norme française. (1998). *Mesure de la capacité d'adsorption de bleu de méthylène d'un sol ou d'un matériau rocheux*.

Norme Française. (2000). *Particle size analysis-Laser Diffraction methods*.

Norme Française. (2017). *Reconnaissance et essais géotechniques-Essais de laboratoire sur les sols-Partie 5: Essai de chargement par palier à l'œdomètre* (ISO 17892-5). Article ISO 17892-5.

Ridley, A. M., & Wray, W. K. (1996). Suction measurement: A review of current theory and practices. In E. E. Alonso & P. Delage (Eds.), *1st Int. Conf. on Unsaturated Soils*.

Romero, E. (1999). *Characterisation and thermo-hydromechanical behaviour of unsaturated boom clay: an experimental study*. Univesitad Politecnica de Cataluna.

U.S.D.A. (1950). Diagnosis and Improvement of saline and alkali soils. *Soil Science Society of America Journal*, *18*, 348.

Vanapalli, S., Nicotera, M. V., & Sharma, R. (2008). Axis translation and Negative Water Column Techniques for Suction Control. *Geotechnical and Geological Engineering*, *26*(6), 645–660.

CHAPTER 5- ANALYSIS OF EXPERIMENTAL RESULTS

5.1. Introduction

This chapter presents the experimental results obtained in this dissertation. The results are analyzed and discussed as they are presented.

Initially, the geotechnical properties and geological characterization of eolian soils of Mayapo are presented, describing the soil mineralogy, the soil structure, the contacts between grains, and the distribution of minerals in the soil in order to know their influence in the volumetric behaviour of the eolian soils. Three components of suction are determined and analyzed: matric, total, and osmotic suction. The total and matric suction are analyzed with a double water retention curve to know the influence of the soil structure in the suction behaviour of the soils, the osmotic suction was analyzed using the pore water by squeezing technique. The results are also correlated to the geological and geotechnical characteristics.

Subsequently, the collapse potential of the eolian soils of Mayapo is determined through quantitative criteria by double oedometer tests. The maximum load when the soil presents the maximum collapse potential is also determined by the oedometer tests at different vertical net stresses. An analysis of results and their correlation with the geological and geotechnical properties is presented.

The influence of suction in the eolian soils of Mayapo is analyzed by the results of the unsaturated tests at suction controlled. First, the volumetric behaviour of the soil at different suction levels is analyzed by compressibility curves. Based on the results of the oedometer tests at constant suction, a constitutive model of the eolian soils is proposed based on the Barcelona Basic Model (BBM) proposed by Alonso et al., 1990. The model allows us to know the elastic domain of the eolian soils and the Loading collapse (LC) curve from which the soil presents irreversible deformations. By last, two unsaturated tests at different stress and suction path has been conducted in order and to evaluate the volumetric behaviour at different paths and to correlate the results with the LC curve.

5.2. Geotechnical classification and characterization of the eolian soils of Mayapo.

This section presents the geotechnical classification and characterization of the eolian soils of Mayapo. Table 5-1 presents the physical index of the eolian sands including the water content, specific gravity, void ratio, and saturation.

Table 5-1. Results of physical index of the eolian soils of Mayapo.

Sample	Moisture content (%)	Void ratio (e)	Specific Gravity
1A	5,5	0,605	2,68
1B	3,8	0,604	2,68
1C	5,1	0,605	2,65
2A	4,2	0,897	2,61
2B	5,6	0,78	2,62
2C	3,1	0,645	2,62
3A	12,2	0,755	2,64
3B	5,1	0,876	2,62
4A	7,4	0,813	2,63
4B	7,9	0,810	2,65
4C	5,4	0,686	2,64

The results of physical index are plotted in Figure 5-1. The results of the index properties do not exhibit large variations. The specific weight of solids is between the range of 26,10 and 26,80 kN/m^3. The samples present low moisture content, representing a low degree of saturation between 10 to 30 These values are representative of sands. The void ratio varies from 0,61 to 0,89. These values are representative of loose silty sand and loose uniform sand, according to Coduto, 1999.

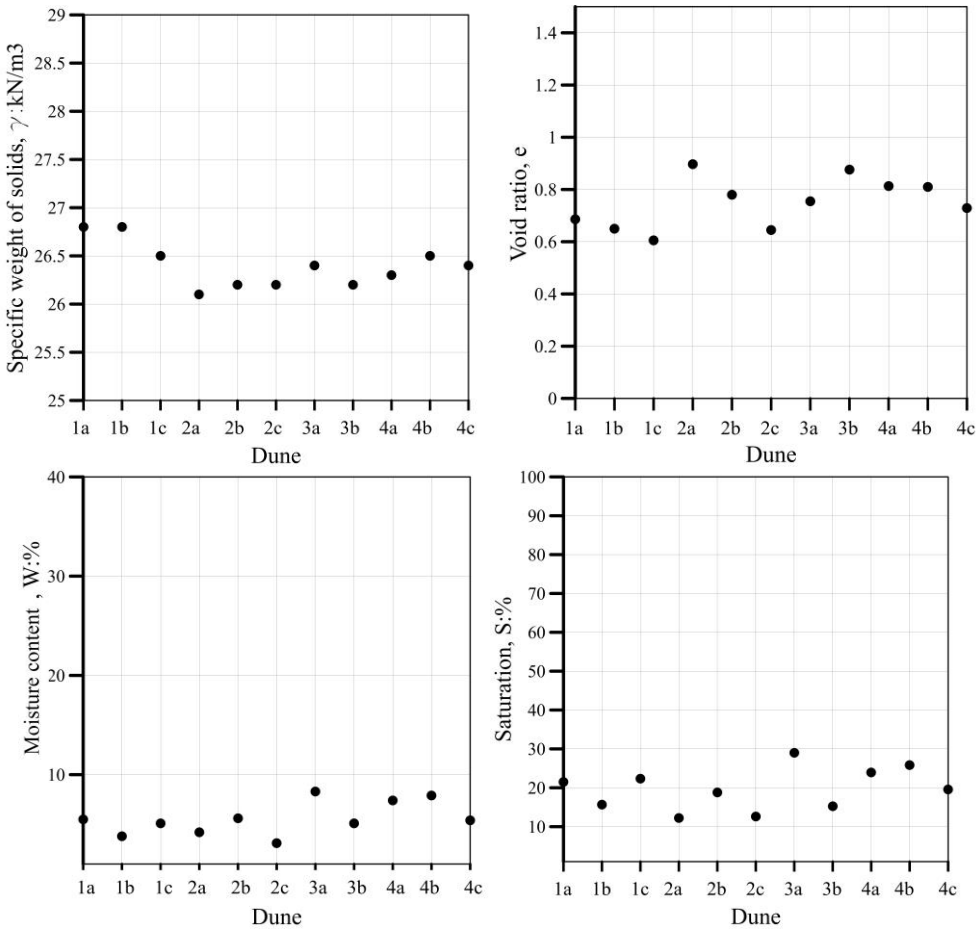

Figure 5-1. Results of physical index of eolian soils of Mayapo.

Although the physicals index are similar between the dunes and these properties are representative of loose uniform sand, there are small variations in the results, in the order of 20%, that could be due to are undisturbed samples and the soil structure, density, and porosity for each sample could be slightly different. These differences can also be presented from the origin of the material.

5.2.1. Particles size distribution by sedimentation method

Figure 5-2 shows the results of eolian soil particle size cumulative distribution in natural and deflocculated state. Table 5-2 presents the percent of the sand silt a clay particle, uniformity coefficient (Cu), and Curvature Coefficient (Cc) of the eolian soils.

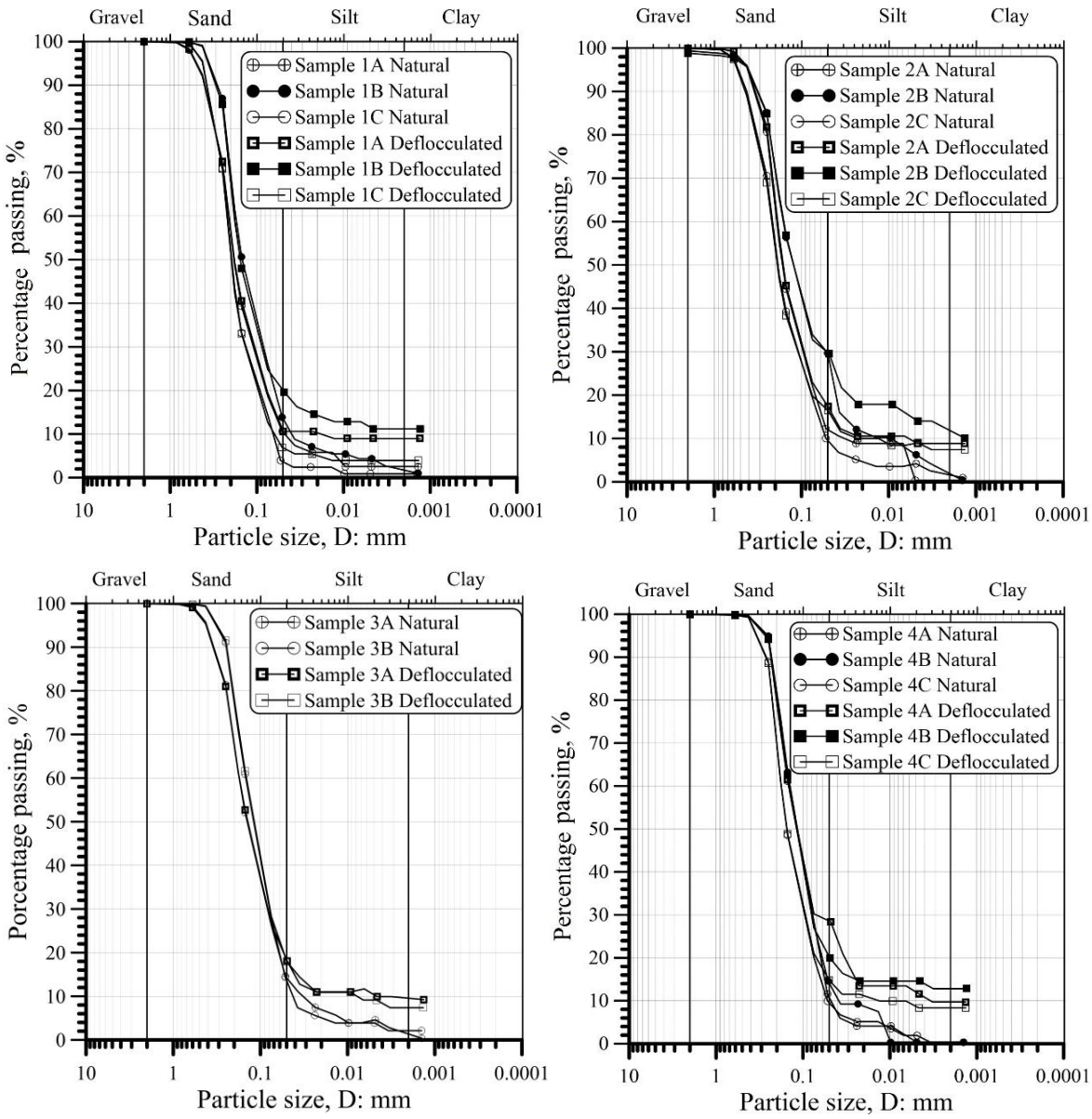

Figure 5-2. Particle size distribution obtained by sedimentation method for eolian soils of Mayapo.

According to the Unified soil Classification System, the classification for each sample of the eolian soils was Silty Sand (SM). The soil constituted sand with very low fines content. The soil is poorly graded soil. For the plasticity, the eolian soils were classified as non-plastic.

Table 5-2. Summary of grain size percentage, Cu and Cc of eolian soils.

	Sand ID	Sand (%)	Silt (%)	Clay (%)	Uniformity coefficient (Cu)	Coefficient of curvature (Cc)
1A	Natural	81,29	16,16	2,55	3,84	1,16
	Deflocculated	80,54	10,46	9,00	--	--
1B	Natural	73,92	21,69	4,39	4,50	0,98
	Deflocculated	75,17	13,63	11,2	--	--
1C	Natural	85,59	13,52	0,89	3,23	1,43
	Deflocculated	87,32	8,76	3,92	--	--
2A	Natural	78,01	21,65	0,34	4,75	0,04
	Deflocculated	77,05	14,15	8,80	--	--
2B	Natural	66,06	27,68	6,26	9,00	0,69
	Deflocculated	67,22	18,78	14,00	--	--
2C	Natural	80,68	15,14	4,18	3,81	1,04
	Deflocculated	80,18	10,82	9,00	--	--
3A	Natural	73,76	21,65	4,59	5,14	0,99
	Deflocculated	73,45	16,65	9,90	--	--
3B	Natural	72,17	23,96	3,87	3,55	0,88
	Deflocculated	71,77	19,12	9,11	--	--
4A	Natural	71,50	28,12	0,38	3,20	0,80
	Deflocculated	69,75	18,65	11,60	--	--
4B	Natural	72,33	27,31	0,36	3,33	0,94
	Deflocculated	73,01	12,39	14,60	--	--
4C	Natural	79,90	18,17	1,93	3,27	1,01
	Deflocculated	78,99	12,70	8,31	--	--

Despite the soil being classified as silty sand (SM), the sedimentation process of these soils occurs during several events causing the soil heterogeneity, as flaser beddings as detailed Chapter 3. The compositions of the bed flaser are mainly clay and sands with different sorting. The soil heterogeneity influences the volumetric behaviour of the soil directly.

Figure 5-3 shows a graphic representation of the coefficient of curvature (Cc) and coefficient of uniformity (Cu) of the eolian soils. The coefficient of curvature has a range of 0 to 1,50, and the coefficient of uniformity is in a range of 3,20 to 4,50, excepting the sample 2 with Cu of 9. The general results evidence that the soil is poorly graded, and the particles are uniforms. The uniformity in soil particles in the eolian soils could give a more porous structure to the soil and contribute to the collapse behaviour.

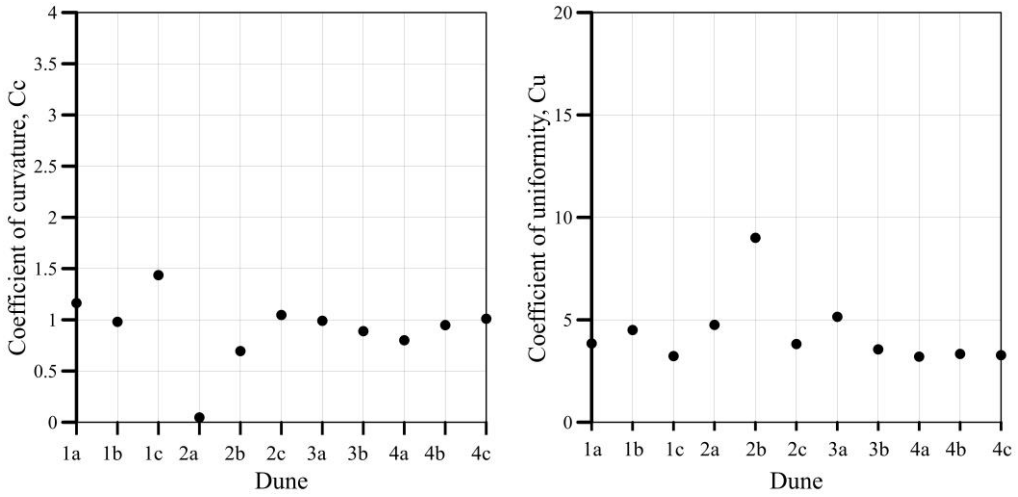

Figure 5-3. Left: Coefficient of curvature (Cc) of the eolian soils. Right: Coefficient of uniformity (Cu) of the eolian soils.

Figure 5-4 shows a graphic representation of fines percentage and the clay particles percentage in the natural and deflocculated eolian soils. The eolian soils have an average of 25% fines and a maximum of 33%. The fines maintain a similar percentage in the natural and deflocculated soils. This behaviour demonstrates that most of the aggregates are present only in fines size particles, and the sand particles present a low amount of aggregates.

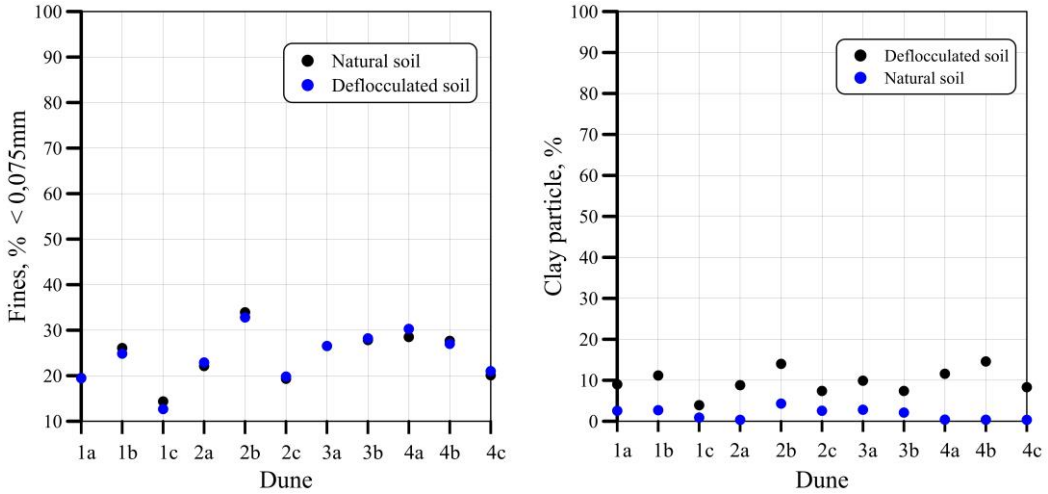

Figure 5-4. Left: Fines percentage of the eolian soils. Right: Clay particles of the eolian soils.

To evaluate the clay aggregated in the eolian soils, the expressions proposed by Araki, 1997 were used. It is shown in Eq 5-1 and 5-2. The clay percentages were obtained from the

granulometry tests with and without deflocculant. Figure 5-5 shows the results of the clay aggregated, and clay aggregated percentage of the eolian soils.

$$\text{Clay aggregates (\%)} = \text{Deflocculated clay size (\%)} - \text{Natural clay size (\%)} \qquad \text{Eq. 5-1}$$

$$\text{Clay aggregates percentage (\%)} = \frac{\text{Clay aggregates (\%)}}{\text{Deflocculated clay size (\%)}} \qquad \text{Eq. 5-2}$$

The eolian soil of Mayapo presents a small amount of clay aggregates in a range of 9 to 19 percent, the clay aggregates percentage in the soil varies from 65 to 97 percent.

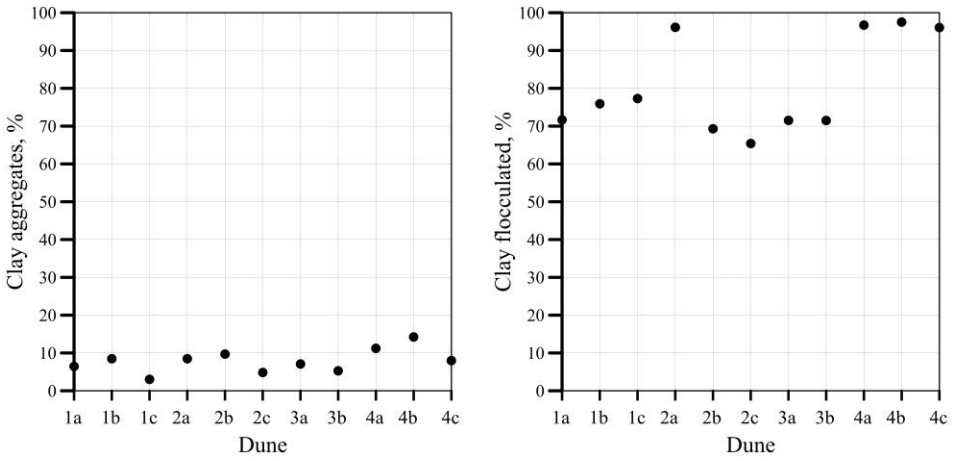

Figure 5-5. Right: Clay aggregated of the eolian soil of Mayapo (Equation 5-1). Left: Clay aggregates percentage of the eolian soils (Equation 5-2).

5.2.2. Particle size analysis using laser diffraction method

Figure 5-1 and Figure 5-6 shows the results of the granulometry curves of the four dunes in natural state obtained by the laser diffraction method. The soil was classified as silty sand (SM). The predominant grain size in the eolian soil of Mayapo is sand of 0,03 millimeters in diameter. Also, there are silt particles with 0,03 mm of diameter. The curves obtained are bimodal due to two-particle size predominant.

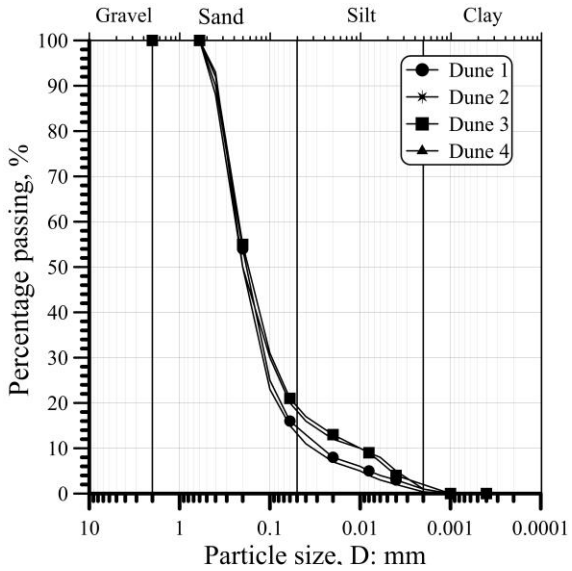

Figure 5-6. Results of granulometry by laser diffraction method.

Figure 5-7 shows the relation between particle size analysis results by the laser diffraction and hydrometer tests without deflocculant. The fines percentage in the laser method varies from 15 to 20 %. The fines percentage obtained by laser diffraction is similar to the results of the sedimentation method.

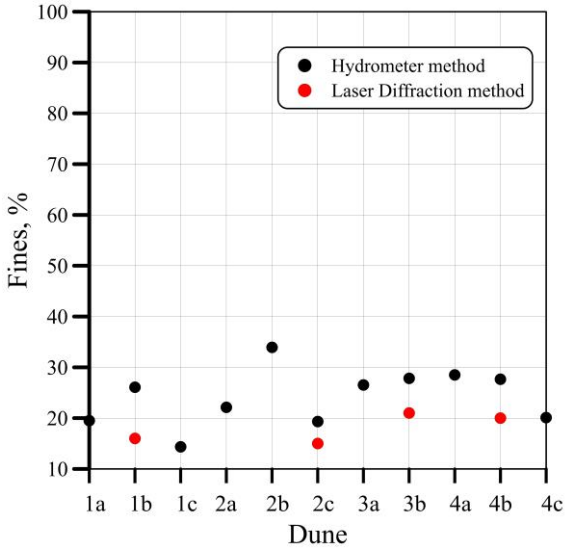

Figure 5-7. Comparison between fines percentage of laser diffraction and hydrometer test without deflocculant. Both methods are useful to obtain the percentage of the fines of the eolian soils.

5.2.3. Particle size analysis using blue of methylene method

The volume of blue of methylene introduced for the measurement was 60 cc, the total of VBS was 1,30, see Table 5-3. The passing percentage of 80 μm is 28,5. According to the Norme française 11-300, 1992, the soils is classified as B_5 how is shown in Figure 5-8, the soils are classified as very silty sands and gravels. The classification coincides with the USCS classification realized with the hydrometer tests.

Table 5-3. Results of particle size analysis using blue of methylene method.

Mass (g)	54,84
Moisture content (%)	1,74
Dry mass (g)	53,91
Volume de Blue introduced (10 g/l)	60 cc
VBS	1,3
Passing 80 μm (%)	28,5

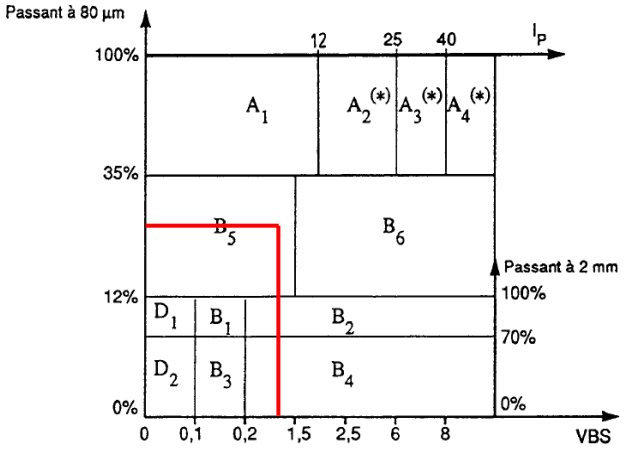

Figure 5-8. Eolian soils classification Norme française 11-300, 1992.

The soil classification and analysis of the percentage of the particles, the void ratio, and the soil density demonstrate that the soil presents similar physical index. Therefore, the tests of microstructure and volumetric behaviour were carried out in the four dunes studied. The main target is to have a better comprehension of the general behaviour of eolian soil of Mayapo regarding the geology, soil structure, suction and volumetric behaviour.

5.3. Microstructure

5.3.1. X-ray diffraction

Figure 5-9 shows the results of X-ray Diffraction carried out in the dune 4 of the eolian soil of Mayapo. The Figure 5-9 shows the minerals and its percentage in the sample. The predominant component of the eolian soil of Mayapo is α quartz or quartz low. This mineral was formed in low temperatures.

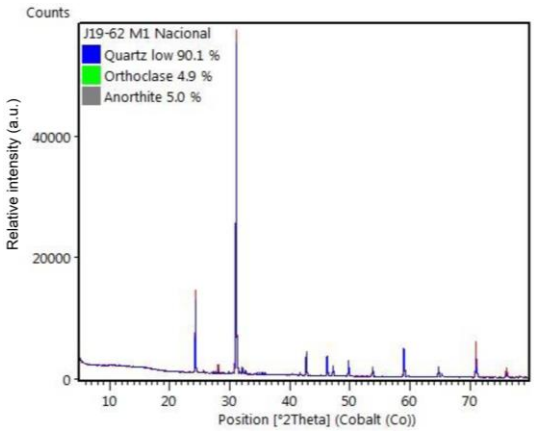

Figure 5-9. DRX results of the eolian soils of Mayapo.

The DRX results showed that the eolian sands are predominantly composed of quartz in 90,1%. It also presents minerals of Anorthite with 5% and orthoclase with 4,9%, a variety of plagioclase and feldspars, respectively. These minerals are characterized as igneous rock formers. It can infer that the origin of eolian soil studied is igneous rocks. Most of the sand-size particles of the eolian soils of Mayapo are composed of quartz crystals, this mineral is representative of these kinds of soils, which is resistant to the physical and chemical weathering.

5.3.2. Microstructural analysis with thin sections.

Figure 5-10 shows the results of the analysis of the thin section through the petrographic microscope. Thin Sections from each dune were observed, seeking to identify the minerals present and the contact between grains. The thin sections analysis shows that the mineralogic characteristics of the eolian soils are similar. Due to this, the analysis presented in this section is according to the four thin section results.

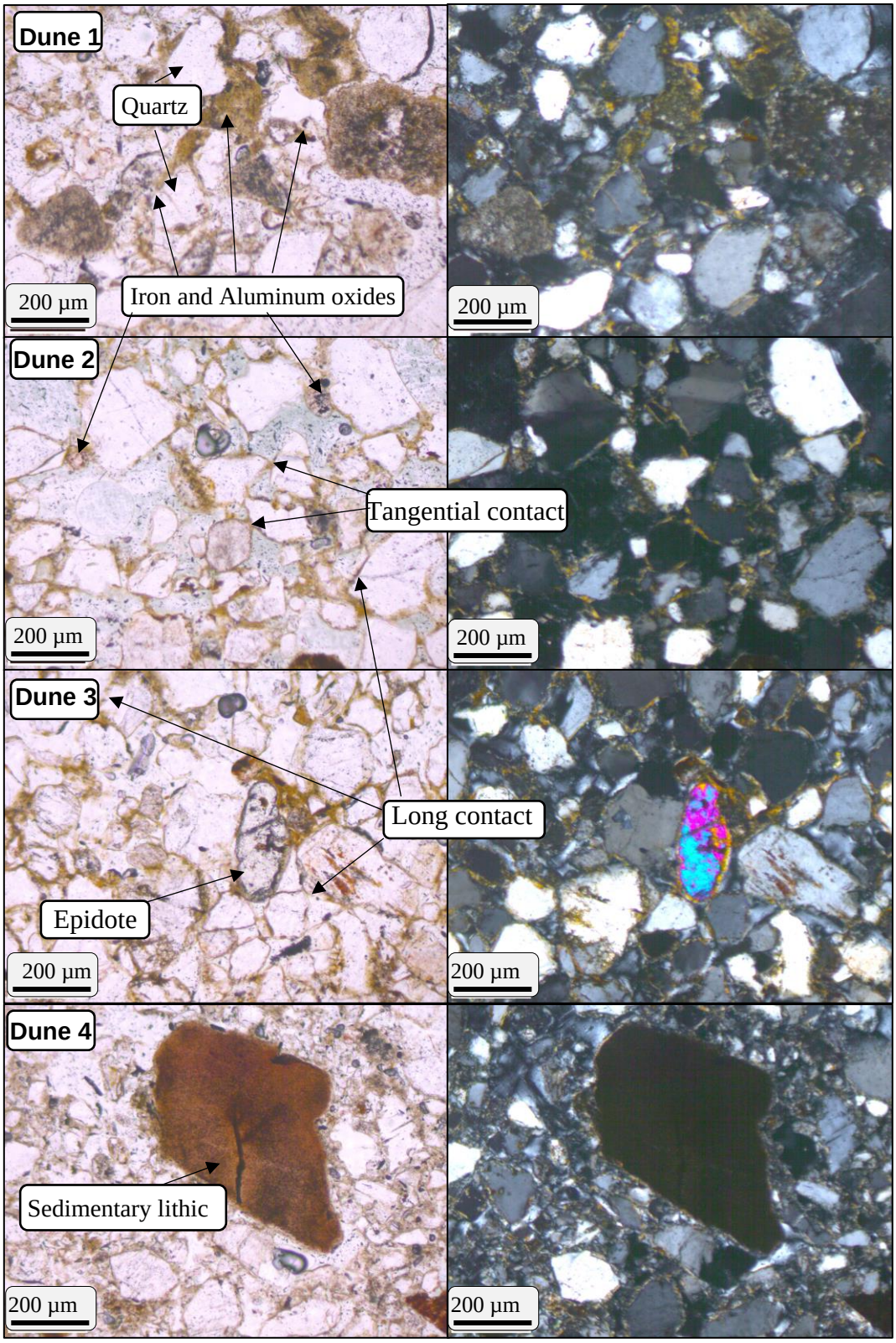

Figure 5-10. Micrographics of thin sections.

The soil presents similar grain size, according to granulometry analysis results, where the eolian soil is classified as poorly graded. The soil contains more sand-size grains than clay minerals.

The particles of the eolian soils are terrigenous minerals. The thin sections confirm the information of the x-ray diffraction test. The soil is mainly composed of crystals of quartz, plagioclases, and feldspars, minerals typic of these kinds of soils. Other minerals are present, such as titanium, zircon. In general, the crystals show evidence of reworking, and the minerals are formed in igneous environments.

The crystals of quartz present are colorless, fractured with fluid intrusions. The shape of quartz crystals is subangular to angular, evidencing that the wind transport was short, and the mineral could have more mechanic resistance. Also, it presents intrusions of zircon. The epidote crystals are also present in the eolian soils. This mineral is fractured with intrusions. The feldspars are present as grains and clay minerals, they are very fractured and reworked. Also, some opaque fine-granular minerals are distributed in the matrix, generally anhedral due to wear during eolic transport. The soil presents sedimentary lithics of mudstone with organic material.

There are two types of contacts: tangential contact or punctual contact and long contact. The contacts between the silt and sand particles are observed represented in light brown color, composed of iron and aluminum oxide. The contacts act as a bonding material and can be assimilated apparent cementation between the grains. This behaviour is typic of soil from arid regions when the temperature and the oxides, carbonates, or silica generate this cementation.

According to the geological history, the minerals presented are originally formed in igneous rocks, the origin could have from rocks of the river next to the eolian soils region, which has contribution from different geological formations. After that, the eolian soils presented sort transport, evidencing in the angular shape mineral.

5.3.3. Scanning electronic microscopy (SEM) for direct fabric viewing

Figure 5-11 shows four photomicrographs of the eolian soils with a magnification of 110x. These images have been taken of the undisturbed samples of the eolian soils from Mayapo. Also, it is presented the digitized and processed photomicrographs. The Scanning electronic microcopy was also used to analyses the thin sections, which is presents in EDS results.

These deposits comprise angular, silt, and sand-size particles. The grains have marked edges and are characterized primarily by conchoidal breakage patters, v-shaped pits, and curved grooves. Angular grains are evidencing that transport distance was short. Many impacts may be observed on the grain surface that is typical of eolian transport because of the impact of the edges of some grains against others during transport. This particle shape can influence soil structure stability.

Figure 5-11 also shows graphic representations of the SEM photomicrographs of eolian soil. The black and white scale was used to differentiate pores from the soil particles. Dark pixels are the pores, and the white pixels are the soil particles. Some results of the analysis of graphic representations are shown in Table 5-4. The diameter of the grains is of the order of 90 µm. The porosity percentage is an average of 26 %. However, these values were calculated of a small section of the sample, and it just give an idea of these values in all samples

Table 5-4. Results of analysis of graphic representation of SEM Photomicrographs.

Dune	Porosity (%)	Size grain prom (µm)
1	24	80
2	26	87
3	24	98
4	20	98

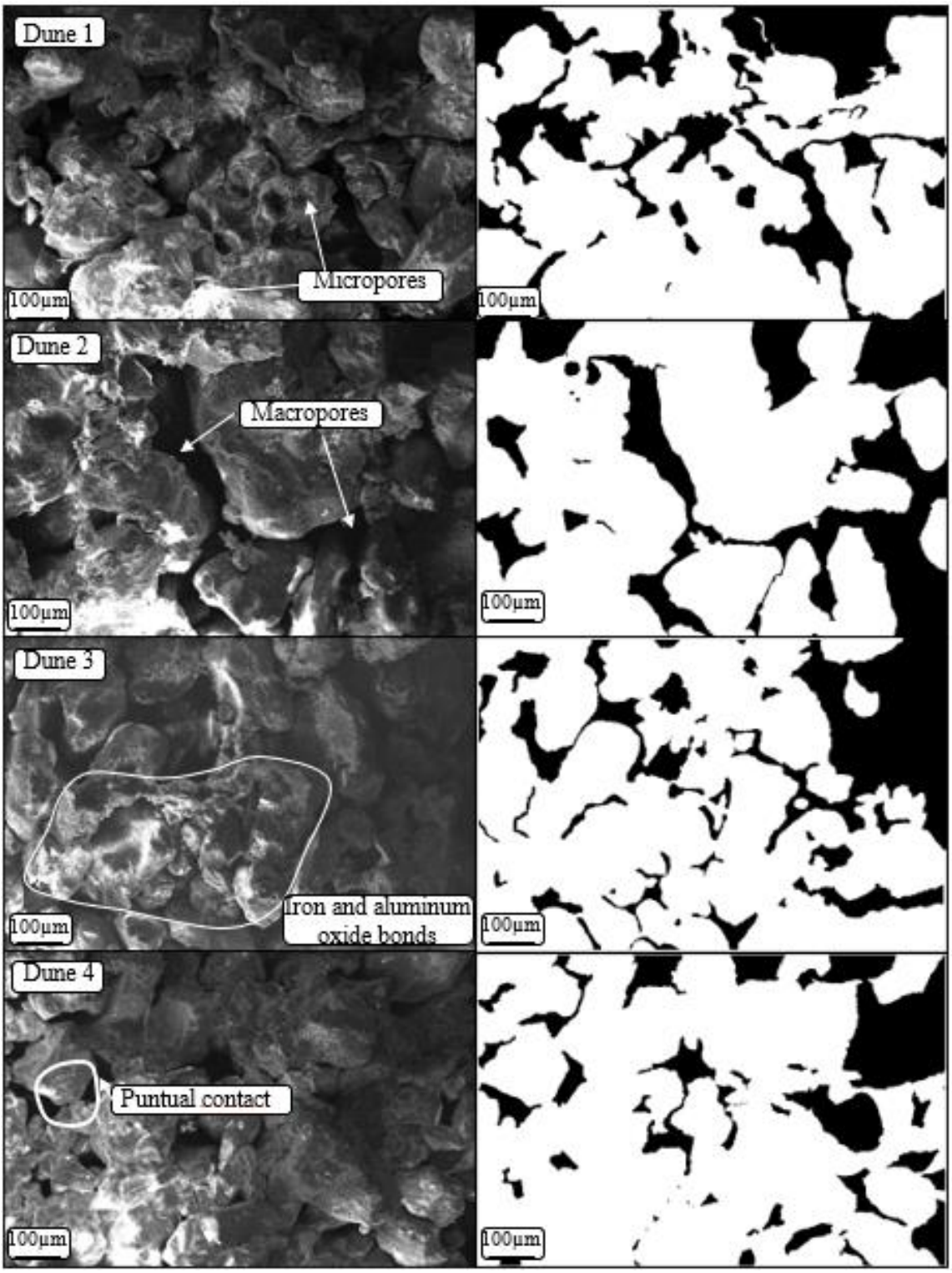

Figure 5-11. SEM Photomicrographs of eolian soils and the graphic representation of porosity in the samples. Pores are black and particles white.

The eolian soils present some punctual contacts, as shown in Figure 5-11. This type of contact could cause particles to slide over each other, leading to a rearrangement of the structure. Particles with punctual contact are mostly naked, making the soil more susceptible to collapse.

The soil presents large and continuous macropores. Due to this, the eolian soils have a low density, high permeability. The micropores are also present in the eolian soils it can be observed between the soil aggregates. The micropores presented contributes to the collapse behaviour and the susceptibility, but the total collapse of eolian soils could be controlled by the presence of macropores.

The SEM analysis can be reinforced considering the results of the analysis of particle size distribution. The type of porosity of the eolian soils is associated with the particle size of the eolian soil. The soil is composed mostly of grains sand-size, which is associated with the presence of the macropores. The low presence of micropores is attributed to the low percentage of fines in the soil. It can be inferred that the eolian soils have a behaviour typic of the granular soils.

5.3.4. Energy dispersive X-ray spectrometry EDS

The element distributions maps of eolian soils are shown in this section. The dispersive energy X-ray spectrometry with SEM is used to determine the distribution of chemical elements in the section studied. Table 5-5 shows the elemental composition in weight percent of the dunes.

Table 5-5. Elemental composition in weight percent of the dunes.

Names of elements	Elemental composition -weight (%)			
	Dune 1	Dune 2	Dune 3	Dune 4
Silica (Si)	43,20	38,88	39,06	42,16
Oxygen (O)	52,06	49,51	51,95	50,79
Aluminum (Al)	2,36	5,22	3,80	2,69
Iron (Fe)	0,90	2,43	1,87	1,02
Sodium (Na)	0,24	0,85	0,51	0,49
Chlorine (Cl)	0,37	----	0,42	0,41
Titanium (Ti)	----	1,14	0,18	----
Calcium (Ca)	----	1,08	1,12	----
Potassium (K)	0,87	0,89	0,81	0,86
Magnesium (Mg)	----	----	0,28	----

Figure 5-12 to Figure 5-19 shows the distribution of the elements of the dunes. Each figure is composed of an SEM micrograph, a graphic representation of the percentage of the element, and the distribution maps for each element in the section analyzed, see Figure 5-13.

The four EDS spectra show very similar results, i.e.., the presence of silica, oxygen, iron, aluminum, chlorine, sodium have similar relative intensities. The silica (Si) and oxygen (O) are present on the map with the same distribution. The combined distribution of these elements can be interpreted as the presence of quartz mineral.

The salts are evidenced in chorine (Cl), and sodium (Na) maps. The salt particles are not in the contact between the grains, but it is presented in the disseminated form. It can be inferred that the collapse behaviour would not be governed by the dissolution of these salts. However, the presence of salt particles affects the suction of the eolian soil, attracting more water to the soil.

The calcium element is concentrated in a region of the calcium map. It can be inferred that the element is a seashell fragment. The calcium is not forming carbonates bonding in the eolian soils. It was the hypothesis raised at the beginning of the research because the dunes were sampling in blocks and the dunes were formed in marine environments.

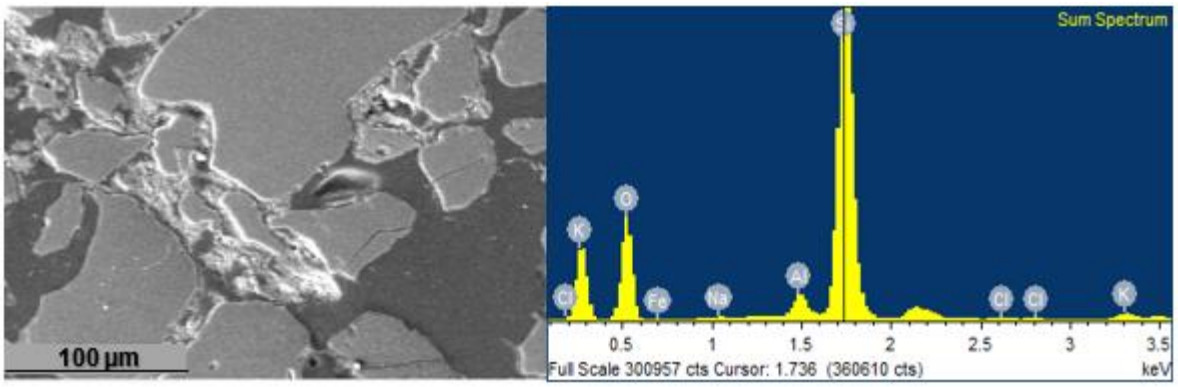

Figure 5-12. SEM images and EDS spectra of element dune 1.

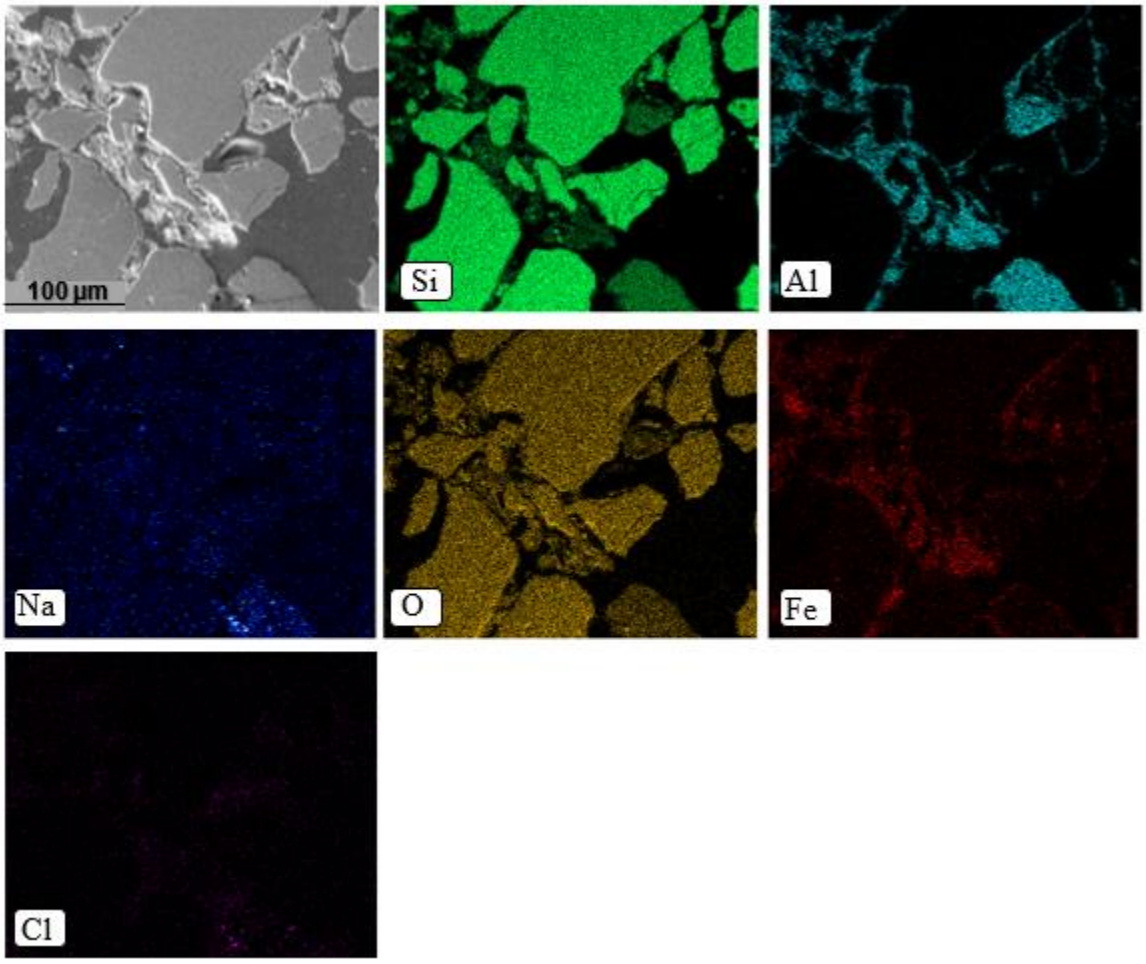

Figure 5-13. Element distributions maps using SEM-EDS dune 1.

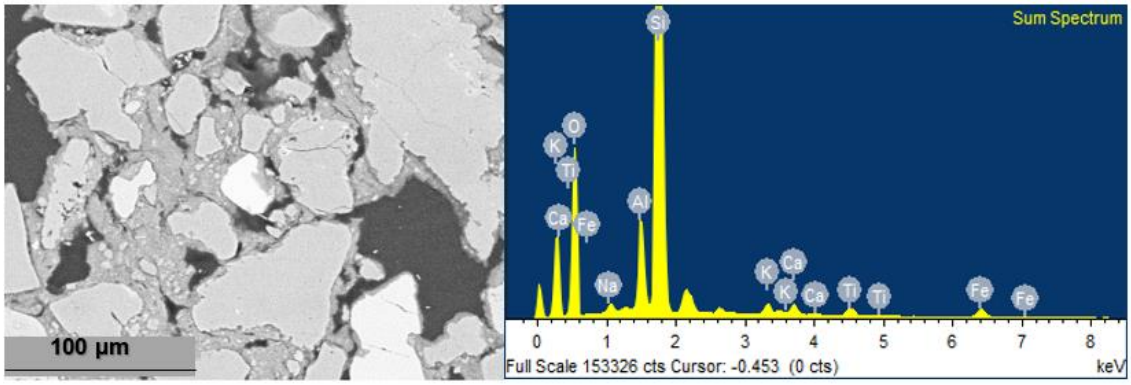

Figure 5-14. SEM images and EDS spectra of element dune 2.

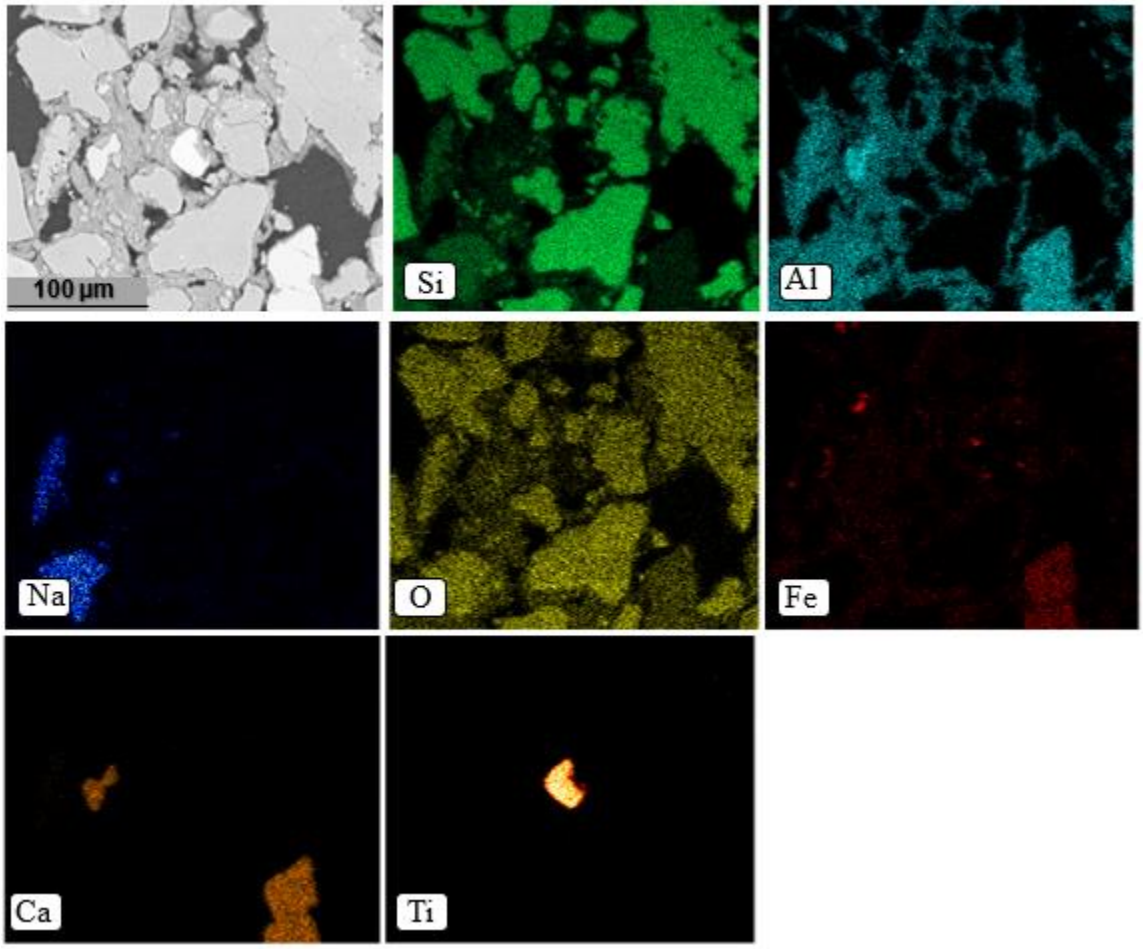

Figure 5-15. Element distributions maps using SEM-EDS dune 2.

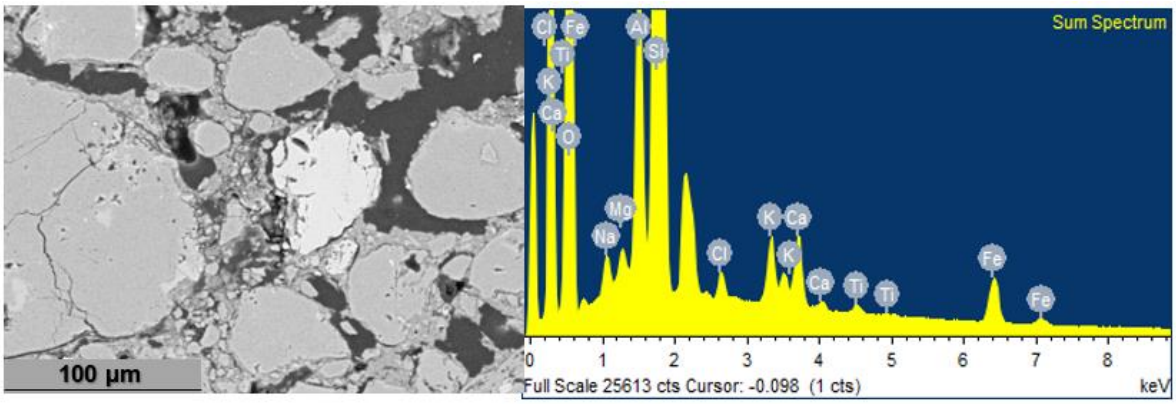

Figure 5-16. SEM images and EDS spectra of element dune 3.

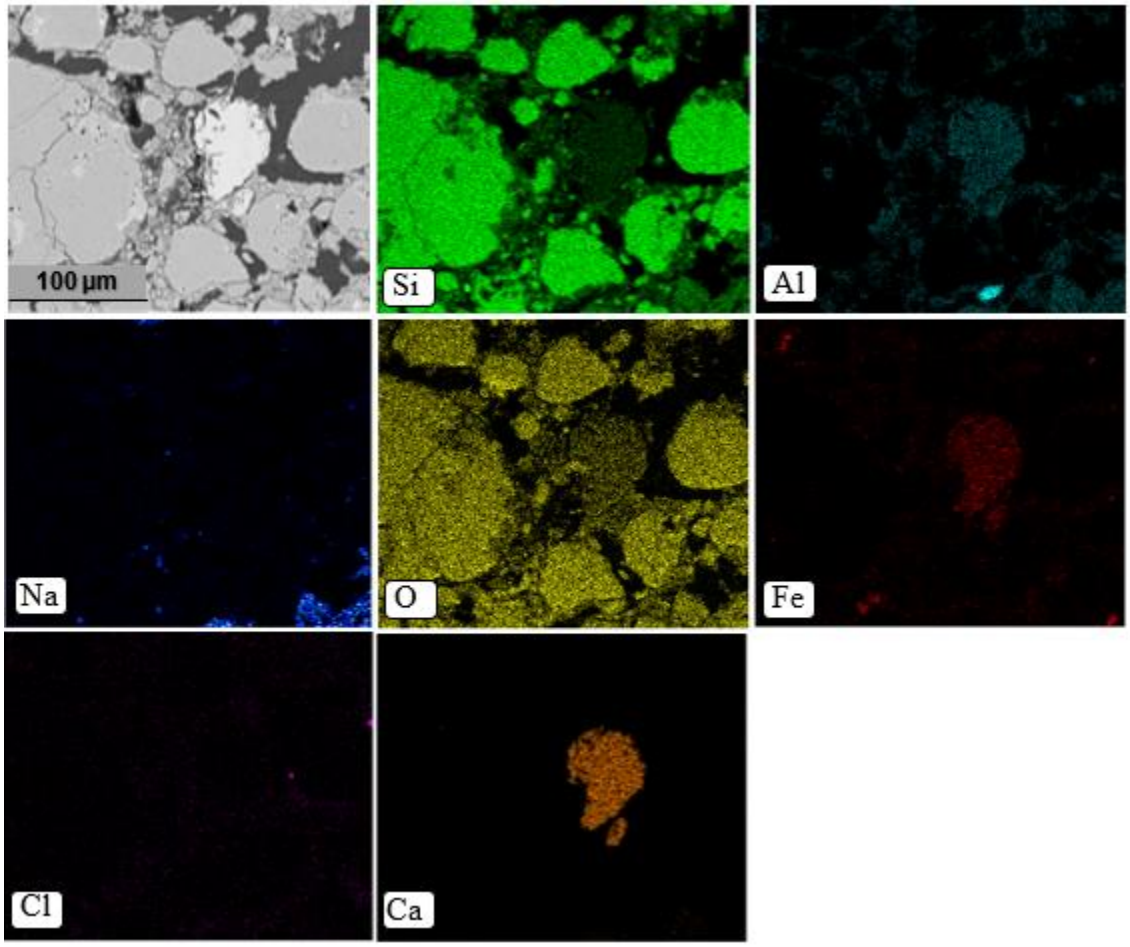

Figure 5-17. Element distributions maps using SEM-EDS dune 3.

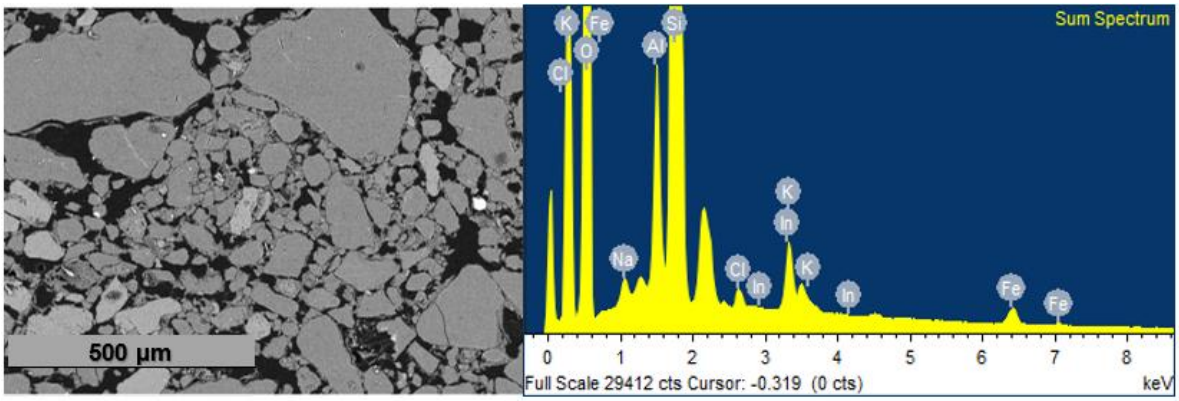

Figure 5-18. SEM images and EDS spectra of element dune 4.

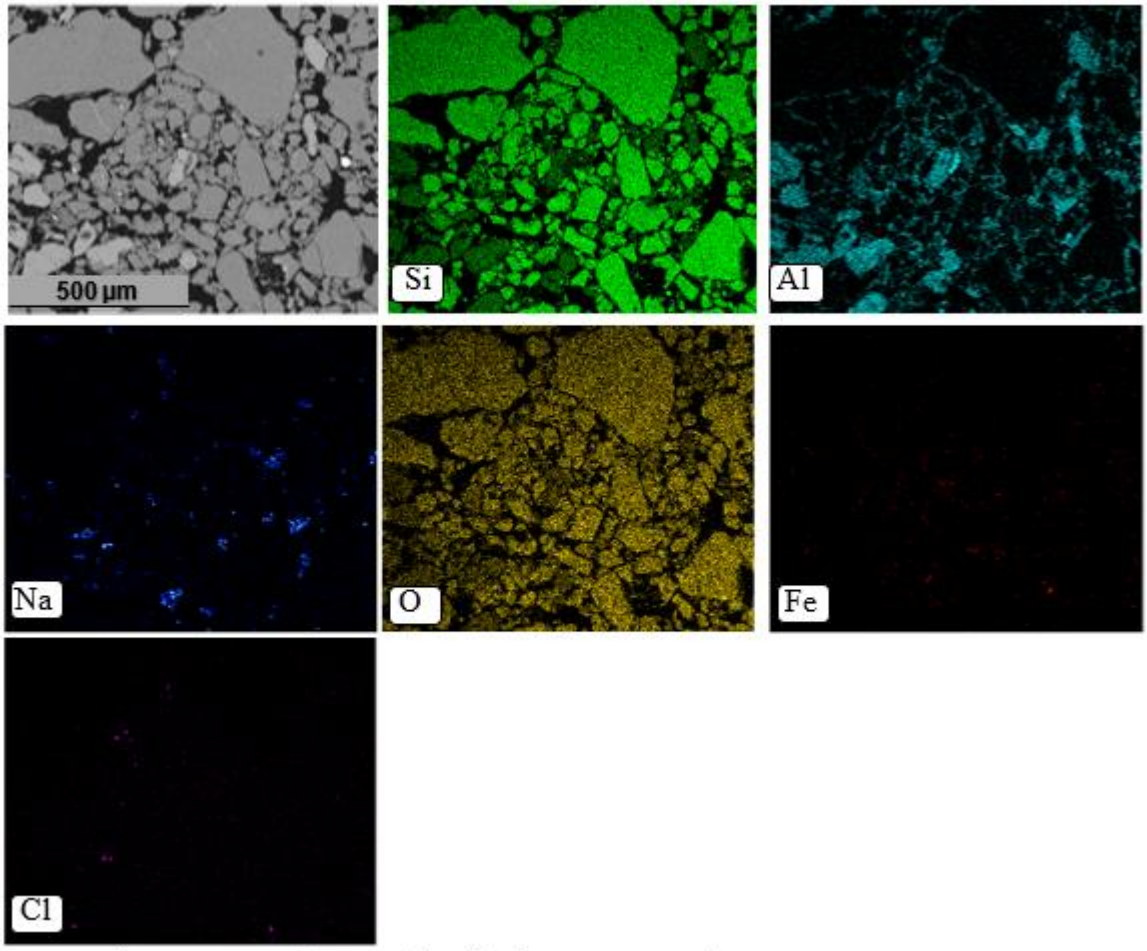

Figure 5-19. Element distributions maps using SEM-EDS dune 4.

The Aluminum (Al) and Iron (Fe) elements are distributed around the minerals of quartz and feldspars, providing further evidence that the aluminum oxides and iron oxides act as a bonding material between grains as show the results obtained in thin sections. The four EDS spectra show similar results, i.e.., the presence of silica, oxygen, iron, aluminum, chlorine, sodium have similar relative intensities. The bonding of aluminum and iron oxides are bordering the grains in all samples of the eolian soils. However, the Aluminum and Iron elements do not exceed 6% in the EDS micrographs. It can be inferred that although these oxides can have influence in the soil behaviour acting as a bonding material, the total collapse behaviour won´t be controlled by this cementation due to the low percentage of these.

5.4. Suction measurement

5.4.1. Water retention curve. Total and matric suction measurement

The results of suction measured using the paper filter method is presented in this section. The water retention curve (WRC) linking suction and equivalent degree of saturation is given by the following modified van Genuchten, 1980 equation:

$$S_e = \frac{Sr - Sr_{res}}{Sr_{max} - Sr_{res}} = \left(1 + \left(\frac{P_g - P_L}{P}\right)^{\frac{1}{1-\lambda}}\right)^{-\lambda} \quad \text{Eq. 5-3}$$

Where,

S_e is the equivalent saturation degree.

Sr, Sr_{max}, Sr_{res} are the actual, the maximum and the residual saturation degree.

$P =$ The air entry value.

λ = A model parameter, the shape function for retention curve.

P_g and $P_L =$ The gas and liquid pressure.

For Van Genuchten equation Sr_{max} is 1 and Sr_{res} is 0. Figure 5-20 shows fitted simple water retention curves for total and matric suction according to the experimental data of dunes 1 and 4. The red line represents the simple water retention curves for total suction, and the blue

line is the simple water retention curves for matric suction. A simple WRC can be fitted for both soils. It means that related to the water attraction to the soil, the behaviour of the dune is similar.

The simple water retention curves represent the behaviour of the macropores. The parameters obtained from the simple water retention curves based on the Van Genuchten equation are Po that represents the air entry values (AEV), and λ representing the slope to which the soil desaturates. The results are summarized in Table 5-7.

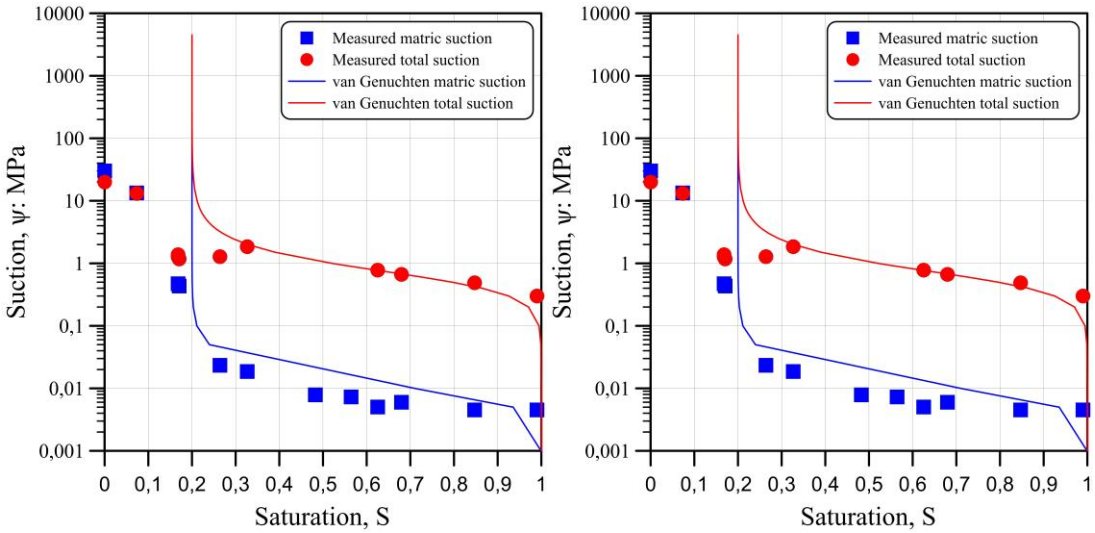

Figure 5-20. Simple water retention curves (WCR) for dune 1 and 4.

Table 5-6. Po and λ parameters from water retention curves of the eolian soils.

Suction	Pores	Po: Air entry value (AEV). kPa	λ (parameter in function of curve shape).
Matric	Macropores	15	0,70
Total		550	0,60

However, the simple water retention curve is not sufficient to fully represent the suction of the eolian soils. Due to this, a double water retention curves proposed by Durner, 1994 was calculated. The double retention curve describes properly the retention characteristics of soil with the heterogenous pore systems: macropores and micropores. It can be obtained by the following equation constructed by a linear superposition of sub-curves of the Van Genuchten type:

$$S_e = \frac{Sr - Sr_{res}}{Sr_{max} - Sr_{res}} = w_1[WRC]_1 + w_2[WRC]_2 \qquad \text{Eq. 5-4}$$

Where,

S_e is the equivalent saturation degree of each structural level

Sr, Sr_{max}, Sr_{res} are the actual, the maximum and the residual saturation degree of each structural level (micro and macro)

w are weighting factors for the sub-curves, subject to $0 < w < 1$ and $\Sigma w = 1$

$[WRC]_1$ is the water retention curve Van Genuchten type for macropores

$[WRC]_2$ is the water retention curve Van Genuchten type for micropores

Figure 5-21 and Figure 5-22 show the water retention sub-curves for the macropores and micropores of the eolian soils.

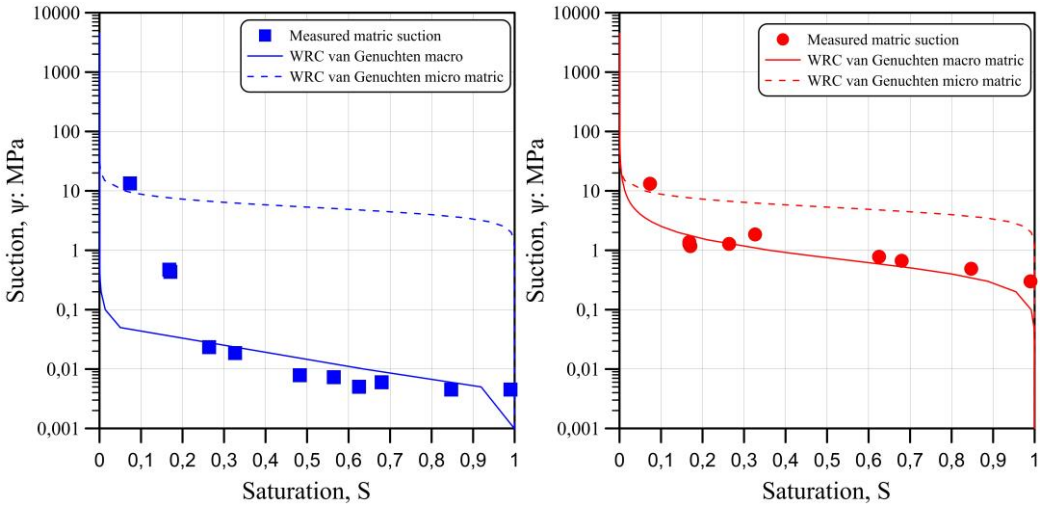

Figure 5-21. Water retention curve of macro-structure and micro-structure of dune 1.

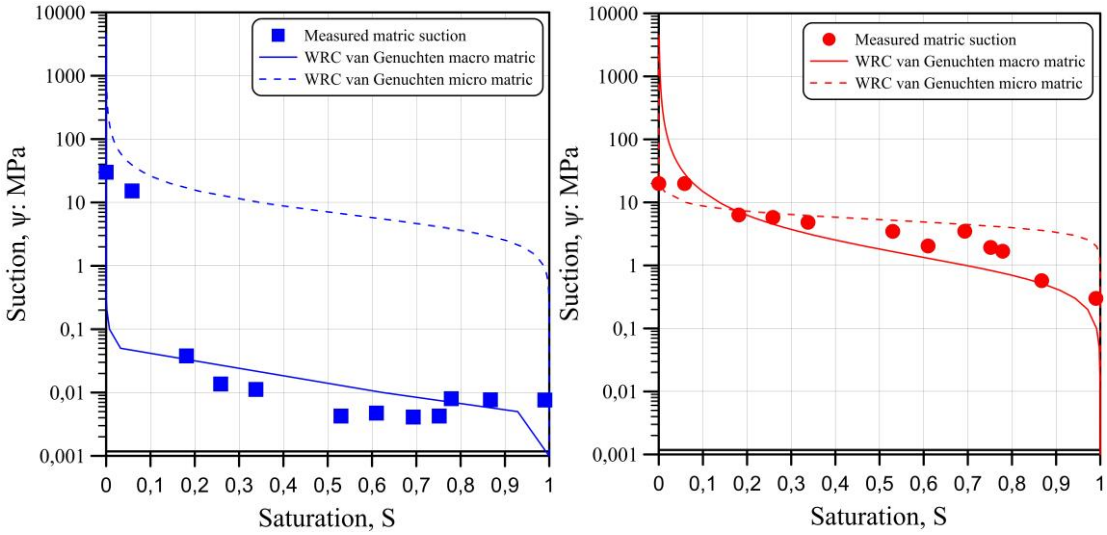

Figure 5-22. Water retention curve of macro-structure and micro-structure of dune 4.

To construct the double water retention curves for the eolian soils, a weighting factor of 0,20 was assigned for micropores and 0,80 for the macropores. These weighing factors were assigned according to the granulometry distribution. it shows the double water retention curves for the eolian soils using Durner, 1994 equation. Figure 5-23 It can be observed that the curve bends at a saturation of 0,20. This behaviour shows that the weight of the microstructure is very low and corresponds to the small fraction of clay present between grains of soil.

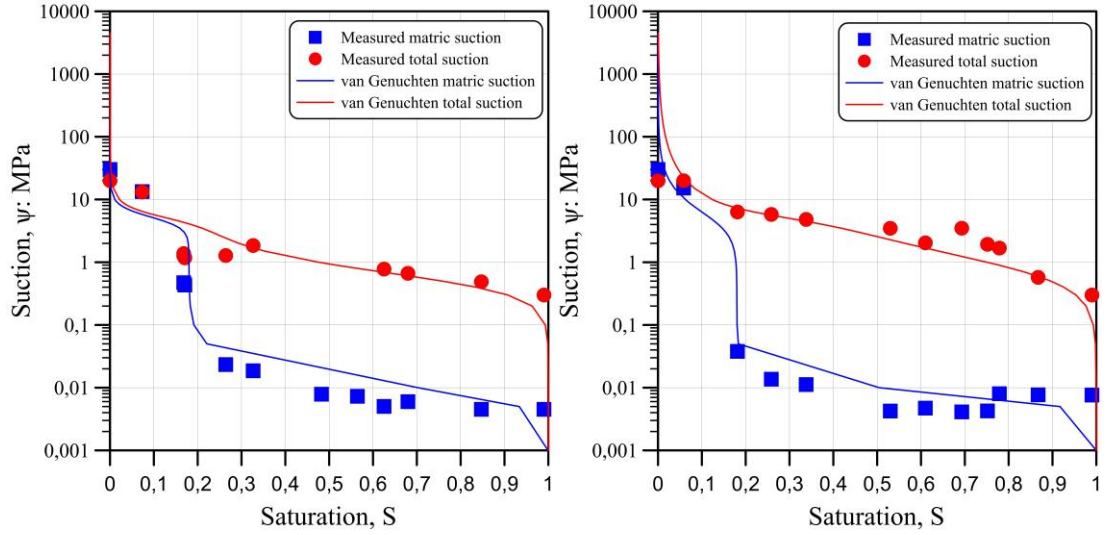

Figure 5-23. Double water retention curves (WRC) of dune 1 and 4 respectively.

The parameters obtained from the double water retention curves are Po, the air entry values (AEV), and λ representing the slope to which the soil desaturates. The results are summarized in Table 5-7.

Table 5-7. Po and λ parameters from water retention curves of the eolian soils.

Suction	Pores	Dune 1		Dune 4	
		Po (AEV)	λ	Po (AEV)	λ
Matric	Macro	10	0,65	10	0,68
	Micro	5000	0,8	5000	0,58
Total	Macro	550	0,6	550	0,45
	Micro	5000	0,8	5000	0,80

Po: Air entry value (AEV) kPa. λ: Parameter in function of curve shape

It can be demonstrated that at low saturation degrees, the water flow can be controlled by the fines present in the micropores. From 0 to 20% of saturation, and the water will come out of the soil with greater difficulty because the micropores govern the suction at these degrees of saturation. According to the physical index tests, the eolian soils have saturation values in the order of 20% in its natural state, representing high suction levels, generating interparticle forces, and providing stiffened to the soil. These high levels of suction can influence the collapse behaviour due to, with small increases in saturation, the suction will become governed by the macropores, and the suction will decrease sharply.

5.4.2. Pore water extraction by squeezing technique. Osmotic suction measurement

With the purpose of determining the osmotic suction in the eolian soils was to use the pore water extraction by squeezing technique. The electrical conductivity of the pore water from the eolian soils in saturated conditions was 8,46 mS/cm = 8460 µS/cm. The osmotic suction of this pore water containing mixtures of dissolved salts, estimated from the electrical conductivity is $\pi = 315$ kPa according to USDA,1950, and $\pi = 365$ kPa obtained from the NaCl calibration curve of Romero, 1999. Figure 5-24 shows the electrical conductivity results of osmotic suction, the relationships between osmotic suction, and osmotic suction obtained by Wan et al., 1995, calculated as the numerical difference between total and matric suction obtained with filter paper technique.

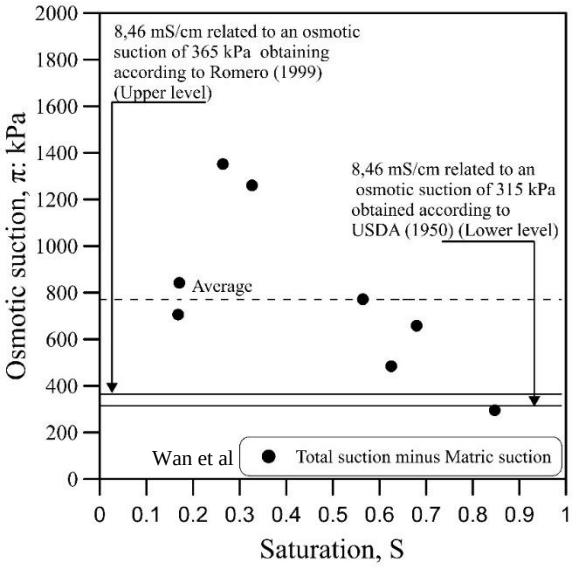

Figure 5-24. Electrical conductivity and filter paper techniques for osmotic suction measurement.

Figure 5-24 also shows that the value estimated of osmotic suction based on the electrical conductivity is agreed with the osmotic suction obtained by Wan et al., 1995, for the highest saturation degree. This close agreement, also demonstrated in Romero, 1999, indicates the reliability of the pore water extraction by squeezing technique for osmotic suction measurements, and certain support of the validity of matric and osmotic suctions being components of total suction. Also, it can be inferred that the osmotic suction appears to be dependent on the saturation degree.

Figure 5-24 shows that with the decreased in saturation degree, the osmotic suction increases for the region of macropores. Subsequently, the matric suction plays an important role in the total suction, increasing its value by the presence of fines, causing a decrease in osmotic suction.

The osmotic suction can be physically explained by the presence of salts particle shows in the EDS test results. The salt concentration influences the osmotic suction and the total suction of the eolian soil. Osmotic suction could affect the hydraulic conditions of the eolian soil. It can govern the water flow and attract more water to the soil, increasing the saturation

degree. The increase in saturation causes a decrease in total suction in the soil, affecting the volumetric behaviour of soil.

5.5. Volumetric behaviour

5.5.1. Classical oedometers

5.1.1.1. Double oedometer test

The double oedometer tests were carried out to know if the eolian soils from Mayapo are collapsible. Test results from double oedometer tests are shown in Figure 5-25, when vertical net stress applied is plotted versus Void ratio.

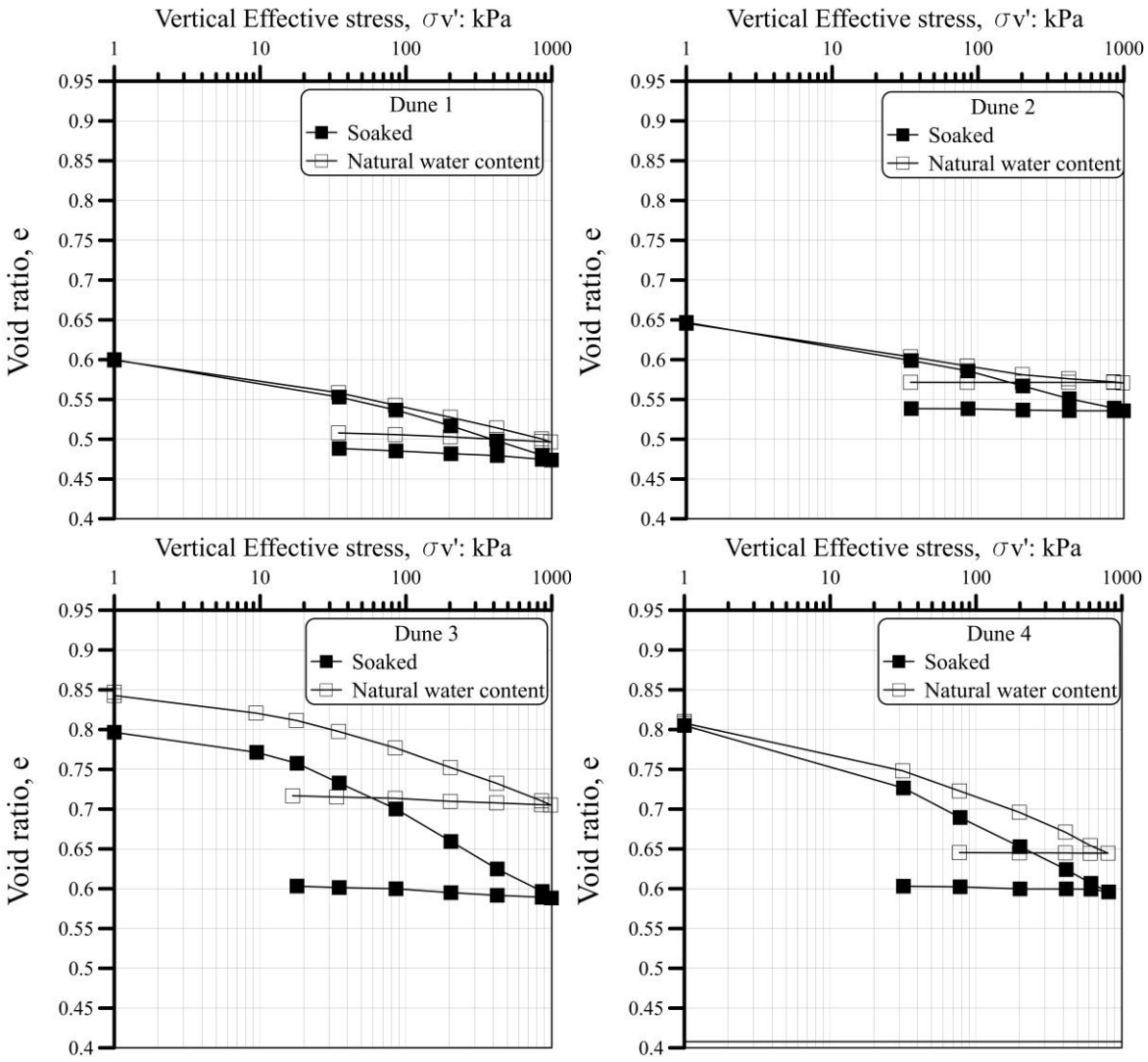

Figure 5-25. Compression curve from double oedometer tests of eolian soils.

Table 5-8 shows the initial conditions of the double oedometer tests and the results of the collapse potential. The initial matric suction of each oedometer test was determined from the eolian soil Water retention curve (WRC) and using the initial moisture content of each test.

Table 5-8. Initial conditions of the oedometer tests and CP of the eolian soils.

Dune	%w initial	Saturation initial (%)	Matric suction initial (kPa)	e_0	CP (%)	Severity of the problem
1	6,64	29	40	0,600	1,56	A Moderate problem
2	7,34	22	80	0,65	2,28	A Moderate problem
3	3,84	15	4000	0,847	4,49	A Moderate problem
4	4,73	15	4000	0,810	2,73	A Moderate problem

According to the results shown in Table 5-8, the eolian soils were classified related to the severity of the problem as a moderated problem based on Jennings and Knight, 1957 classification. It can be denoted the maximum collapse is presented in dune 3, which has the lower moisture content and the highest void ratio. However, the value of collapse potential for this dune can be considerate as problematic in practical engineering.

The collapse presented can be explained by the high quantity of macropores, which contribute to the overall collapse due to the particle rearrangement in the soil. Although the grains are covered by the bonding of iron and aluminum oxides, the percentage of these is very low, and the particles rearrange easier between the macropores. Regarding the micropores, this can contribute to the initial soil collapse due to the suction decreases rapidly when the soil gets wet, decreasing the suction also. However, the most amount of collapse is due to the soil rearrangement in the macropores.

The suction also plays an important role in the results of the collapse potential. As suction decreases and soil wets, water menisci coalesce, and the empty pores are flooded, and it causes a loss in the soil stiffness. On the other hand, it can be inferred that the collapse potential increases as the initial matric suction increases. This indicates that higher initial matric suction levels try to maintain the meta-stable bound between particles without significant settlement but eventually collapse upon inundation (Alonso et al., 1990).

The high initial suction levels in dunes 3 and 4 also indicate that the initial suction is initially governed by the micropores as shown in the double water retention curve. However, the suction decreases rapidly during the saturation process due to the matric suction will become governed by macropores, and the soils experience more collapse.

Although these results give a little knowledge about the role of suction in the collapse behaviour, the classical oedometer tests are not sufficient to explain fully the influence of the suction on the volumetric behaviour of the soils, therefore, it will be investigated using suction-controlled tests.

Table 5-9 shows the compression index, recompression index, and the yield stress from the compressibility curves of the double oedometer tests. The results indicate that the compression index Cc and Cr are lower in soaked specimens than the specimens in natural states. Also, the yield stress values are lower in specimens collapsed. These results can indicate that the stiffness of the eolian soils decreases when the soil is collapsed due to the bonding materials (water meniscus and ferromagnesian minerals) are dissolved and transported by water (Rogers, 1995).

Table 5-9. Cc, Cr and yield stresses from compressibility curves of the eolian soils.

Dune	Soaked			Natural		
	Cc	Cr	Yield stress (kPa)	Cc	Cr	Yield stress (kPa)
1	0,061	0,035	40	0,058	0,032	60
2	0,042	0,077	50	0,041	0,027	60
3	0,091	0,050	25	0,072	0,023	40
4	0,091	0,052	40	0,079	0,040	60

Comparing the compression index Cc y Cr in the natural and soaked state between dunes, it can be denoted a higher difference in dunes 3 and 4 than in dunes 1 and 2. Due to this, it is inferred that in dunes 3 and 4, the change in the stiffness is greater, and therefore, the collapse potential is higher. These results are consistent with the physical index, due to the initial moisture content is smaller and the void ratio are higher for dunes 3 and 4, as shown Table 5-8.

Figure 5-26 show the normalized curves from the compressibility curve of the double oedometer tests.

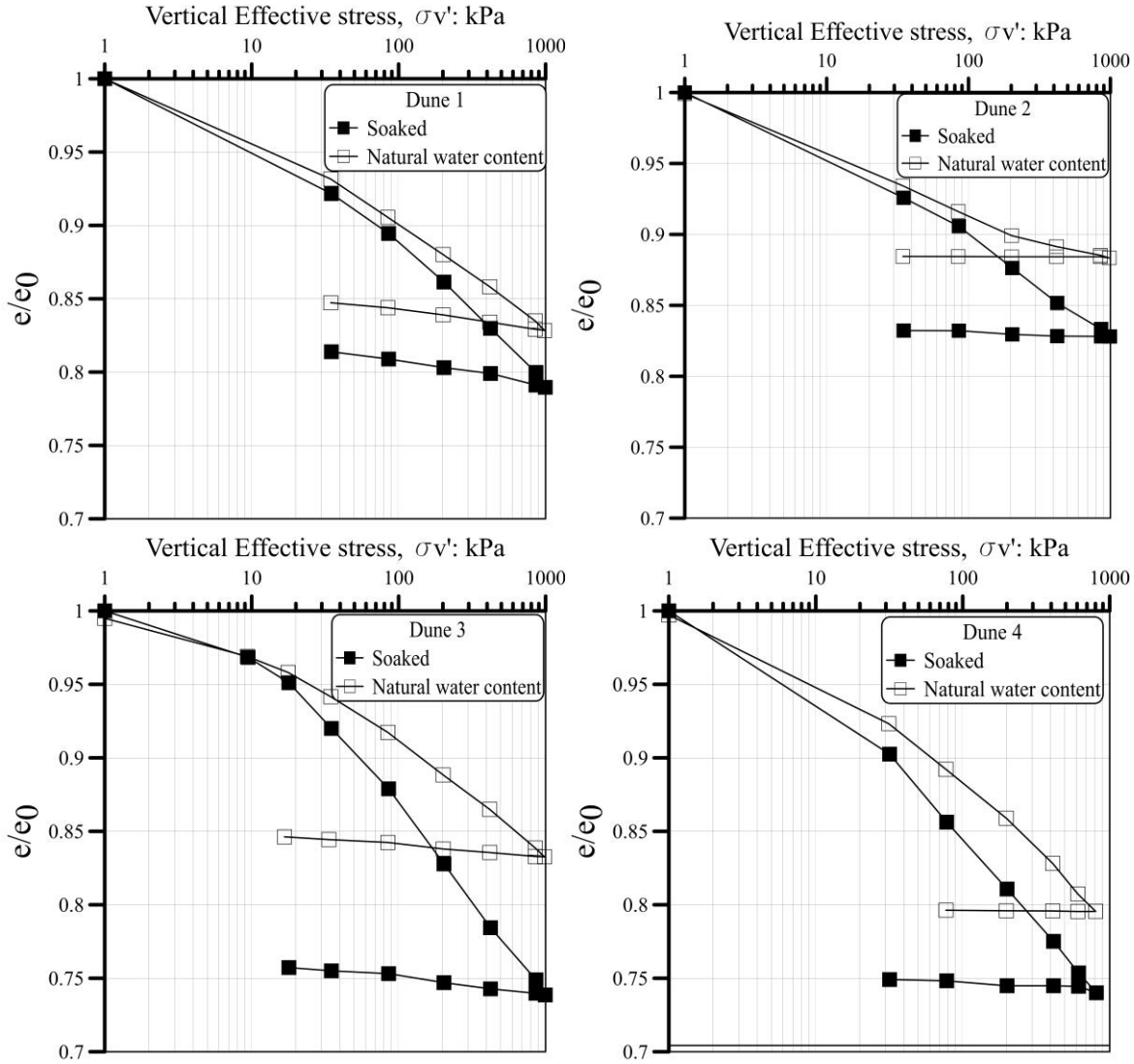

Figure 5-26. Compressibility curves normalized of double oedometer tests.

Figure 5-27 shows a graphic representation of the influence of the void ratio variable in the collapse behaviour for the double oedometer tests. It is denoted that the collapse potential increase with the increment of the initial void ratio. Dune 3 presents the maximum collapse potential with a void ratio of 0,847.

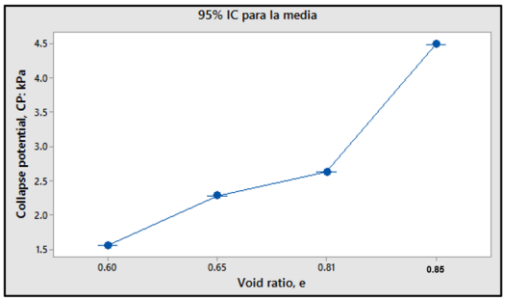

Figure 5-27. Graphic of interval of the factor collapse potential (Minitab analysis).

5.1.1.2. **Oedometer tests under different vertical effective stresses**

Figure 5-28 and Figure 5-29 show the results of oedometer tests under different vertical effective stresses on several samples of the eolian soils of Mayapo. Table 5-10 shows the initial condition for the tests. The tests were corrected to a common initial average void ratio. The saturation degree is quite low (Sr<19%). According to water retention curves of the eolian soil of Mayapo (Figure 5-23), the soil suction initial is very high, in the order of 300 kPa of suction for dune 1, 3, and 4. For dune 2, the suction is in the order of 800 kPa approximately.

Table 5-10. Initial condition of oedometer tests under different vertical effective stresses.

Dune	e_0	e_0 average	Soaking load (kPa)	Initial saturation degree (%)
1	0,697	0.69	80	17,90
	0,691		200	18,10
	0,690		400	18,87
	0,697		800	18,35
2	0,770	0,77	80	8,74
	0,771		200	10,14
	0,761		400	10,13
	0,760		800	8,84
3	0,724	0,72	80	17,89
	0,718		200	18,03
	0,723		400	17,92
	0,732		800	17,68
4	0,709	0,71	80	16,50
	0,715		200	16,74
	0.716		400	16,43
	0.712		800	15,31

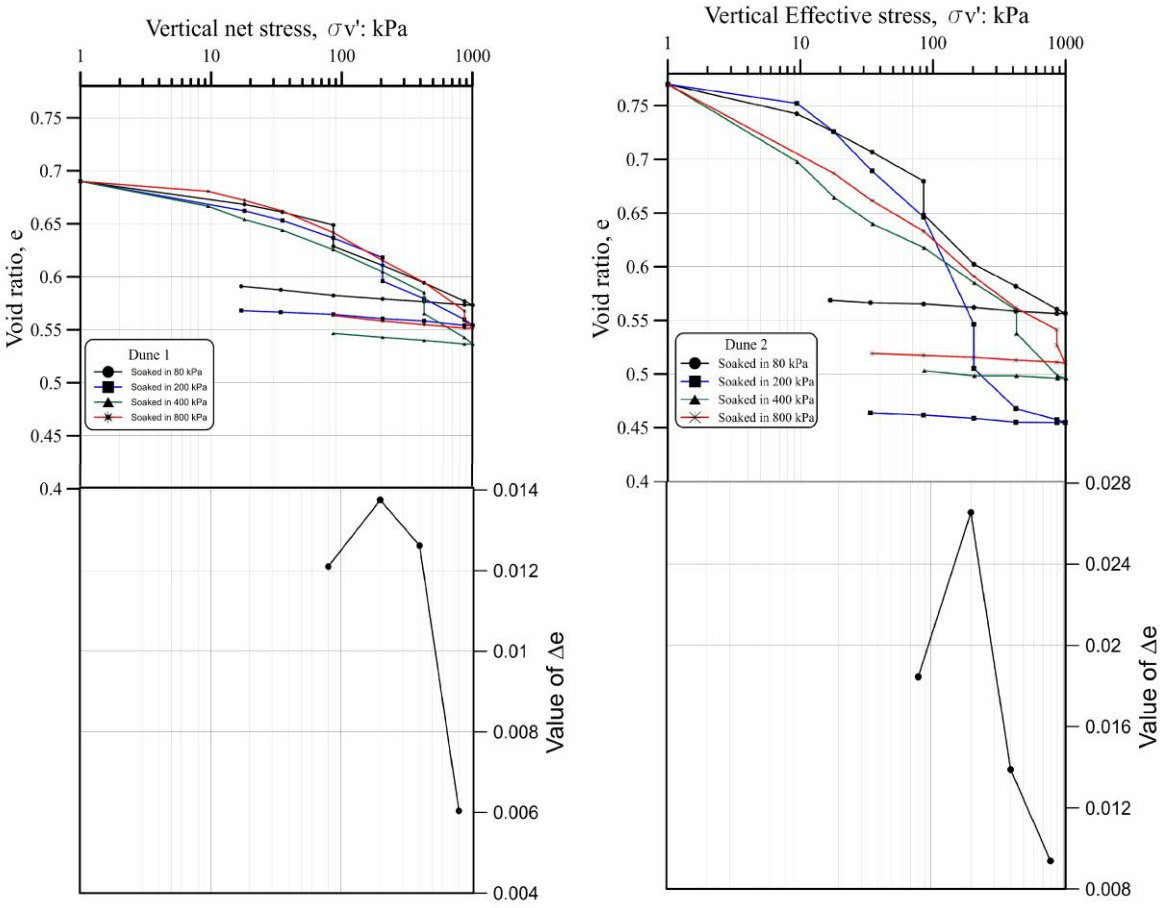

Figure 5-28. Compressibility curves of dune 1 and 2 under different vertical effective stresses.

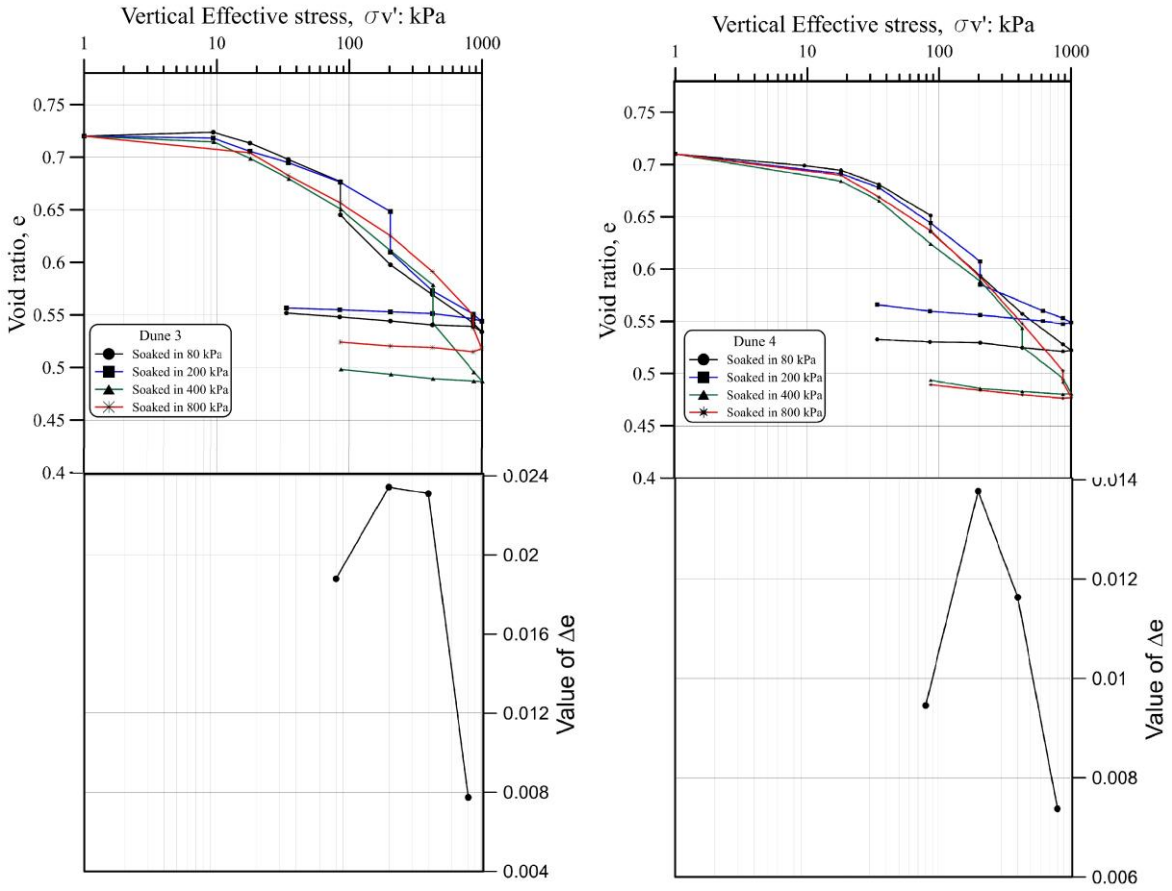

Figure 5-29. Compressibility curves of dune 3 and 4 under different vertical effective stresses.

The results of the collapse potential based on Jennings and Knight, 1957 method are summarized in Table 5-11. The maximum collapse in the eolian soils is at 200 kPa of vertical effective stress. It also observed that the maximum collapse is in dune 2, where the initial saturation degree is low and consequently presents a high suction level. There may be deducted that a saturation degree affects the collapse behaviour of the eolian soils.

Table 5-11. Collapse potential results of oedometer tests under different vertical effective stresses.

Dune	$e_0\ prom$	Soaking load	Collapse potential (%)	Severity of the problem
1	0,69	80	1,21	Moderate problem
		200	1,37	Moderate problem
		400	1,26	Moderate problem
		800	0,6	No problem
2	0,77	80	1,8	Moderate problem
		200	2,6	Moderate problem
		400	1,38	Moderate problem
		800	0,9	No problem
3	0,72	80	1,87	Moderate problem
		200	2,34	Moderate problem
		400	1,3	Moderate problem
		800	0,77	No problem
4	0,71	80	0,94	No problem
		200	1,37	Moderate problem
		400	1,16	Moderate problem
		800	0,73	No problem

A reduction in the collapse deformation is observed as the magnitude of the vertical stress applied increases. This trend is due when applying large stress, the pore volume in the soil is reduced, and it is created a new denser structure, which avoids the development of collapse strains. These results also confirm the typical behaviour of unsaturated soil exposed in the experimental test of Booth, 1975; Yudhbir, 1982, the collapse in an unsaturated soil increase up to maximum value, and the value decreases to a negligible value (Alonso et al., 1987).

This behaviour can also be explained by the consolidation phenomenon. When the soil is loaded up to 200 kPa, it can maintain the bonding between grains in unsaturated conditions, and the larger strains will take place when the soil is wetted. On the other hand, when higher loads are applied after collapse (400 and 800 kPa), the bonding between the grains will break by load instead of by wetting, and when the soil will be soaked will suffer lower strains.

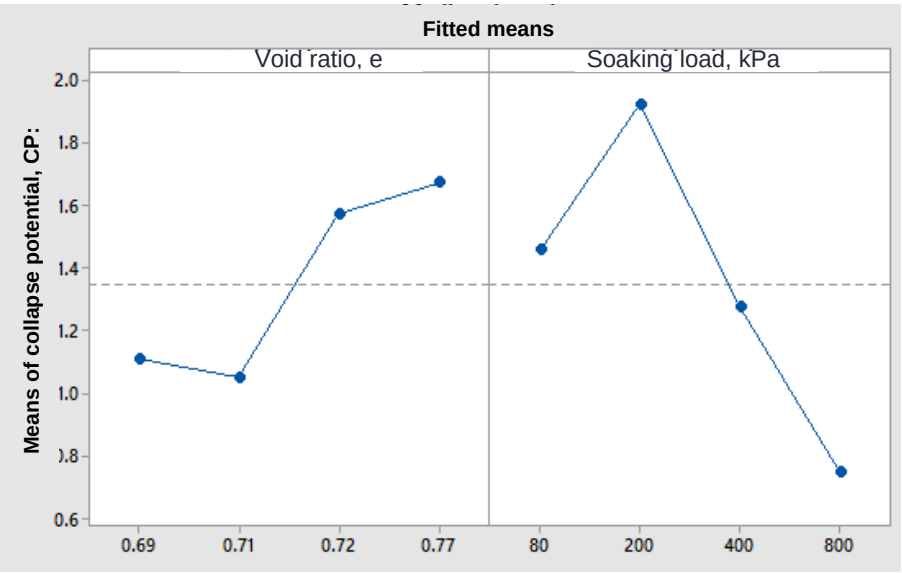

Figure 5-30. Graphic of principal effects of factors for collapse potential (Minitab analysis).

Figure 5-30 shows the average of the collapse potential in each level of the factors, it gives the principal effects of the factors in the variable response. Table 5-12 and Table 5-13 show the results of fitted means of collapse potential.

Table 5-12. Fitted means of collapse potential for void ratio.

Dune	Void ratio	Collapse potential Fitted means
1	0,69	1,11
2	0,77	1,67
3	0,71	1,05
4	0,72	1,83

Table 5-13. Fitted means of collapse potential for soaking load.

Soaking load	Collapse potential Fitted means
80	1,45
200	1,95
400	1,53
800	0,75

For the void ratio, the collapse potential increased with the increased in the initial void ratio. The vertical effective stress in which the soil experiences the maximum collapse is at 200 kPa for all dunes.

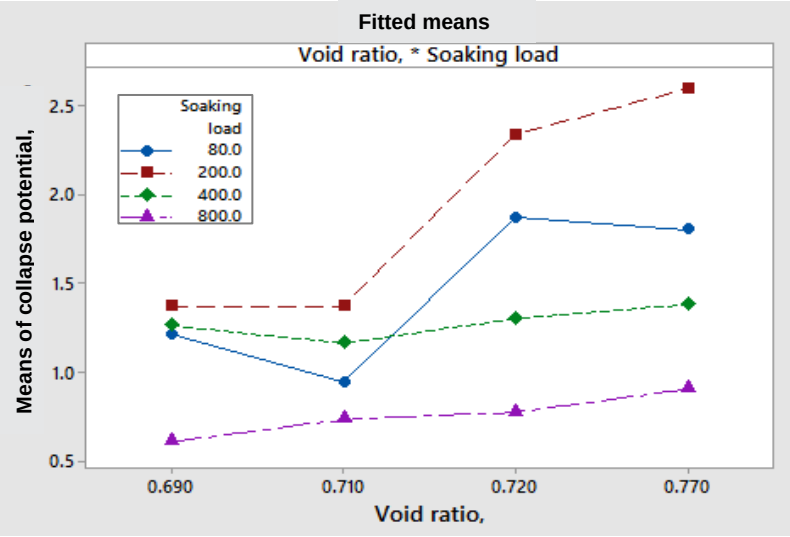

Figure 5-31. Graphic of factor interaction of factors for collapse potential (Minitab analysis).

Figure 5-31 shows the interaction between void ratio and soaking load in the collapse potential. Each curve represents the collapse potential at the same soaking load for the four dunes analyzed. It can be inferred that the maximum collapse is present at 200 kPa of soaking load. Evaluating the simple effects, the void ratio change is not significant in the collapse behaviour for soaking loads of 400 and 800 kPa. The changes in void ratio have more significance in the soaking load of 200 kPa, in which the collapse potential is the highest. Table 5-14 shows the saturation degree and the collapse potential obtained for each dune.

Table 5-14. Fitted means of collapse potential for saturation degree.

Dune	Saturation, S	Collapse potential Fitted means
1	18,30	1,11
2	9,46	1,67
3	17,88	1,57
4	16,24	1,05

A low level of saturation in the eolian soils, the collapse potential increases. It can be observed in the saturation of 9,46 the collapse potential is the highest. This behaviour can be associated with suction. However, this information could not be enough to have a complete

comprehension of the suction influence in the volumetric behaviour of the eolian soil because of the saturation degree changes during the test and the lack of control of this variable.

Figure 5-32 shows a scheme of the saturation increase caused by a strain increase. With a load increment, unsaturated soil will suffer strains, decreasing the air volume (Va). Even if the water maintains the same volume, the relationship between the water volume (Vw) and void volume (Vv), which represents the saturation degree, will increase because the Vv will decrease with each load increment.

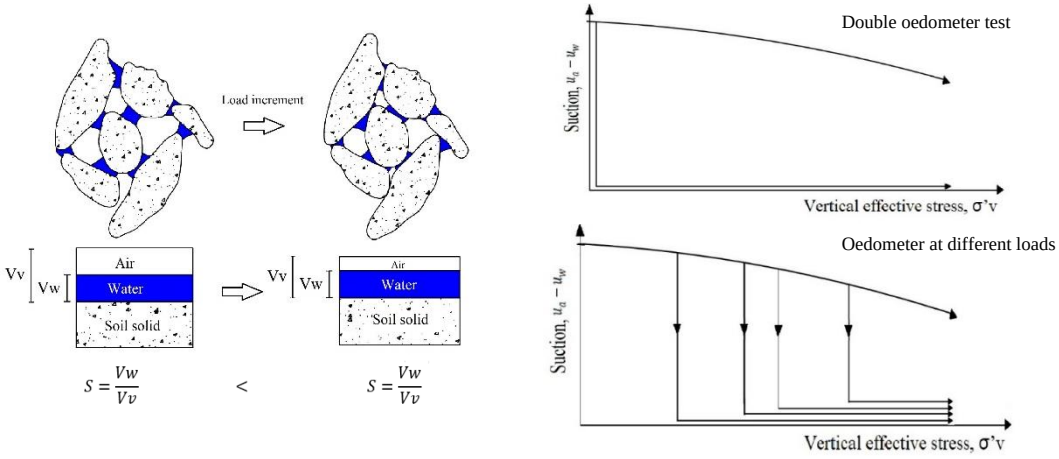

Figure 5-32. Left: Scheme of the increase in saturation with the increase in deformation. Right: Suction and stress paths of double oedometer and oedometer at different vertical effective stress tests (Alonso et al., 1990).

For this reason, suction-controlled tests were carried out in order to study the suction influence in the volumetric behaviour of the eolian soils.

5.5.2. Unsaturated oedometer tests

The volumetric behaviour of the eolian soils has been analyzed through two independent variables of stress state: $(\sigma_v - u_a)$ net stress and matric suction $(u_a - u_w)$, where σ_v is the total stress, and u_a and u_w correspond to the pressure of the gas and liquid phase respectively. The study of these unsaturated soils was based on the Barcelona Basic Model propose by Alonso et al., 1990. The suction levels for suction controlled oedometer tests are selected based on the water retention curve WRC of the dunes obtained with the paper filter

method. The suction levels range is 10 kPa to 300 kPa, in which the soil presents large changes in suction levels with small changes in the saturation degree.

5.5.2.1. Suction-controlled oedometer test: constant suction.

Five oedometer tests at constant matric suction of 0, 30, 100, 200, and 300 kPa were conducted to know the volumetric behaviour of dune 4 of the eolian soils and obtain yield stress and the stiffness parameters as κ(s) λ(s). Table 5-15 shows the initial conditions of the tests carried out. Figure 5-33 shows the compressibility curves of the eolian soils obtained from the unsaturated tests at constant suction.

Table 5-15. Conditions of the unsaturated tests at constant suction for Dune 4.

Suction (kPa)	e_0	Initial moisture content (%)	Inicial saturation degree (%)
0	0,798	5,0	16,54
30	0,763	5,6	19,20
100	0,753	5,0	17,53
200	0,752	5,2	18,18
300	0,751	3,0	18,74

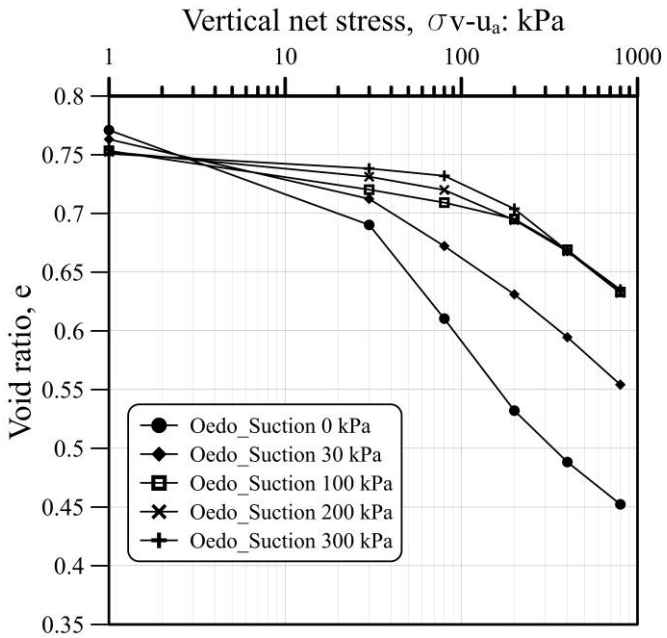

Figure 5-33. Compressibility curves from oedometer tests at constant suction.

In the compressibility test at constant suctions of the eolian soils, the large deformations occur in the soil when the vertical net stress applied reaches yield stress. Also, it can be inferred that the higher the matric suction levels, the larger the yields stress. Therefore, the suction increased. The compression index Cc and recompression index Cr values decrease with the matric suction increment. It means that the suction improves the stiffness of the eolian soils. Table 5-16 shows the saturation final and the yield stress obtained from the compressibility curves. It can be observed that the saturation degree results measured after each test are consistent with the results from the water retention curve of the eolian soils from Mayapo. The suction imposed in the samples is normally reached at these saturation degrees. For the suctions of 200 and 300 kPa, the saturation degree presents similar values due to, as shown by the water retention curve, at low saturation degrees the soil has the biggest changes in suction level and the change of 200 to 300 kPa is small compared with the values presents in this region of the WRC, see Figure 5-23.

Table 5-16. Compressibility parameters of eolian soil of Mayapo at constant suction.

Suction (kPa)	**Final Saturation degree (%)**	**Yield stress (kPa)**	**Cc**	**Cr**
0	89	60	0,145	0,055
30	20,43	70	0,134	0,034
100	18,75	120	0,113	0,026
200	12,21	170	0,112	0,014
300	12,22	180	0,110	0,008

The volumetric behaviour of the eolian soils is described following the constitutive model proposed in Alonso et al., 1990. In Figure 5-34 are plotted the yield stresses obtained at different suction of eolian soils in two-dimensional stress space: vertical net stress ($\sigma_v - u_a$) and suction ($u_a - u_w$). A yield surface is drawn through these points. The yield surface allows knowing the reversible compressive volumetric strains for any stress path of loading (L), collapse (C), or both in the elastic domain. Also, it can predict irreversible compressive volumetric strain for any stress loading or collapse paths. The LC curve obtained for the eolian soils support the concept of the LC model.

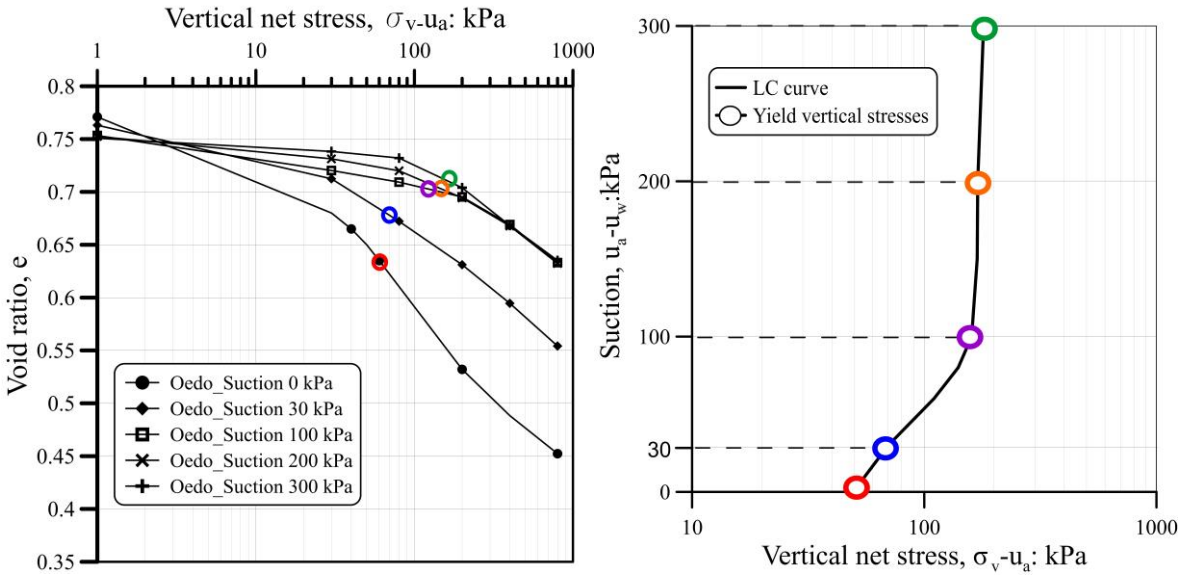

Figure 5-34. LC curve of eolian soil of Mayapo from experimental test at constant suction.

It can be observed in LC curve that the yield stress moves further to the right as suction increases. The suction in the soil allows the soil to sustain higher applied stress: The higher the suction, the higher the stress can be sustained before yield.

A theoretical yield curve can be obtained by the equation proposed by Alonso et al., 1990)(Reznik, 2007)(Reznik, 2007)(Reznik, 2007)(Reznik, 2007)(Reznik, 2007):

$$p_0 = p_c \left(\frac{p_0^*}{p_c}\right)^{\frac{\boldsymbol{\lambda(0)-\kappa}}{\boldsymbol{\lambda(s)-\kappa}}} \text{ and } \boldsymbol{\lambda(s) = \lambda(0)[r + (1-r)e^{-\beta s}]} \qquad \text{Eq. 5-5}$$

Where,

λ(s) = Compressibility parameters in the post-yield range

κ(s) = Compressibility parameter in the pre-yield range

r = Parameter defining the maximum macrostructural soil stiffness

p^c = Reference stress

β = Parameter controlling the rate of increase of macrostructural soil stiffness with suction

P_0^* = Yield stress at saturated conditions

$$\lambda = \frac{Cc}{Ln(10)} \qquad \text{Eq. 5-6}$$

$$k = \frac{Cr}{Ln(10)} \qquad \text{Eq. 5-7}$$

To obtain los parameters of theorical yield curve is assumed k_o=1. Then,

$$p = \frac{\sigma_1+\sigma_2+\sigma_3}{3} = \frac{\sigma_1+2\sigma_3}{3} = \frac{\sigma_1+2(k_o*\sigma_1)}{3} \quad \text{Eq. 5-8}$$

The compressibility parameters of eolian soils obtain from the compressibility curves at different constant suction values are summarized in Table 5-17.

Table 5-17. Parameters of the eolian soils from compressibility curves and the theoretical yield stress.

Suction (kPa)	**λ(s)**	**κ(s)**	**r ($^{\lambda(s)}/_{\lambda(o)}$)**	p^c	β	**Theoretical Yield stress (kPa)**
0	0,063	0,024				50
30	0,058	0,014	0,92			69
100	0,049	0,011	0,78	1,3	2,5	156
200	0,048	0,006	0,77			163
300	0,047	0,003	0,76			180

The compressibility parameters values κ and λ decrease with the increase in matric suction. This implies that the suction contributes to the stiffening of the eolian soils subjected to external stresses. Figure 5-35 shows the approximation between the experimental LC curve of the eolian soils with theoretical yield stress and experimental yield stress. A remarkable similarity is observed between the theoretical and experimental results. The LC curve allows to solve boundary value problems and evaluate closer to real situations in engineering.

The evolution of the LC curve can be obtained from the theoretical LC curve of the eolian soils. Figure 5-36 shows a scheme of the evolution of the LC curve. After yield stress in the compressibility curves, the soil will suffer plastic volumetric strains, which would be equal to the irreversible plastic volumetric strains of the LC curve. The soil state will follow new paths of loading and (or) collapse and the yield curve will move from position LC_1 to LC_2. The new LC curve is associated with the final plastic strains of the compressibility curves (Δ), representing the new yield stresses of the soil. The LC_2 curve can be obtained with the yield stress at saturated conditions and using the theoretical equation proposed by Alonso et al., 1990.

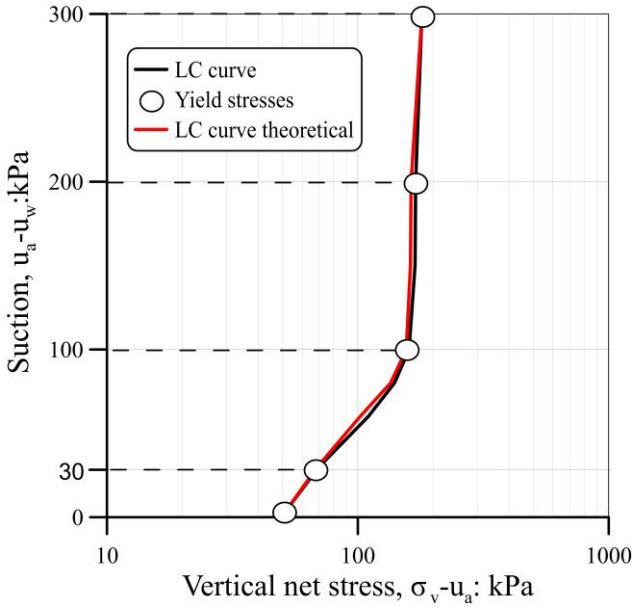

Figure 5-35. Approximation between theoretical loading collapse curve and the experimental loading collapse curves.

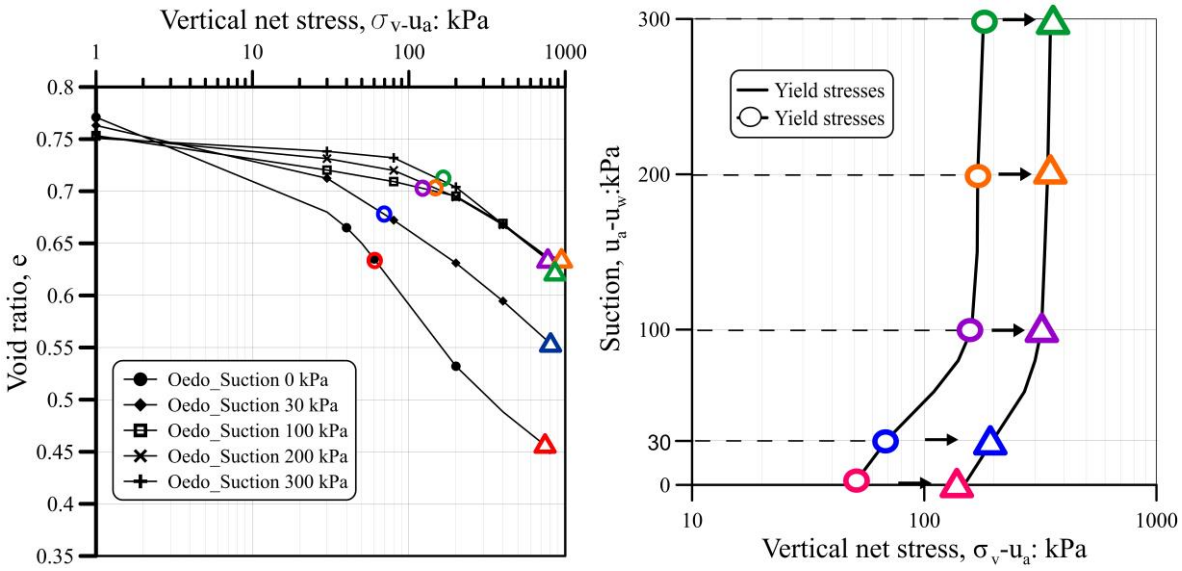

Figure 5-36. Evolution of the Loading Collapse curve of the eolian soil.

5.5.2.2. Suction controlled oedometer tests: stress paths.

These tests are focus on the analysis of volumetric behaviour of the eolian soils associated with suction and vertical net stress changes. The tests start from the same state of 10 kPa of vertical net stress and 200 kPa of suction, and the final state is at 300 kPa of vertical net stress and 30 kPa of suction. The paths from each test are detailed in

Figure 5-37. The initial and final conditions of the tests are summarized in Table 5-18.

Table 5-18. Initial and final conditions of the suction controlled oedometer tests., Dune 4.

Test	e_0	W% initial	S final (%)	W % final	Cc	Cr
5	0,737	3	23,304	4,3	0,176	0,1
6	0,738	2,9	20,67	4,5	0,135	0,051

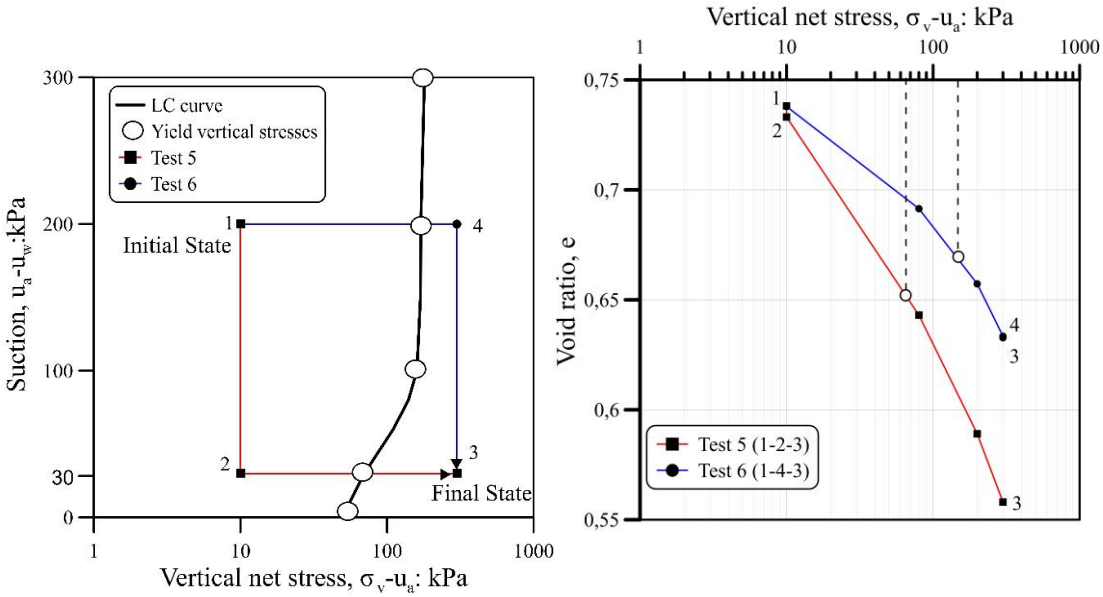

Figure 5-37. Response of the model to alternative loading-collapse paths. Left: Loading collapse of eolian soils Right: Variation of void ratio with vertical net stress applied.

In test 5, represented by path 1-2-3, the soil starts with a small strain by decreasing the suction to 30 kPa. The next path consists of loading at 300 kPa under constant suction of 30 kPa. During this load increment, the soil reaches the yield stress of 70 kPa, and then the soil compresses plastically. It can be noted that the yield stress obtains from the compressibility curve agrees with the yield stress obtained from the LC curve at 30 kPa.

In test 6, presented as path 1-4-3, the soil is loaded to 300 kPa at constant suction of 200 kPa, and then, the suction decreased to 30 kPa. It can be observed that the soil compresses elastically with small strains up to reach the yield stress of 170 kPa, and then, the soil compresses plastically. The results are also associated with the LC curve obtained for the eolian soils due to it can predict the yield stress obtained in the compressibility curve. Once

the soil reaches 300 kPa of net vertical stress, the suction is decreased to 30 kPa inducing settlement.

The results denoted that larger strains occur when the soil is loaded (2-3 and 1-4 paths) instead of when the suction decreases (1-2 and 4-3 paths). Figure 5-38 shows a comparison between the strains of both tests for the suction paths. It can be observed that the strains are very small at suction changes. Therefore, it can deduct that the strains are controlled by the constant suction value in which the soil is loaded. The suction change paths are more important if the soil would have expansive minerals (Romero, 1999).

It can be observed that for test 5 the elastic domain is smaller, and the total strains are larger than for test 6. This can be demonstrated in the compressibility curves, where the total strain in test 5 is 12% larger than the test 6. This behaviour is caused by the suction level in which the soil is loaded. This behaviour also can be denoted comparing the compressive index Cc and re-compressive index Cr results, Cc and Cr are lower at higher suction levels in which the soil is loaded, and the soil stiffness increases. It can be inferred that the Cc and Cr depend on suction.

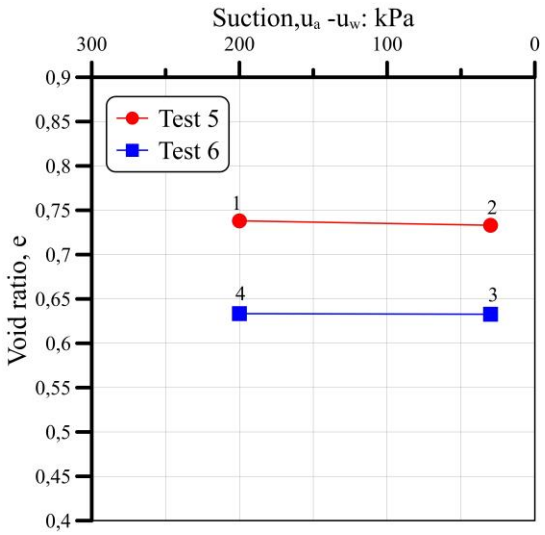

Figure 5-38. Relation of the strains at suction change (collapse path) in unsaturated oedometer tests at different stress paths.

It can be concluded that there is an important dependence of collapse and loading paths in the volumetric behaviour of the eolian soil. The deformations are very small at suction changes. The soils will suffer higher deformations in loading paths at low suction levels due to the soil stiffness is less.

5.6. Procedure of sampling and characterization of the volumetric behaviour of eolian soils.

The methodology and results obtained from the experimental investigation in the eolian soils form Mayapo, Colombia have allowed us to define an experimental procedure for sampling and characterization of the volumetric behaviour of undisturbed eolian soils. The steps are listed as follow:

1. Carry out the soil sampling according to the guideline of standard practices for obtaining intact blocks (see section 4.3).
2. Define the physical properties and geotechnical classification of eolian soils. (see section 4.4)
3. Define the mineral composition, the soil structure, and the distribution of the element by microstructure tests. These features can directly influence volumetric behaviour. (see section 4.5)
4. Determinate the water retention curve for matric and total suction by the paper filter method. The suction plays an important role in the volumetric behaviour of this kind of unsaturated soils. (see section 4.6.1)
5. Define the osmotic suction at a saturated condition by measuring the conductivity electric of the soil pore water extracted by the squeezing method. (see section 4.6.2)
6. Determinate the collapse potential of the soils. The equation used to calculate the collapse behaviour is proposed by Jennings and Knight, 1957, (See section 4.7.2).
7. Define the stress in which the eolian soil has the maximum collapse potential (See section 4.7.2).
8. Determinate compressibility curve of eolian soils at constant suction (see section 4.7.3)

9. Define the experimental yield stresses of the eolian soils from the compressibility curve. (see section 5.5.2.1).
10. Define the Loading-Collapse curve for the eolian soils with the yield stress according to Barcelona Basic Model proposed by Alonso et al., 1987 (see section 5.5.2.1).
11. Define the parameters of the soil from the compressibility curves (see section 5.5.2.1)
12. Obtain the theoretical yield stresses using the Eq. 5-9 proposed by Alonso et al., 1987. (see section 5.5.2.1)
13. Define the theoretical loading collapse curve with the theoretical yield stresses and compare them with the experimental results. It can model the volumetric behaviour of the eolian soil (see section 5.5.2.1).

Figure 5-39 summarized the proposed protocol for sampling and characterization of the volumetric behaviour of the eolian soil.

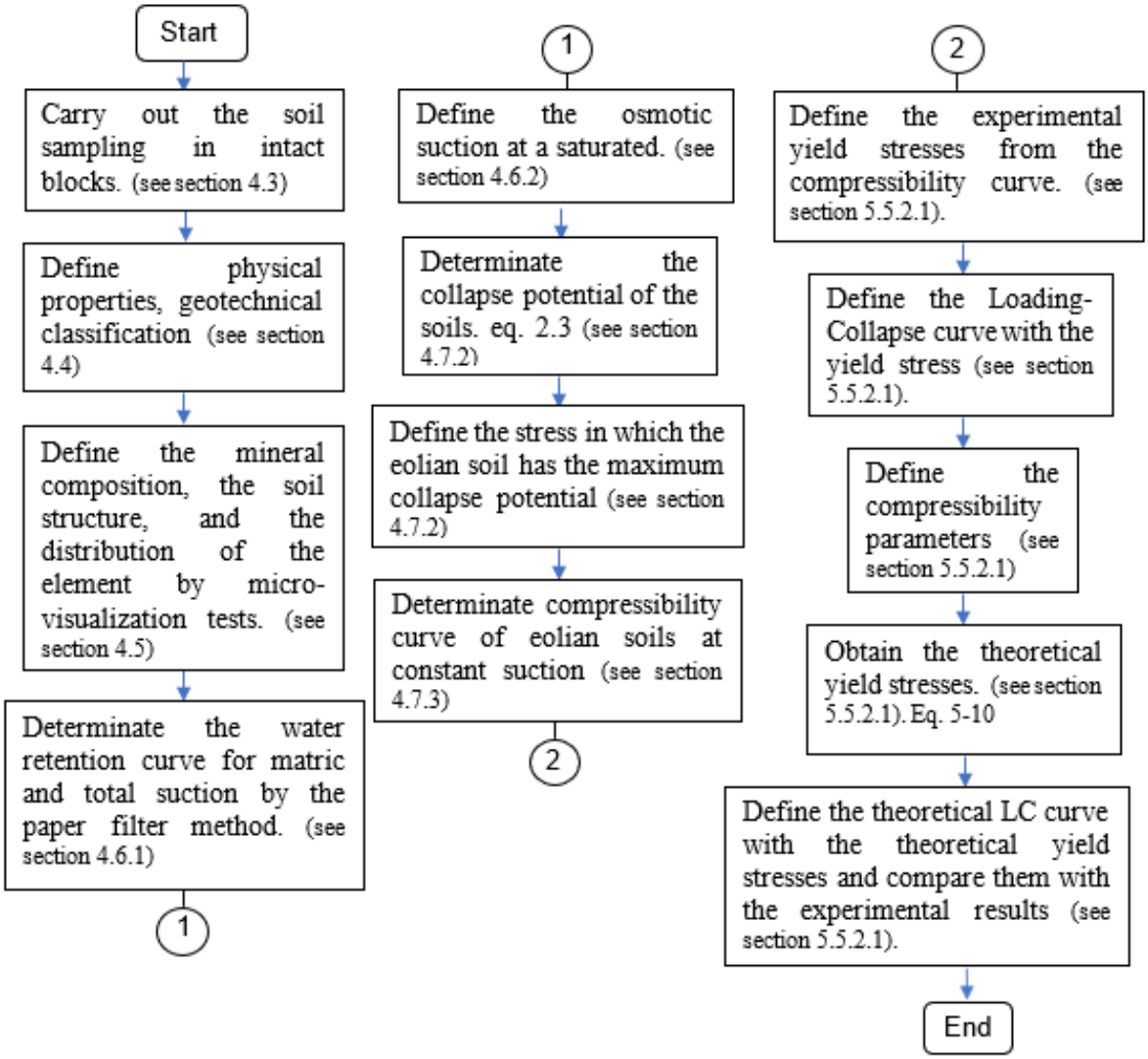

Figure 5-39. Experimental procedure for sampling and characterization of the volumetric behaviour of undisturbed eolian soils.

5.7. Chapter conclusions

- Most of the sand-size particles are composed of quartz crystals. The soil is also composed of plagioclases and feldspars. These minerals are characterized as igneous rocks formed. The shape of crystals is subangular to angular, which could affect the mechanic resistance. The salt particles are also present in the eolian soils, appearing in disseminated form.

- Most of the fine particles are Aluminum and Iron oxides, presented in the contacts between grains. These oxides act as a bonding material and can be assimilated apparent cementation between the grains. The bonding is bordering the grains in all samples of the eolian soils. However, the Aluminum and Iron elements do not exceed 6% in the samples, and this apparent cementation won´t control the collapse behaviour.

- The analysis of the soil structure by SEM allows identifying large and continuous macropores between the grains sand sized. The micropores are also present in the eolian soils between the soil aggregates. But the total collapse of eolian soils could be controlled by the presence of macropores.

- According to the geological history, the eolian soils have minerals representative of the igneous rocks, the origin could have from rocks of the river next to the eolian soils region, which has contribution from different geological formations. After that, the eolian soils presented sort transport until reach the actual localization.

- Double water retention curves for the eolian soils were calculated to have a better comprehension of the suction behaviour and the influence of the porosity (microstructure and macrostructure) in the eolian soil suction. It can be demonstrated that at low saturation degrees (0-20%) the water flow is controlled by the micropores, and the water will come out of the soil with greater difficulty. With small increases in saturation, the suction will become governed by the macropores and will decrease sharply.

- The osmotic suction estimated from the electrical conductivity was π=315 kPa, according to USDA,1950, and π= 365 kPa according to Romero,1999. The value of osmotic suction can be physically explained by the presence of salt particles. The salt concentration influences the osmotic suction and the total suction of the eolian soil, affecting its hydraulic condition. It can govern the water flow and attract more water to the soil, increasing the saturation degree. The increase in saturation causes a decrease in total suction in the soil, affecting the volumetric behaviour of soil.

- Based on the classical oedometer tests results, the collapse potential of the eolian soils was classified as a moderated problem. The collapse potential increase with the increment of the initial void ratio. The suction also plays an important role in the collapse potential. As suction decreases and soil wets, water menisci coalesce, and the empty pores are flooded, and it causes a loss in the soil stiffness. On the other hand, the collapse potential increases as the initial matric suction increases. This indicates that higher initial matric suction levels try to maintain the meta-stable bound between particles without significant settlement but eventually collapse upon inundation. The stiffness of the eolian soils decreases when the soil is collapsed.

- The maximum collapse in the eolian soils is at 200 kPa of vertical effective stress. After that, a reduction in the collapse deformation takes place as the magnitude of the vertical stress applied increases. This trend is due when applying large stress, the pore volume in the soil is reduced, and it is created a new denser structure, which avoids the development of collapse strains.

- The unsaturated oedometer tests allowed to understand the influence of suction on the volumetric behaviour of the eolian soils. The suction allows the soil to sustain higher applied stress: The higher the suction, the higher is the stress that can be sustained before yield. The suction increases the stiffness of the eolian soils. A constitutive model was proposed to describe the volumetric behaviour of the eolian soil. The model is represented by a Loading Collapse (LC) curve, and to allow knowing the reversible compressive volumetric strains for any stress path of loading (L), collapse (C), or both

in the elastic domain and to predict irreversible compressive volumetric strain for any stress loading or collapse paths.

- The parameters obtained from the oedometer tests at constant suction allowed to calculate yield stresses and drawing a theoretical LC curve. The experimental and theoretical yield curves show a good agreement. This demonstrated a good consistency in the development of the unsaturated tests, and in the volumetric behaviour of the eolian soils although the tests have been done on undisturbed samples.

- There is an important dependence of collapse and loading paths in the volumetric behaviour of the eolian soils. The deformations are very small at suction changes. The soils will suffer higher deformations in loading paths at low suction levels due to the soil stiffness is less.

- It is to highlight that, there is a close relationship between the experimental results of this dissertation. It can be denoted that the bonding material as iron and aluminum oxide and the meniscus water play an important role in the volumetric behavior of the eolian soils of Mayapo, it contributes to the stiffness of the soil. The bonding of the water menisci between grains is the most representative in the eolian soils. Its behaviour is evidenced in the water retention curve of the soil, which shows the suction of the soil at different saturation degree. The component of suction and the water menisci are also related to the macrostructure and the microstructure of the soil. It can be denoted that the low suction levels take place in the macropores where the water menisci present larger areas, conversely, high suction levels take place in micropores where the water menisci area is smaller.

5.8. References

Alonso, E. E., Gens, A., & D., W. (1987). Groundwater Effects in Geotechnical Engineering. *The Ninth European Conference on Soil Mechanics and Foundation Engineering*, *3*.

Alonso, E. E., Gens, A., & Josa, A. (1990). A constitutive model for partially saturated soils G ”. *Géotechnique*, *40*(3), 405–430.

Araki, M. S. (1997). *Aspectos Relativos às Propriedades dos Solos Porosos Colapsíveis do Distrito Federal*. University of Brasília, College of Technology.

Booth, A. R. (1975). The factors influencing collapse settlement in compacted soils. *6th. Reg. Conf. for Africa on SMFE*, 57–63.

Coduto, D. (1999). Geotechnical engineering principles and practices. In *Engineers Australia* (Vol. 73, Issue 4). https://doi.org/10.2113/gseegeosci.iii.1.156

Durner, W. (1994). Hydraulic conductivity estimation for soils with heterogeneous pore structure. *Water Resources Research*, *30*(2), 211–223.

Jennings, J., & Knight, K. (1957). The Additional Settlement of Foundations due to a Collapse of Structure of Sandy Subsoils on Wetting. *Proceedings, 4th International Conference on Soil Mechanics and Foundation Engineering, London, 1,* 316–319.

Classification des matériaux utilisables dans la construction des remblais et des couches de forme d´infrastructures routières, (1992).

Reznik, Y. M. (2007). Influence of physical properties on deformation characteristics of collapsible soils. *Engineering Geology*, *92*(1), 27–37. https://doi.org/https://doi.org/10.1016/j.enggeo.2007.03.001

Rogers, C. D. F. (1995). *Types and Distribution of Collapsible Soils*. 1–17.

Romero, E. (1999). *Characterisation and thermo-hydromechanical behaviour of unsaturated boom clay: an experimental study*. Univesitad Politecnica de Cataluna.

van Genuchten, M. T. (1980). A Closed-form Equation for Predicting the Hydraulic Conductivity of Unsaturated Soils. *Soil Science Society of America Journal*, *44*(5), 892–898.

Wan, A. W. L., Gray, M. N., & Graham, J. (1995). On the relations of suction , moisture content and soil structure in compacted clays. In E. E. Alonso & P. Delage (Eds.), *1st.*

International Conference on Unsaturated Soils (Issue December, pp. 215–222).

Yudhbir, Y. (1982). Collapsing behavior of collapsing soils. *7th Southeast Asia Geotechnical Conference*, 915–930.

CHAPTER 6- GENERAL CONCLUSION AND FUTURE WORK

6.1 General conclusions

All conclusions were described in each chapter of this dissertation. Therefore, the general conclusions are detailed below:

Although the eolian soils of Mayapo present a moderate collapse potential, in specific levels of factor the soil experiment more collapse, when the soil is soaked at 200 kPa of loading, the void ratio greater than 0.8, saturation degrees values higher that 20 %, when the macropores governs the soil suction. These values levels must be considered in construction in this area studied.

The eolian soils are collapsible, and there is a close relationship between the volumetric behaviour with the soil structure: The collapse is governed by the macropores. The suction also plays an important role: The macropores govern most of the suction soils. There are important variations in suction at low saturation degrees, which is governed by micropores.

The understanding of the geological characteristics and its relationship with the collapse potential allow to contribute to the knowledge of the influence of mineralogy and structure in the volumetric behaviour of this kind of soils.

The importance of the LC curve results justifies performing controlled suction tests, due to it is possible to have a better understanding of the influence of suction on collapse, because in classical oedometer tests, the suction is not controlled and measured. The model constitutive realized of the eolian soils is an important contribution in the knowledge of eolian soils. It is noteworthy that although the tests were carried out on undisturbed samples, and the variation in the initial properties of the soil could affect the results, the consistency in the results obtained was good.

6.2.Recommendations and future work

The experimental research of this thesis has allowed a better understanding of the volumetric behaviour of the eolian. However, there are some natural extensions to this work that would help expand and strengthen the results. The new lines of work are described below:

Due to the eolian soils are formed in arid regions, the change in the ambient temperature can affect the volumetric behaviour of the soil. An experimental program of unsaturated tests at

constant suction is proposed in order to analyze the volumetric behaviour at different relative humidity, and to compare with the results obtain in this research.

Numerical simulation can be developed considering certain field situation and using the parameters obtained from double water retention curves of the eolian soils and the parameters obtained from Loading collapse (LC) curve to predict the future behaviour of the eolian soil at a certain situation.

From the point of view of unsaturated tests, the testing techniques developed could be improved, including the measurement of lateral forces. It would allow expanding the knowledge of the evolution of k0 with suction and the influence in the constitutive model proposed.

New stress paths of loading collapse are suggested, including the soil wetting at different loads in order to know the maximum load when the soil can experience the maximum collapse at constant suction.

It is also proposed unsaturated oedometer tests, testing eolian soils with denser structure, to know the experimental yield stresses with this new soil structure. This would make it possible to verify whether the soil under this condition has a behaviour that can be explained with the evolution of the loading collapse curve and the parameters derived from the tests carried out in this research.

It is suggested to carry out the tests with repeatability. For this research, this process was not carried out for all tests because of the high cost of transport from the site of extraction of the soils to the site of testing, and the time required for the realization of the test. However, this investigation is an important improvement in the knowledge of the volumetric behaviour of the eolian soils in Colombia.